HOMO RES SACRA

ՀԱՅ-ՌՈՒՍԱԿԱՆ ՀԱՄԱԼՍԱՐԱՆ

ԼՐԱԲԵՐ

ՀԱՅ-ՌՈՒՍԱԿԱՆ ՀԱՄԱԼՍԱՐԱՆԻ

ՍԵՐԻԱ

ՖԻԶԻԿԱՄԱԹԵՄԱՏԻԿԱԿԱՆ
ԵՎ ԲՆԱԿԱՆ ԳԻՏՈՒԹՅՈՒՆՆԵՐ

№ 2

ՀՌՀ Հրատարակչություն

Երևան 2020

РОССИЙСКО-АРМЯНСКИЙ УНИВЕРСИТЕТ

В Е С Т Н И К

РОССИЙСКО-АРМЯНСКОГО УНИВЕРСИТЕТА

СЕРИЯ:

ФИЗИКО-МАТЕМАТИЧЕСКИЕ И ЕСТЕСТВЕННЫЕ НАУКИ

№ 2

Издательство РАУ

Ереван 2020

Печатается по решению Ученого совета РАУ

Вестник РАУ, № 2. – Ер.: Изд-во РАУ, 2020. – 125 с.

Журнал входит в перечень периодических изданий,
зарегистрированных ВАК РА и РИНЦ

Российско-Армянский университет, 2020 г.

ISBN 1829-0450

МАТЕМАТИКА И ИНФОРМАТИКА

UDC 519.178

Поступила: 14.10.2020г.
Сдана на рецензию: 23.10.2020г.
Подписана к печати: 04.11.2020г.

TWO NP-COMPLETE PROBLEMS ON LOCALLY-BALANCED 2-PARTITIONS OF GRAPHS

A. Gharibyan

Chair of Discrete Mathematics and Theoretical Informatics, YSU, Armenia

aramgharibyan@gmail.com

ABSTRACT

A 2-partition of a graph G is a function $f: V(G) \rightarrow \{0,1\}$. A 2-partition f of a graph G is a locally-balanced with a closed neighborhood if for every $v \in V(G)$, $\left| |\{u \in N_G[v]: f(u) = 0\}| - |\{u \in N_G[v]: f(u) = 1\}| \right| \leq 1$, where $N_G[v] = N_G(v) \cup \{v\}$. In this paper we prove that the problem of the existence of locally-balanced 2-partition with a closed neighborhood is NP-complete for some restricted classes of graphs. In particular, we show that the problem of deciding if a given graph has a locally-balanced 2-partition with a closed neighborhood is NP-complete even for subcubic bipartite graphs and odd graphs with maximum degree 3.

Keywords: Locally-balanced 2-partition, NP-completeness, bipartite graph, subcubic bipartite graph, odd graph.

Introduction

In this paper all graphs are finite, undirected, and have no loops or multiple edges. Let $V(G)$ and $E(G)$ denote the sets of vertices and edges of a graph G, respectively. The set of neighbors of a vertex v in G is denoted by $N_G(v)$. Let $N_G[v] = N_G(v) \cup \{v\}$. The degree of a vertex $v \in V(G)$ is denoted by $d_G(v)$ and the maximum degree of vertices in G by $\Delta(G)$. A graph G is odd if the degree of every vertex of G is odd. The terms and concepts that we do not define can be found in [1,2].

The concept of locally-balanced 2-partition of graphs was introduced by Balikyan and Kamalian [3] in 2005. Locally-balanced 2-partitions of graphs can be considered as a special case of equitable colorings of hypergraphs [4]. Berge [4] obtained some sufficient conditions for the existence of equitable colorings of hypergraphs. Ghouila-Houri [5] characterized unimodular hypergraphs in terms of partial equitable colorings and proved that a hypergraph $H = (V, E)$ is unimodular if and only if for each $V_0 \subseteq V$ there is a 2-coloring $\alpha: V_0 \rightarrow \{0,1\}$ such that for every $e \in E$, $||e \cap \alpha^{-1}(0)| - |e \cap \alpha^{-1}(1)|| \leq 1$. In [6-9], it was considered the problems of the existence and construction of proper vertex-coloring of a graph for which the number of vertices in any two color classes differ by at most one. In [10], 2-vertex-colorings of graphs were considered for which each vertex is adjacent to the same number of vertices of every color. In particular, Kratochvil [10] proved that the problem of the existence of such a coloring is NP-complete even for the $(2p, 2q)$-biregular $(p, q \geq 2)$ bipartite graphs. Moreover, he also showed that the problem of the existence of the aforementioned coloring for the $(2,2q)$-biregular $(q \geq 2)$ bipartite graphs can be solved in polynomial time. Gerber and Kobler [11,12] suggested to consider the problem of deciding if a given graph has a 2-partition with nonempty parts such that each vertex has at least as many neighbors in its part as in the other part. In [13], it was proved that the problem is NP-complete. In [3], Balikyan and Kamalian proved that the problem of existence of locally-balanced 2-partition with an open

neighborhood of bipartite graphs with maximum degree 3 is NP-complete. In 2006, they also proved [14] that the problem of existence of locally-balanced 2-partition with an closed neighborhood of bipartite graphs with maximum degree 4 is NP complete. In [15,16], the necessary and sufficient conditions for the existence of locally-balanced 2-partitions of trees were obtained. In [17], Balikyan obtained the necessary and sufficient conditions for the existence of locally-balanced 2-partitions of bipartite cactus graphs. In [18], Gharibyan and Petrosyan obtained the necessary and sufficient conditions for the existence of locally-balanced 2-partitions of complete multipartite graphs. Recently, Gharibyan [19] studied locally-balanced 2-partitions of even and odd graphs. In particular, he gave necessary conditions for the existence of locally-balanced 2-partitions of these graphs.

In the present paper we study the complexity of the problem of the existence of locally-balanced 2-partition with a closed neighborhood of graphs. In particular, we prove that the problem of deciding if a given graph has a locally-balanced 2-partition with a closed neighborhood is NP-complete even for subcubic bipartite graphs and odd graphs with maximum degree 3.

Main Results

Before we formulate and prove our main results, we introduce some terminology and notation. If φ is a 2-partition of a graph G and $v \in V(G)$, then define $\#[v]_\varphi$ and $\varphi^*(v)$ as follows:

$$\#[v]_\varphi = |\{u \in N_G[v]: \varphi(u) = 1\}| - |\{u \in N_G[v]: \varphi(u) = 0\}|,$$

$$\varphi^*(v) = \begin{cases} -1, & if\ \varphi(v) = 0, \\ 1, & if\ \varphi(v) = 1. \end{cases}$$

If F is a graph and $\{v_1, \dots, v_k\} \subseteq V(F)$, then we call a graph $F < v_1, \dots, v_k >$ *reduction element* with an input set $\{v_1, \dots, v_k\}$.

For a reduction element $F < v_1, \dots, v_k >$ and a graph H, we define a new graph $G = (F < v_1, \dots, v_k > \cup\ H)_{E'}$ as follows:

$$V(G) = V(F) \cup V(H),$$

$$E(G) = E(F) \cup E(H) \cup E',$$

where $E' \subseteq \{uv : v \in \backslash\{v_1, \dots v_k\}, u \in V(H)\}$.

We denote by $V = \{x_1, \dots, x_n\}$ a finite set of variables. A literal is either a variable x or a negated variable $\overline{x}$. We denote by $L_V = \{x, \overline{x} : x \in V\}$ the set of literals. A *clause* is a set of literals, i.e., a subset of L_V, and a k-*clause* is one which contains exactly k distinct literals. A clause is *monotone* if all of its involved variables contain no negations.

We define a function $NAE_n : \{0,1\}^n \to \{0,1\}$ in the following way:

$$NAE_n(x_1, x_2, \dots, x_n) = \begin{cases} 0, & if\ x_1 = x_2 = \cdots = x_n, \\ 1, & otherwise. \end{cases}$$

If c is a monotone k-clause and $x_{i_1}, x_{i_2}, \dots, x_{i_k} \in c$, then define $NAE_k(c)$ as follows:

$$NAE_k(c) = NAE_k(x_{i_1}, x_{i_2}, \dots, x_{i_k})$$

Let us now consider the following.

Problem 1 (NAE-3-Sat-E4)

Instance: Given a set $V = \{x_1, \dots, x_n\}$ of variables and a collection $C = \{c_1, \dots, c_k\}$ of monotone 3-clauses over V such that every variable appears in exactly four clauses,

Question: Is $f(x_1, \dots, x_n) = NAE_3(c_1) \& \cdots \& NAE_3(c_k)$ formula satisfiable?

The following was proved.

Theorem 1. *([20]). Problem 1 is NP-complete.*

Lemma 2. If φ is a locally-balanced 2-partition with a closed neighbourhood of graph $G = (V, E)$, then for every $v \in V(G)$ with $d_G(v) = 1, \varphi(u) \neq \varphi(v), where\ uv \in E(G)$.

Proof. Suppose φ is a locally-balanced 2-partition with a closed neighbourhood of G. Let us consider a vertex $v \in V(G)$, where $d_G(v) = 1$, then

$$\#[v]_\varphi = 0 = |\{u: u \in N_G[v]\ and\ \varphi(u) = 1\} - \{u: u \in N_G[v]\ and\ \varphi(u) = 0\}|,$$ hence $$|\{u:\ u \in N_G[v]\ and\ \varphi(u) = 1\} = \{u: u \in N_G[v]\ and\ \varphi(u) = 0\}|,$$

which implies that $\varphi(v) \neq \varphi(u)$.

Let us define a graph F_1 as follows

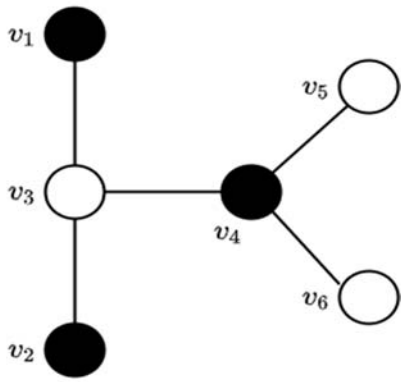


Fig. 1. The graph F_1.

Lemma 3. If graph F_1 has φ locally-balanced 2-partition with a closed neighbourhood, then $\varphi(v_1) = \varphi(v_2) = \varphi(v_5) = \varphi(v_6)$ and $\varphi(v_3) = \varphi(v_4) = 1 - \varphi(v_1)$.

Proof. Suppose φ is a locally-balanced 2-partition with a closed neighbourhood of G. By Lemma 2, we obtain

$$\varphi(v_5) \neq \varphi(v_4),$$
$$\varphi(v_6) \neq \varphi(v_4).$$

Hence

$$\varphi(v_5) = \varphi(v_6). \tag{1}$$

Since $d_G(v_4)$ is odd and φ is a locally-balanced 2-partition with a closed neighbourhood, we obtain $\#[v_4]_\varphi = 0$. From this and taking into account (1), we have

$$\varphi(v_4) = \varphi(v_3) \neq \varphi(v_5). \tag{2}$$

Using the same assumption for v_3 and taking into account (2), we get

$$\varphi(v_1) = \varphi(v_2) \neq \varphi(v_3).$$

For $i \in \mathbb{N}$, let us define F_2^i graph as follows:

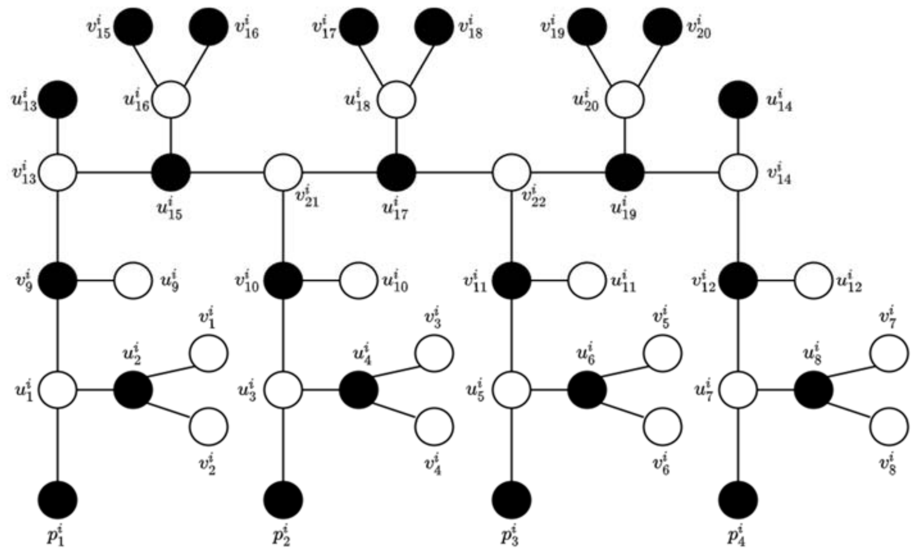


Fig. 2. The graph F_2^i.

Lemma 4. If graph $G = (F_2^i < p_1^i, p_2^i, p_3^i, p_4^i > \cup H)_{E'}$ has φ locally-balanced 2-partition with a closed neighbourhood, then $\varphi(p_1^i) = \varphi(p_2^i) = \varphi(p_3^i) = \varphi(p_4^i)$.

Proof. Suppose φ is a locally-balanced 2-partition with a closed neighbourhood of G. Without loss of generality we may assume that $\varphi(u_1^i) = 1$. By Lemma 3, we obtain

$$\begin{gathered}\varphi(u_2^i) = \varphi(u_1^i) = 1,\\ \varphi(v_1^i) = \varphi(v_2^i) = \varphi(p_1^i) = \varphi(v_9^i) = 0.\end{gathered} \tag{3}$$

By Lemma 2 and taking into account (3), we have

$$\varphi(u_9^i) = 1 - \varphi(v_9^i) = 1. \tag{4}$$

From (3) and (4), we get

$$\varphi(v_{13}^i) = \varphi(v_9^i) = 0. \tag{5}$$

By Lemma 2 and taking into account (5), we get

$$\varphi(u_{13}^i) = 1 - \varphi(v_{13}^i) = 1. \tag{6}$$

By Lemma 3 and (6), we have

$$\begin{gathered}\varphi(u_{15}^i) = \varphi(u_{16}^i) = 1,\\ \varphi(v_{15}^i) = \varphi(v_{16}^i) = \varphi(v_{21}^i) = 0.\end{gathered} \tag{7}$$

By Lemma 3 and taking into account (7), we obtain

$$\begin{gathered}\varphi(u_{17}^i) = \varphi(u_{18}^i) = 1.\\ \varphi(v_{17}^i) = \varphi(v_{18}^i) = \varphi(v_{22}^i) = 0.\end{gathered} \tag{8}$$

By Lemma 3 and (8), we have

$$\begin{gathered}\varphi(u_{19}^i) = \varphi(u_{20}^i) = 1,\\ \varphi(v_{14}^i) = \varphi(v_{19}^i) = \varphi(v_{20}^i) = 0.\end{gathered} \tag{9}$$

From (7) and (8), we get

$$\varphi(v_{21}^i) = \varphi(v_{10}^i) = 0. \tag{10}$$

By Lemma 2 and taking into account (10), we obtain

$$\varphi(u_{10}^i) = 1 - \varphi(v_{10}^i) = 1. \tag{11}$$

By Lemma 3 and taking into account (11), we obtain

$$\varphi(u_3^i) = \varphi(u_4^i) = 1,$$
$$\varphi(v_3^i) = \varphi(v_4^i) = \varphi(p_2^i) = 0. \quad (12)$$

From (8) and (9), we get

$$\varphi(v_{11}^i) = \varphi(v_{22}^i) = 0. \quad (13)$$

By Lemma 2 and taking into account (13), we have

$$\varphi(u_{11}^i) = 1 - \varphi(v_{11}^i) = 1. \quad (14)$$

By Lemma 3 and (14), we obtain

$$\varphi(u_5^i) = \varphi(u_6^i) = 1,$$
$$\varphi(v_5^i) = \varphi(v_6^i) = \varphi(p_3^i) = 0. \quad (15)$$

By Lemma 2 and (9), we have

$$\varphi(u_{14}^i) = 1 - \varphi(v_{14}^i) = 1. \quad (16)$$

From (9) and (16), we get

$$\varphi(v_{12}^i) = \varphi(v_{14}^i) = 0. \quad (17)$$

By Lemma 2 and (17), we have

$$\varphi(u_{12}^i) = 1 - \varphi(v_{12}^i) = 1. \quad (18)$$

By Lemma 3 and taking into account (18), we obtain

$$\varphi(u_7^i) = \varphi(u_8^i) = 1,$$
$$\varphi(v_7^i) = \varphi(v_8^i) = \varphi(p_4^i) = 0. \quad (19)$$

By (3), (12), (15) and (19), we have

$$\varphi(p_1^i) = \varphi(p_2^i) = \varphi(p_3^i) = \varphi(p_4^i) = 0.$$

From the proof of Lemma 4, it follows the following result.

Lemma 5. If φ is a *2-partition of a graph* $G = (F_2^i < p_1^i, p_2^i, p_3^i, p_4^i > \cup H)_{E'}$, $\varphi(p_j^i) = \varphi(v_l^i)$ $(1 \le j \le 4, 1 \le l \le 22)$ and $\varphi(u_j^i) = 1 - \varphi(p_1^i)$ $(1 \le j \le 20)$, then $\#[v_j^i]_\varphi = 0$ $(1 \le j \le 22)$, $\#[u_j^i]_\varphi = 0$ $(1 \le j \le 20)$ and $\#[p_j^i]_\varphi = \sum_{w \in \{a\,:\,ap_j^i \in E'\}} \varphi^*(w)$ $(1 \le j \le 4)$.

Problem 2.

Instance: A bipartite graph G with $\Delta(G) = 3$.

Question: Does G has a locally-balanced 2-partition with a closed neighbourhood?

Theorem 6. *Problem 2 is NP-complete.*

Proof. It is easy to see that Problem 4 is NP-complete since a nondeterministic algorithm need only guess a 2-partition of vertices and for each vertex of graph check in polynomial time whether its closed neighbourhood is locally-balanced. For the proof of the NP-completeness, we show a reduction from Problem 1 to Problem 4. Let $\mathcal{I} = (V, C)$ be an instance of Problem 1. We must construct a bipartite graph G, such that G has a locally-balanced 2-partition with a closed neighbourhood if and only if $f(x_1, \dots, x_n) = NAE_3(c_1) \,\&\, \cdots \,\&\, NAE_3(c_k)$ formula is satisfiable. Let us construct a graph G in such a way:

$$V(G) = \left(\bigcup_{i=1}^{n} V\,(F_2^i < p_1^i, p_2^i, p_3^i, p_4^i >)\right) \cup \{q_1, q_2 \dots, q_k\},$$

$$E(G) = \{(p_i^t, q_j)\text{: } 1 \le i \le n, 1 \le j \le k, x_i \in c_j$$

and it is x_i's t-th appearance in the formula}.

It is not hard to see that the graph G can be constructed from V and C in polynomial time, since we used only $46n + k$ vertices. Clearly G is a bipartite graph. Since each clause contains exactly three distinct literals and $\Delta(F_2^i < p_1^i, p_2^i, p_3^i, p_4^i >) = 3$, we have $\Delta(G) = 3$. Suppose $(\beta_1, \dots, \beta_n)$ is a true assignment of $f(x_1, \dots, x_n)$. We show that G has locally-balanced 2-partition with a closed neighbourhood. Let us define a 2-partition φ of G by two steps as follows:

1. For any $\in V(F_2^i < p_1^i, p_2^i, p_3^i, p_4^i >)$ $(1 \le i \le n)$,

$$\varphi(w) = \begin{cases} \beta_i, \ if \ \ w = p_l^i, & where \ 1 \le l \le 4, \\ \beta_i, \ if \ \ w = v_l^i, & where \ 1 \le l \le 22, \\ 1 - \beta_i, \ if \ \ w = u_l^i, & where \ 1 \le l \le 20. \end{cases}$$

2. For any $q_i \in V(G)$ $(1 \le i \le k)$,

$$\varphi^*(q_i) = -\sum_{w \in N_G(q_i)} \varphi^*(w).$$

Let us show, that φ is a locally-balanced 2-partition with a closed neighbourhood. First, let us consider vertices of a subgraph $F_2^i < p_1^i, p_2^i, p_3^i, p_4^i > (1 \le i \le n)$.

Let us consider three cases:

Case 1: $v_l^i \in V(G)$ $(1 \le l \le 22)$

By definition of φ and Lemma 5, we obtain

$$\#[v_l^i]_\varphi = 0.$$

Case 2: $u_l^i \in V(G)$ $(1 \le l \le 20)$

By definition of φ and Lemma 5, we have

$$\#[u_l^i]_\varphi = 0.$$

Case 3: $p_l^i \in V(G)$ $(1 \le l \le 4)$

By definition of φ, Lemma 5 and taking into account, that vertex p_l^i has only one neighbour outside of subgraph $F_2^i < p_1^i, p_2^i, p_3^i, p_4^i >$, we get

$$|\#[p_l^i]_\varphi| \le 1.$$

Now, let us consider the remaining vertices. Let $q_i \in V(G)$ $(1 \le i \le k)$. By definition of φ, we get

$$\varphi^*(q_i) = -\sum_{w \in N_G(q_i)} \varphi^*(w),$$

which implies that

$$\#[q_i]_\varphi = -\sum_{w \in N_G(q_i)} \varphi^*(w) + \sum_{w \in N_G(q_i)} \varphi^*(w) = 0.$$

Conversely, suppose that α is a locally-balanced 2-partition with an open neighbourhood of G. By Lemma 4 we have $\alpha(p_1^i) = \alpha(p_2^i) = \alpha(p_3^i) = \alpha(p_4^i)$. Let us define an assignment of $f(x_1, \dots, x_n)$ as follows: $x_i = \alpha(p_1^i)$ $(1 \le i \le n)$. Let $c_i \in C$ $(1 \le i \le k)$ and $c_i = \{x_{j_1}, x_{j_2}, x_{j_3}\}$. From this and taking into account that $|\#(q_i)_\alpha| \le 1$, $\alpha(p_1^i) = \alpha(p_2^i) = \alpha(p_3^i) = \alpha(p_4^i)$ and $d_G(q_i) = 3$, we obtain

$$NAE_3(x_{j_1}, x_{j_2}, x_{j_3}) = 1,$$

which implies that $f(x_1, \dots, x_n)$ is satisfiable.

For $i_1, l_1, i_2, l_2, i_3, l_3 \in \mathbb{N}$, let us define a graph $F_3^{i_1,l_1,i_2,l_2,i_3,l_3}$ as follows:

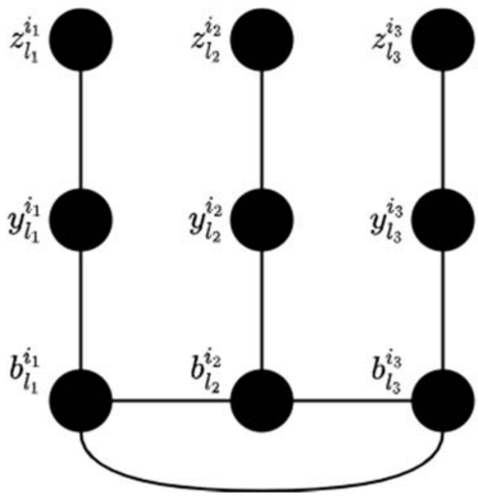


Fig. 3. The graph $F_3^{i_1,l_1,i_2,l_2,i_3,l_3}$.

Problem 3.

Instance: An odd graph G with $\Delta(G) = 3$.

Question: Does G has a locally-balanced 2-partition with a closed neighbourhood?

Theorem 7. *Problem 3 is NP-complete.*

Proof. It is easy to see that Problem 5 is NP-complete since a nondeterministic algorithm need only guess a 2-partition of vertices and for each vertex of graph check in polynomial time whether its closed neighbourhood is locally-balanced. For the proof of the NP-completeness, we show a reduction from Problem 1 to Problem 5. Let $\mathcal{J} = (V, C)$ be an instance of Problem 1. We must construct an odd graph G such that G has a locally-balanced 2-partition with a closed neighbourhood if and only if $f(x_1, \dots, x_n) = NAE_3(c_1) \,\&\cdots\&\, NAE_3(c_k)$ formula is satisfiable. Let us construct a graph G in such a way:

$$V(G) = \left(\bigcup_{i=1}^{n} V\left(F_2^i < p_1^i, p_2^i, p_3^i, p_4^i >\right)\right) \cup \{q_1, q_2 \dots, q_k\}$$

$$\cup \{w\colon \in V(F_3^{i_1,l_1,i_2,l_2,i_3,l_3}), where\ c_j = \{x_{i_1}, x_{i_2}, x_{i_3}\}$$

and it is x_{i_1}'s l_1-th, x_{i_2}'s l_2-th and x_{i_3}'s l_3-th appearances in the formula, $1 \le j \le k\}$,

$$E(G) = \{e, q_j p_{l_1}^{i_1}, q_j p_{l_2}^{i_2}, q_j p_{l_3}^{i_3}, y_{l_1}^{i_1} p_{l_1}^{i_1}, y_{l_2}^{i_2} p_{l_2}^{i_2}, y_{l_3}^{i_3} p_{l_3}^{i_3}\colon e \in E(F_3^{i_1,l_1,i_2,l_2,i_3,l_3}),$$

$where\ c_j = \{x_{i_1}, x_{i_2}, x_{i_3}\}$ and it is x_{i_1}'s l_1-th, x_{i_2}'s l_2-th and x_{i_3}'s l_3-th

appearances in the formula, $1 \le j \le k\} \cup \left(\bigcup_{i=1}^{n} E\left(F_2^i < p_1^i, p_2^i, p_3^i, p_4^i >\right)\right)$.

The graph G has $46n + 10k$ vertices, so it can be constructed from V and C in polynomial time. Clearly, G is a bipartite graph. Since each clause contains exactly three distinct literals, $\Delta(F_2^i < p_1^i, p_2^i, p_3^i, p_4^i >) = 3$, $\Delta(F_3^{i_1,l_1,i_2,l_2,i_3,l_3}) = 3$ and by the construction of G, we have $\Delta(G) = 3$. Suppose $(\beta_1, \dots, \beta_n)$ is a true assignment of $f(x_1, \dots, x_n)$. We show that G has locally-balanced 2-partition with a closed neighbourhood. Let us define a 2-partition φ of G by three steps as follows:

1. For any $w \in V(F_2^i < p_1^i, p_2^i, p_3^i, p_4^i >)$ $(1 \le i \le n)$

$$\varphi(\mathrm{w}) = \begin{cases} \beta_i, \; if \;\; w = p_l^i, & where\ 1 \le l \le 4, \\ \beta_i, \; if \;\; w = v_l^i, & where\ 1 \le l \le 22, \\ 1-\beta_i, \; if \;\; w = u_l^i, & where\ 1 \le l \le 20. \end{cases}$$

2. For any $q_i \in V(G)\ (1 \le i \le k)$

$$\varphi^*(q_i) = -\sum_{w \in N_G(q_i)} \varphi^*(w).$$

3. For any $w \in V(F_3^{i_1,l_1,i_2,l_2,i_3,l_3})\ (1 \le i_1, i_2, i_3 \le n,\ 1 \le l_1, l_2, l_3 \le 4)$

$$\varphi(\mathrm{w}) = \begin{cases} 1-\varphi(q_j), \; if \;\; w = y_{l_t}^{i_t} \; and \; p_{l_t}^{i_t} q_j \in E(G), where\ 1 \le t \le 3,\ \ 1 \le j \le k, \\ \varphi(q_j), \; if \;\; w = z_{l_t}^{i_t} \; and \; p_{l_t}^{i_t} q_j \in E(G), where\ 1 \le t \le 3,\ \ 1 \le j \le k, \\ 1-\varphi(p_{l_t}^{i_t}), \; if \;\; w = b_{l_t}^{i_t} \; and \; p_{l_t}^{i_t} q_j \in E(G), where\ 1 \le t \le 3,\ \ 1 \le j \le k. \end{cases}$$

Let us show that φ is a locally-balanced 2-partition with a closed neighbourhood. First, let us consider vertices of a subgraph $F_2^i < p_1^i, p_2^i, p_3^i, p_4^i > (1 \le i \le n)$.

Let us consider three cases.

Case 1: Let $v_l^i \in V(G)\ (1 \le l \le 22)$

By definition of φ and Lemma 5, we have

$$\#[v_l^i]_\varphi = 0.$$

Case 2: Let $u_l^i \in V(G)\ (1 \le l \le 20)$

By definition of φ and Lemma 5, we get

$$\#[u_l^i]_\varphi = 0.$$

Case 3: Let $p_l^i \in V(G)$ and $(p_l^i, q_j) \in E(G)\ (1 \le l \le 4)$

By definition of φ and Lemma 5, we obtain

$$\#[p_l^i]_\varphi = \varphi^*(q_j) + \varphi^*(y_l^i) = 0.$$

Now, let $q_i \in V(G)$ $(1 \leq i \leq k)$. By definition of φ, we get

$$\varphi^*(q_i) = -\sum_{w \in N_G(q_i)} \varphi^*(w),$$

which implies that

$$\#[q_i]_\varphi = -\sum_{w \in N_G(q_i)} \varphi^*(w) + \sum_{w \in N_G(q_i)} \varphi^*(w) = 0. \qquad (20)$$

Finally, let us consider vertices of a subgraph $F_3^{i_1,l_1,i_2,l_2,i_3,l_3}$ $(1 \leq i_1, i_2, i_3 \leq n,\ 1 \leq l_1, l_2, l_3 \leq 4)$. Let us consider three cases.

Case A: Let $z_{l_t}^{i_t} \in V(F_3^{i_1,l_1,i_2,l_2,i_3,l_3})$ and $p_{l_t}^{i_t} q_j \in E(G)$ $(1 \leq t \leq 3)$

By definition of φ, we get

$$\#[z_{l_t}^{i_t}]_\varphi = \varphi^*(z_{l_t}^{i_t}) + \varphi^*(y_{l_t}^{i_t}) = \varphi^*(q_j) + (-\varphi^*(q_j)) = 0.$$

Case B: Let $y_{l_t}^{i_t} \in V(F_3^{i_1,l_1,i_2,l_2,i_3,l_3})$ and $p_{l_t}^{i_t} q_j \in E(G)$ $(1 \leq t \leq 3)$

By definition of φ, we obtain

$$\#[y_{l_t}^{i_t}]_\varphi = \varphi^*(y_{l_t}^{i_t}) + \varphi^*(z_{l_t}^{i_t}) + \varphi^*(p_{l_t}^{i_t}) + \varphi^*(b_{l_t}^{i_t})$$
$$= -\varphi^*(q_j) + \varphi^*(q_j) + \varphi^*(p_{l_t}^{i_t}) + (-\varphi^*(p_{l_t}^{i_t})) = 0.$$

Case C: Let $b_{l_t}^{i_t} \in V(F_3^{i_1,l_1,i_2,l_2,i_3,l_3})$ and $p_{l_t}^{i_t} q_j \in E(G)$ $(1 \leq t \leq 3)$

By definition of φ and (20), we have

$$\#[b_{l_t}^{i_t}]_\varphi = \varphi^*(b_{l_1}^{i_1}) + \varphi^*(b_{l_2}^{i_2}) + \varphi^*(b_{l_3}^{i_3}) + \varphi^*(y_{l_t}^{i_t})$$
$$= -\varphi^*(p_{l_1}^{i_1}) - \varphi^*(p_{l_2}^{i_2}) - \varphi^*(p_{l_3}^{i_3}) - \varphi^*(q_j) = -\#[q_j]_\varphi = 0.$$

Conversely, suppose that α is a locally-balanced 2-partition with an open neighbourhood of G. By Lemma 4, we have $\alpha(p_1^i) = \alpha(p_2^i) = \alpha(p_3^i) = \alpha(p_4^i)$. Let us define an assignment of $f(x_1, \dots, x_n)$ as follows:

$x_i = \alpha(p_1^i)$ $(1 \le i \le n)$. Let $c_i \in C$ $(1 \le i \le k)$ and $c_i = \{x_{j_1}, x_{j_2}, x_{j_3}\}$. From this and taking into account that $|\#(q_i)_\alpha| \le 1$, $\alpha(p_1^i) = \alpha(p_2^i) = \alpha(p_3^i) = \alpha(p_4^i)$ and $d_G(q_i) = 3$, we obtain

$$NAE_3(x_{j_1}, x_{j_2}, x_{j_3}) = 1,$$

which implies that $f(x_1, \dots, x_n)$ is satisfiable.

REFERENCES

1. *Chartrand G., Zhang P.* Chromatic Graph Theory, Discrete Mathematics and Its Applications. CRC Press (2009).
2. *West D.B.* Introduction to Graph Theory. N.J. Prentice–Hall (2001).
3. *Balikyan S.V., Kamalian R.R.* On-Completeness of the Problem of Existence of Locally – balanced 2- partition for Bipartite Graphs with $\Delta(G) = 3$. Dokl ady NAN RA 105: 1 (2005), 21–27.
4. *Berge C.* Graphs and Hypergraphs. Elsevier Science Ltd (1985).
5. *Ghouila–Houri A.* Caractérisation des matrices totalement unimodulaires, C.R. Acad. Sci . Paris 254 (1962), 1192–1194.
6. *Hajnal A., Szemeredi E.* Proof of a Conj ecture of P. Erdős. Combinatorial Theory and Its Applications. II Proc. Colloq., Balatonfüred (1969). North-Holland (1970), 601–623.
7. *Meyer W.* Equitable Coloring. American Mathematical Monthly, 80: 8 (1973), 920–922.
8. *Kostochka A.V.* Equitable Colorings of Outerplanar Graphs. Discrete Mathematics, 2 58 (2002), 373–377.
9. *Werra de D.* On Good and Equitable Colorings. In Cahiers du C.E. R.O.17 (1975), 417–426.
10. *Kratochvil J.* Complexity of Hyper graph Coloring and Seidel's Switching. Graph Theoretic Concepts in Computer Science, 29th International Workshop, WG 2003, Elspeet, The Netherlands, Revised Papers, 2880 (2003), 297–308.
11. *Gerber M., Kobler D.* Partitioning a graph to satisfy all vertices, Technical report, Swiss Federal Institute of Technology, Lausanne, 1998.

12. *Gerber M., Kobler D.* Algorithmic approach to the satisfactory graph partitioning problem, European J. Oper. Res. 125 (2000), 283–291.
13. *Bazgan C., Tuza Zs., Vanderpooten D.* The satisfactory partition problem, Discrete Applied Mathematics 154 (2006), 1236–1245.
14. *Balikyan S.V., Kamalian R.R.* On-completeness of the Problem of Existence of Locally-balanced 2-partition for Bipartite Graphs with $\Delta(G) = 4$. Under the Extended Definition of the Neighbourhood of a Vertex. Doklady NAN RA, 106: 3 (2006), 218–226.
15. *Balikyan S.V.* On Existence of Certain L ocally-balanced 2-partition of a Tree. Mathematical Problems of Computer Science, 30 (2008), 25–30.
16. *Balikyan S .V, Kamalian R.R.* On Existence of 2-partition of a Tree, which Obeys the Given Priority. Mathematical Problems of Computer Science, 30 (2008), 31–35.
17. *Balikyan S.V.* On locally-balanced 2-partition of some bipartite graphs // Proceedings of the XV international conference "Mathematics. Computing. Education", Dubna, Russia, 2008, 13p.
18. *Gharibyan A.H., Petrosyan P.A.* Locally-balanced 2-partitions of Complete Multipartite Graphs. Mathematical Problems of Computer Science, 49 (2018), 7–17.
19. *Gharibyan A.H.* On Locally-balanced 2-partitions of some classes of graphs, Proceedings of the Yerevan State University, Physical and Mathematical Sciences 54(1) (2020), 9–19.
20. *Darmann A., Döcker J.* On a simple hard variant of Not-All-Equal 3-Sat. Theoretical Computer Science, 815 (2020), 147–152.

ДВЕ NP-ПОЛНЫЕ ЗАДАЧИ О ЛОКАЛЬНО-СБАЛАНСИРОВАННЫХ 2-РАЗБИЕНИЯХ ГРАФОВ

А.Г. Гарибян

АННОТАЦИЯ

2-Разбиением графа G называется функция $f: V(G) \to \{0,1\}$. 2-Разбиение f графа G называется локально-сбалансированным с закрытой окрестностью, если для любой вершины $v \in V(G)$, $\big||\{u \in N_G[v]: f(u) = 0\}| - |\{u \in N_G[v]: f(u) =$

$1\}|\big| \leq 1$, где $N_G[v] = N_G(v) \cup \{v\}$. В настоящей работе доказано, что задача существования локально-сбалансированного 2-разбиения с закрытой окрестностью NP-полна для некоторых классов графов. В частности, доказано, что задача определения: имеет ли данный граф локально-сбалансированное 2-разбиение с закрытой окрестностью, является NP-полной в классе субкубических двудольных графов и нечетных графов максимальной степени 3.

Ключевые слова: локально-сбалансированное 2-разбиение, NP-полнота, двудольный граф, субкубический двудольный граф, нечетный граф.

УДК 004.051 Поступила: 13.08.2020г.
Сдана на рецензию: 17.08.2020г.
Подписана к печати: 09.10.2020г.

POST-OCR CORRECTION OF ARMENIAN TEXTS USING NEURAL NETWORKS

Sh.T. Tigranyan, T.G. Ghukasyan

Ivannikov Laboratory for System Programming at Russian-Armenian University, Yerevan, Armenia

shtigranyan@ispras.ru, tsggukasyan@ispras.ru

ABSTRACT

In this work the problem of post-processing OCR errors for the Armenian language is addressed. We employ a two-step approach to the task: (i) OCR error detection via multilayer perceptron, and (ii) error correction via a convolutional neural network-based sequence transducer. The proposed post-processing methods allow to reduce word error rate of Tesseract OCR by 23.5% on the articles of Soviet-Armenian Encyclopedia, achieving results comparable to commercial solutions.

Keywords: OCR, postprocessing, machine learning.

1. Introduction

Optical character recognition (OCR) is the process of converting handwritten, typewritten or printed text images into machine-readable text. Due to various factors such poor image quality or inaccuracy of OCR tools, a number of errors may occur at different stages of OCR, such as text detection, word boundary detection, character segmentation, character classification. The occurrence of such errors prevents OCR from correctly

recognizing characters, causing spelling errors and obscuring the meaning of the text. Therefore, in tasks where accuracy of textual information is crucial, further post-processing of OCR results is needed before using them.

There are various tools that perform OCR of Armenian-language texts, however few of them are freely available. Tesseract [1] is an open source tool for OCR, which supports many languages, including Armenian. The problem with Tesseract is that its performance declines steeply for low-resolution images or texts with rare fonts, leading to a higher rate of text recognition errors (e.g. ‘ւոեււակը’ instead of ‘տեսակը’; 'փոււից' instead of 'փուլից') in older texts. Manual post-OCR correction of texts requires a lot of time and human resources, thus research is carried out in the direction of automating that work. Considering the presence of a large number of non-digitized literature and other textual resources, the creation of such a tool is of great importance for the Armenian language. Therefore, in this work we attempt to address that problem and explore methods of automating the post-processing step. The proposed methods can be used for the collection and analysis of textual information, in the development of plagiarism detection systems, and computer linguistics.

Following [2], a paper dedicated to OCR post-processing for the English language, we pursue a two-stage solution, developing a separate model for detecting errors and then employing another model for correcting them. In this work, we explored various algorithms both for error detection and error correction task, with the focus on machine learning-based approaches, given their success in related tasks [3][4]. The algorithms are described in detail in Section 2, and Section 3 provides the results of the experiments and their analysis.

2. Models

This section describes the post-processing pipeline for OCR texts. OCR output is first pre-processed to remove line breaks and word wrapping, then its tokens are classified to detect errors, and finally the detected errors are corrected and replaced using an error correction method (Figure 1). The

main tasks, error detection and error correction, are described in detail below.

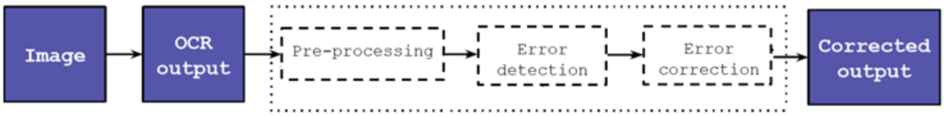


Figure 1. OCR output post-processing steps.

2.1. OCR error detection

The first task is to detect erroneous words among words recognized by OCR. Common erroneous words contain letters of different registers (e.g. ‘բորԲՈՔային’), extra spaces (e.g. ‘Մ ե թ ո դ ա կ ա ն’), more than one consecutive character ‘ւ’ (this character usually occurs only after character ‘ո’), misclassification of similar-looking characters (e.g. ‘պա-տերազմի’).

Dictionary lookup: As baseline solution for the first task dictionary lookup was used. To implement this algorithm, a dictionary was built on the basis of texts from the Armenian Wikipedia, news articles and fiction [5]. In this method, a token was considered erroneous if it was not present in the dictionary and considered correct otherwise.

Naïve Bayes: Using word unigram and character n-grams (n = 1, 2, 3) as features, we trained a multinomial Naïve Bayes classifier[1] which classifies a word being erroneous (1) or not (0).

MLP: To classify the words, we also trained MLP with two hidden layers and 128 neurons in each layer. For MLP, the same features were used as in Naïve Bayes.

[1] https://scikit-learn.org/stable/modules/generated/sklearn.naive_bayes.MultinomialNB.html

2.2. OCR error correction

The second task is the correction of the erroneous words detected in the first task. We explored 3 methods for this task: a dictionary lookup baseline based on Levenshtein distance, attentional encoder-decoder, and a simpler convolutional neural network-based sequence transducer.

Dictionary Lookup: For this algorithm, we built a word-frequency dictionary, using the same corpus as in error detection. For each erroneous word, the algorithm performed the following steps:

1. The Levenshtein editing distance between this word and each word in the dictionary was calculated.
2. The word with the minimum distance was returned as a correction; if there were more than one such word, the most common word was returned.

In addition, we also separately constructed and tested a word bigram-based dictionary lookup. This was motivated by the presence of examples, where the token was incorrectly separated by a space or the space was missing between two tokens.

Sequence-to-sequence: We explored the possibility of using Transformer [6], an attentional encoder-decoder model, to correct OCR errors as sequence-to-sequence task. The input sequence were the characters of the detected erroneous token, and the character sequence of its correction were the output of the decoder. To implement and train the network, we used OpenNMT-tf sequence learning toolkit [7]. The size of input and output dictionaries was limited to 150 characters, with shared 32-dimensional embeddings.

Rybak et al.: During experiments, as the initial results of Transformer were unsatisfactory and also taking into account the time and resources required for its proper hyperparameter tuning and training, we opted for a simpler sequence transduction model based on a convolutional neural network, using the architecture from [8]. Originally developed for lemmatization, we thought [9] would also adapt well for this task, considering the similar nature of them. In this model, each input erroneous word was represented as a character-based word vector using a dilated

convolutional neural network and a trainable word-level vector. To get the final features, both word representations were concatenated and fed into biLSTM. Dimensionality of the features was reduced with a single fully connected layer (FCL). The output of the FCL was fed into the dilated CNN, final layer of which computed the probabilities of one-hot encoded characters of the corrected word.

The full list of the hyperparameters of neural networks is provided in Appendix A.

3. Experiments

3.1. Dataset

As a dataset for this task, we used the scanned pages and their transcriptions from the Armenian Soviet Encyclopedia[2], available under the digitization project held by Armenian Wikisource. The choice of this source for the dataset was determined primarily by the availability of scanned images of its articles and proofread and corrected versions of them. This source was also fitting for our experiments, because of its old-fashioned font and page structure which presented a challenge for OCR.

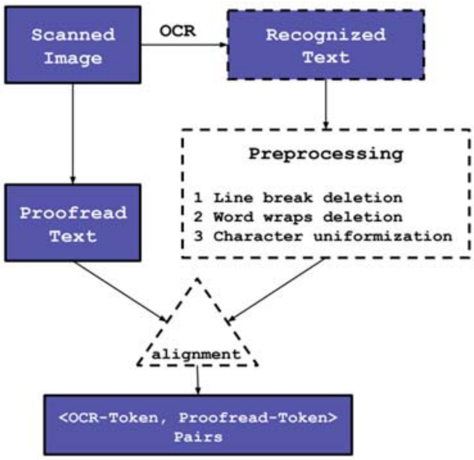


Figure 2. Dataset generation scheme.

[2] https://hy.wikisource.org/wiki/Կատեգորիա:Սրբագրված_ինդեքս

To generate datasets for training and evaluation, we applied OCR to the scanned images of the articles and aligned the output to the proofread versions (Figure 2). In the first step of dataset generation, we extracted texts from scanned images using Tesseract[3] and then applied some pre-processing.

During pre-processing, for each extracted text, the following changes were made:

1. **Line breaks deletion**

   Line breaks were deleted both in the original and recognized texts.

2. **Word wrap removal**

   In accordance with the rules of word wrapping in Armenian, the letter ‘ը’ may appear in a wrapped word. If the letter ը appears before the hyphen or the part of the word before the hyphen has the form (one or more letters) ը (consonant), then the letter ը is also deleted, in other cases the letter ը remains since we have no information, whether this letter was in word before word wrapping or not. For example, the word ‘ջը-րանցքը’ after word wrap deletion will have the following form ‘ջրանցքը’, the word ‘շըր-ջանի’ becomes ‘շրջանի’, and the word ‘մտահըղա-ցում’ becomes ‘մտահղացում’.

3. **Character uniformization**

   When extracting texts, the same punctuation mark can be extracted in different forms. For example, a hyphen in different parts of the text has a different length. All variants of the same mark were brought to the same form using homoglyphs[4] library.

Then, to align the tokens in original and extracted texts we used git diff terminal function. Based on the output of the function, we were able to generate a dataset consisting of 2.2 million <OCR token; proofread token> pairs (matching pairs were labeled with 1, and the rest with 0). Erroneous samples comprised approximately 20% of the dataset. The dataset was randomly divided into training (80%), validation (10%) and test (10%) sets,

[3] https://pypi.org/project/pytesseract/
[4] https://pypi.org/project/homoglyphs/

so that the ratio of data by classes was maintained. The same split was used across error detection and error correction tasks. For the latter, we employed only the pairs that contained errors.

When training neural networks for the problem of error correction, difficulties arose due to the presence of “hard” samples such as extracted words whose originals were in a foreign language, tokens containing numbers, punctuation error, words containing many letter errors. To facilitate network learning, samples of the above types were either filtered out or simplified. Neural networks were trained and validated only on this cleaned set, but all models were tested on both cleaned and full sets.

3.2. Results and Discussion

Table 1.

Performance of Error Detection Models

Model	Accuracy	Precision	Recall	F-1
Dictionary lookup	87.6%	69.5%	69.4%	69.4%
Naïve Bayes	89.0%	73.3%	74.2%	73.8%
MLP	95.2%	95.8%	80.0%	87.5%

Error detection: To evaluate the performance of developed models we used accuracy, precision, recall, and F-1. The results of the described models for error detection task are provided in Table 1. Dictionary-based baseline and Naïve Bayes classifier demonstrated relatively lower precision, which in the case of the former might be possible to improve with expanded vocabulary.

The best result was achieved by MLP, which produced 95.8% precision and 80.0% recall. This means that on average only 1 out of 20 predicted errors was actually error-free. Looking at the false negatives, around 15% represented cases of a punctuation mark being misrecognized as another (‘.’ instead of ‘,’), which the classifier failed to detect. Among

the remaining false negatives, 36.6% were tokens containing uppercase letters (e.g. ‘իՆԱՄԱԿԱԼՈՒԹՅՈՒՆ’, ‘օրՈք’, ‘Ճյուղը’ etc), some of which could be captured with additional feature engineering. It should also be noted that many of the misclassified tokens were correct words when taken in isolation.

Table 2.

Performance of error correction models

Model	Accuracy on cleaned test set	Accuracy on full test set
Dictionary lookup	22.00%	12.10%
Dictionary lookup (bigrams)	25.35%	13.81%
Rybak et al.	21.62%	17.48%

Error correction: Rybak et al. neural network produced the highest accuracy overall on this task (Table 2). However, on cleaned example set, its performance was matched (or in case of bigrams outperformed) by the dictionary lookup baseline. After 20000 training steps, Transformer managed to achieve only 6.95% development accuracy, after which the training was discontinued.

On the full test set, the best result was 17.48%. To better understand the cause of this seemingly low accuracy, we examined the test samples. For over 35% of the test set, OCR token and its proofread version had a Levenshtein distance higher than 5. For these samples, the error correction accuracy was lower than 5% (Figure 3). It should be noted that many of the samples contained numerous misrecognized characters and would be challenging to correct even for human experts. Examples of such samples from the test set are given in Table 3. Therefore, we believe the quality of OCR has a serious limiting effect on the overall potential of post-processing methods. Adding context information can potentially help with some of

these examples, however effective mechanisms of encoding context would be required.

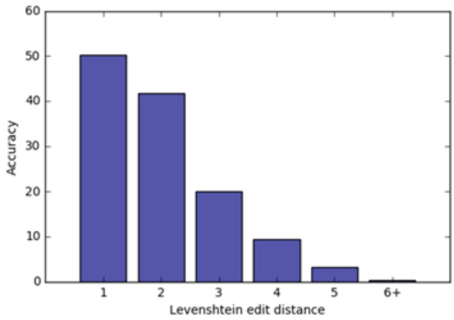


Figure 3. The accuracy of Rybak et al. error correction model based on edit distance between OCR token and its proofread version.

Extracted word	Original word
զադոյթացւււմը	գաղութացումը
սնոտդատությունը	քննադատությունը
աւզեցոդծուրլամբ	այգեգործությամբ
նախազնԻհել	նախագահել
գրււեամեյլենանկ	գրահամեքենաեն
<րամարվեւդվ	Հրաժարվելով
տիռաւթննոիռ	տիրույթներից
ոլոլիմերլւ	պոլիմերը
ռաոիոկգայնությանյյ	ռադիոզգայնությունը
առււնյլնացնում	առանձնացնում

Table 3. Examples of "hard" samples.

Comparison with other OCR tools: To analyze the effect of the developed post-processing methods on the quality of text, on randomly selected 100 articles we computed the average word-error rate (WER[5]) between proofread text and OCR output before and after applying post-processing. The combination of best performing models was used for post-processing: MLP for error detection and Rybak et al. for error correction. The average WER score without post-processing was 0.51, but with post-processing it improved by 23.5%, decreasing to 0.39 on average. Figure 4 and 5 illustrate a sample OCR output before and after correction.

We also compared the results with several other OCR tools, both free and commercial (Table 4).

[5] https://en.wikipedia.org/wiki/Word_error_rate

Table 4.

Performance of Tesseract with post-processing against other tools

OCR tool	WER	Access
Convertio	0.27	Commercial
ABBYY FineReader	0.54	Commercial
Google Docs	1.10	Free
Tesseract	0.51	Free
Tesseract + post-processing	0.39	Free

With the developed post-processing methods, Tesseract achieved the highest score, except for a commercial product Convertio[6]. It is worth noting that even without post-processing, Tesseract was able to match the word-error rate of a commercial product like ABBYY FineReader[7]. The result of Google Docs[8] OCR was surprisingly low, and a closer look at its output revealed that the low score was caused by its inability to read text columns correctly.

Հայերը (34 ընտանիք) գաղթել են Էրզրումի գավառի Նորշեն գյուղից , 1830-ին : Մ. Դարբինյան ԾՂԱԼՏՈՒԲՈ , քաղաք Վրացական ՍՍՀ Ծղալտուբոյի շրջանում , Մեծ Կովկասի հարավային նախալեռներում , Քութայիսից 12 կմ հյուսիս-արևմուտք : 17 hq. բն. (1974) : Բալնեոլոգիական առողջարան է : Բուժիչ միջոցները տաք (32 - 396) . թույլ հանքայնացված , ռադոնային աղբյուրներն են ՚ ազոտի բարձր պարունակությամբ : բուժվում են հոդերի , ...
ԾՂԱԿ , Ծ ղ կ ա մ , գյուղ Արևմտյան Հայաստանի Բիթւիսի վիւայեթի խւաթ գավառում , Վանա լճի հյուսիս-արևմտյան ափին : 1909-ին ուներ 60 տուն (496 շունչ) հայ բնակիչ : Զբաղվում էին երկրագործությամբ և անասնապահությամբ : Ուներ եկեղեցի (Ս . Թեոդորոս) և վարժարան : ...

Հայերը (34 ընտանիք) գաղթել են Էրզրումի գավառի Նորշեն գյուղից , 1830-ին : Մ. Դարբինյան ԾՂԱԼՏՈՒԲՈ , քաղաք Վրացական ՍՍՀ Ծղալտուբոյի շրջանում , Մեծ Կովկասի հարավային նախալեռներում , Քութայիսից 12 կմ հյուսիս-արևմուտք : 17 hq. բն. (1974) : Բալնեոլոգիական առողջարան է : Բուժիչ միջոցները տաք (32 - 396) . թույլ հանքայնացված , ռադոնային աղբյուրներն են ՝ ազոտի բարձր պարունակությամբ : բուժվում են հոդերի , ...
ԾՂԱԿ , Ծ ղ կ ա մ , գյուղ Արևմտյան Հայաստանի Բիթլիսի վիլայեթի Խլաթ գավառում , Վանա լճի հյուսիս-արևմտյան ափին : 1909-ին ուներ 60 տուն (496 շունչ) հայ բնակիչ : Զբաղվում էին երկրագործությամբ և անասնապահությամբ : Ուներ եկեղեցի (Ս . Թեոդորոս) և վարժարան : ...
ԾՂՈՏ , հացազգի և թիթեռնածաղկավոր բույսերի չոր

[6] https://convertio.co/
[7] https://www.abbyy.com/ru/finereader/
[8] https://docs.google.com/

ԾՂՈՏ , հացազգի և թիթեռնածաղկավոր բույսերի չոր ցողունը , որ մնում է հասունացած սերմը կամ ՝ ունդը հեռացնելուց հետո : Օգտագործվում է որպես կեր : Լինում են աշնանացան և գարնանացան , հացազգի ու թիթեռնածաղկավոր տարբեր տեսակի բույսերի (ցորենի . գարու , եգիպտացորենի , տարեկանի , վարսակի , սոյայի ևն) Ծ-ներ : Ծ-ի քիմ. կազմը և սննդարարությունը կախված են բույսի տեսակից. կլիմայից , հողից , պահպանման Ժամկետից և այլ պայմաններից : Ծ. պարունակում է շատ քիչ պրոտեին , ճարպ , հանքային նյութեր և վիտամիններ. սակայն հարուստ է թաղանթանյութով (ՏՏ - ՀՏՀ) : Ծ-ի սննդարարությունն ավելացնելու նպատակով այն մշակում են կաուստիկ սոդայի , չհանգած կրի , կարբիդային շւամի լուծույթներով և շոգեխաշում բարձր ճնշման տակ :

Figure 4. OCR output without post-processing, with errors displayed in blue.

ցողունը , որ մնում է հասունացած սերմը կամ ՝ ունդը հեռացնելուց հետո : Օգտագործվում է որպես կեր : Լինում են աշնանացան և գարնանացան , հացազգի ու թիթեռնածաղկավոր տարբեր տեսակի բույսերի (ցորենի . գարու , եգիպտացորենի , տարեկանի , վարսակի , սոյայի ևն) Ծ-ներ : Ծ-ի քիմ. կազմը և սննդարարությունը կախված են բույսի տեսակից , կլիմայից , հողից , պահպանման Ժամկետից և այլ պայմաններից : Ծ. պարունակում է շատ քիչ պրոտեին , ճարպ , հանքային նյութեր և վիտամիններ , սակայն հարուստ է թաղանթանյութով (ՏՏ - ՀՏՀ) : Ծ-ի սննդարարությունն ավելացնելու նպատակով այն մշակում են կաուստիկ սոդայի , չհանգած կրի , կարբիդային շլմմի լուծույթներով և շոգեխաշում բարձր ճնշման տակ :

Figure 5. OCR output after post-processing, with undetected errors displayed in blue and detected but wrongly corrected errors in purple.

Table 5.

The hyperparameters of the MLP model used in error detection task.

Hyperparameter		**Value**
optimizer	batch size	64
	optimizer	Adam
	beta1	0.9
	beta2	0.999
	epsilon	1e-7
	learning rate	0.01
number of hidden layers		2
hidden layers’ activation function		ReLU
number of units in hidden layers		128
number of units in output layer		1
output layer’s activation function		Sigmoid

Table 6.

The hyperparameters of the encoder-decoder neural network used in error correction task.

Hyperparameter		**Value**
optimizer	batch size	4
	optimizer	Adam
	beta1	0.8
	beta2	0.998
	train_steps	20000
	learning rate	0.01
layers		[**“encoder”** : {“layer1” : “Multi-head self-attention", “layer2” : “Dense”, “number of units” : 32, “number of heads in multi-head self-attention" : 8, “Dense inner dimension” : 32, “dropout” : 0.1}, **“decoder”**: {“layer1” : “Multi-head self-attention", “layer2” : "Dense”, “layer 3” : “Multi-head self-attention", “number of units” : 32, “number of heads in multi-head self-attention" : 8, “Dense inner dimension” : 32, “dropout” : 0.1 }]
dropout		0.3
input dictionary size		150
output dictionary size		150
embedding_size		32
maximum_features_length		30
maximum_labels_length		30

Table 7.

The hyperparameters of Rybak et al. neural network used in error correction task.

Hyperparameter		**Value**
optimizer	batch size	100
	optimizer	Adam
	beta1	0.9
	beta2	0.9
	epsilon	1e-4
	learning rate	0.002
layers		default*
dropout		0.25
trained word-level embedding size		10

*https://github.com/360er0/COMBO

4. Conclusion

In this work, we developed a two-stage post-processing solution for rectifying OCR errors in Armenian-language texts. We implemented a multilayer perceptron that with high precision detects OCR errors, and then applied a convolutional neural network-based sequence transducer to correct detected errors. The presented methods were tested on the articles of Soviet-Armenian Encyclopedia, and helped reduce the word-error rate of Tesseract OCR by 23.5%, outperforming some of the commercial products available.

REFERENCES

1. *Smith R.* An overview of the Tesseract OCR engine // Ninth international conference on document analysis and recognition (ICDAR 2007). IEEE, 2007. V. 2. PP. 629–633.
2. *Khirbat G.* OCR post-processing text correction using simulated annealing (OPTeCA) //Proceedings of the Australasian Language Technology Association Workshop 2017. PP. 119–123.
3. *Amrhein C., Clematide S.* Supervised ocr error detection and correction using statistical and neural machine translation methods // Journal for Language Technology and Computational Linguistics (JLCL). 2018. V. 33. №. 1. PP. 49–76.
4. *Mokhtar K., Bukhari S.S., Dengel A.* OCR Error Correction: State-of-the-Art vs an NMT-based Approach //2018 13th IAPR International Workshop on Document Analysis Systems (DAS). IEEE, 2018. PP. 429–434.
5. *Avetisyan K., Ghukasyan T.* Word embeddings for the Armenian language: intrinsic and extrinsic evaluation // «Вестник Российско-Армянского университета: сер.: физико-математические и естественные науки». 2019. №. 1. PP. 59–72.
6. *Vaswani A., Shazeer N., Parmar N., Uszkoreit J., Jones L., Gomez N A., Kaiser L., Polosukhin I.* Attention is all you need //Advances in Neural Information Processing Systems. 2017. PP. 6000–6010.

7. *Klein G. et al.* OpenNMT: Open-Source Toolkit for Neural Machine Translation // Proceedings of ACL 2017, System Demonstrations. 2017. PP. 67–72.
8. *Rybak P., Wróblewska A.* Semi-Supervised Neural System for Tagging, Parsing and Lematization //Proceedings of the CoNLL 2018 Shared Task: Multilingual Parsing from Raw Text to Universal Dependencies. 2018. PP. 45–54.
9. Ibid. PP. 45–54.

ПОСТОБРАБОТКА ОШИБОК OCR В ТЕКСТАХ НА АРМЯНСКОМ ЯЗЫКЕ ПРИ ПОМОЩИ НЕЙРОННЫХ СЕТЕЙ

Ш. Тигранян, Ц. Гукасян

АННОТАЦИЯ

В данной научной статье рассматривается проблема постобработки ошибок OCR для армянского языка. Был применен двухэтапный подход к задаче: (i) обнаружение ошибок распознавания с помощью многослойного персептрона и (ii) исправление ошибок с помощью преобразователя последовательности на основе сверхточной нейронной сети. Предложенные методы постобработки позволяют уменьшить количество ошибок в словах из статей «Армянской советской энциклопедии», распознанных Tesseract OCR, на 23.5%, достигая результатов, сравнимых с коммерческими решениями данной задачи.

Ключевые слова: OCR, постобработка, машинное обучение.

УДК 517.968.4 Сдана на рецензию: 26.11.2020г.
Подписана к печати: 01.12.2020г.

О РАЗРЕШИМОСТИ ОДНОЙ СИСТЕМЫ БЕСКОНЕЧНЫХ АЛГЕБРАИЧЕСКИХ УРАВНЕНИЙ С ВЫПУКЛОЙ НЕЛИНЕЙНОСТЬЮ И С МАТРИЦАМИ ТЕПЛИЦА-ГАНКЕЛЯ

А.А. Сисакян

Армянский Национальный Аграрный университет

sisakyan64@mail.ru

АННОТАЦИЯ

В данной научной статье исследуется система нелинейных бесконечных алгебраических уравнений с матрицами типа Теплица-Ганкеля. Указанная система возникает в дискретных задачах динамической теории p-адических открыто-замкнутых струн. Доказывается существование нетривиальных неотрицательных решений в пространстве ограниченных последовательностей. В конце работы приводятся конкретные примеры указанных систем, имеющие приложения в теории p-адических струн.

Библиография: 5 наименований.

Ключевые слова: нелинейность, выпуклость, матрица Теплица-Ганкеля, монотонность, итерации.

§ 1. Введение и формулировка основного результата

В настоящей работе исследуется следующая система бесконечных алгебраических уравнений с монотонной и выпуклой нелинейностью:

$$Q(x_n) = \sum_{j=0}^{\infty}\left(a_{n-j} - a_{n+j}\right)\lambda_j x_j, \ \ n \in \mathbb{Z}^+ := \mathbb{N} \cup \{0\} \qquad (1)$$

относительно искомого бесконечного вектора$x = (x_0, x_1, \dots, x_n, \dots,)^T$, ($T$ – знак транспортирования). В системе (1) последовательность $\{a_n\}_{n=-\infty}^{\infty}$ удовлетворяет следующим условиям:

1) $a_i > 0, \ i \in \ \mathbb{Z}, \sum_{j=-\infty}^{\infty} a_j = 1$ (условие консервативности),

2) $a_{i+1} < a_i, \ i = 0,1,2, \dots$ (условие монотонности),

3) $a_j = a_{-j}, \ j = 0,1,2, \dots$ (условие симметричности),

4) $\sum_{j=0}^{\infty} ja_j < +\infty$ (условие конечности первого момента).

Последовательность $\{\lambda_j\}_{j=0}^{\infty}$ обладает следующими свойствами:

a) $\lambda_j \geq 1, j = 0,1,2, \dots$,

b) $\sum_{j=0}^{\infty}(\lambda_j - 1) < +\infty$.

Введем следующую величину:

$$M := \ a_0 \sum_{j=0}^{\infty} \ (\lambda_j - 1) < +\infty.$$

Функция Q описывает нелинейность системы (1) и удовлетворяет условиям:

A) Q – такая непрерывная определенная на $\mathbb{R}^+ := [0, \infty)$ функция, что уравнение $Q(u) = (1 + M)u$ имеет решение в $(0, \infty)$.

B) Q – монотонно возрастающая на отрезке $[0, \xi]$, где число $\xi > 0$ является первым положительным корнем уравнения $Q(u) = (1 + M)u$.

C) Q – выпуклая вниз функция на отрезке $[0, \xi]$, причем $Q(0) = 0$,

D) существует число $\eta > 0$ такое,что $Q(\eta) = \eta$.

Система (1), кроме чисто теоретического интереса, имеет приложение в динамической теории p-адических открыто-замкнутых струн для скалярного поля тахионов (см. [1]–[3]). Такие системы встречаются также в дискретных задачах в математической биологии (см. [4]). В частном случае, когда

$$\lambda_j = 1, \qquad (j = 0,1,2, \dots), \qquad Q(u) = au^p + (1 - a)u,$$

где $a \in (0,1]$, $p > 2$ – нечетное число, система (1) и ее двумерный аналог достаточно подробно был исследован в работе [3]. Следует отметить, что соответствующий непрерывный аналог данной системы был исследован в недавней работе Х.А. Хачатряна (см. [5]).

В настоящей статье при условиях 1)-4), a)-b) и A)–D) докажем существование нетривиального неотрицательного и ограниченного решения системы (1), а также исследуем некоторые качественные свойства построенного решения. В конце работы приведем частные примеры функции Q, имеющие прикладной характер.

Основным результатом настоящей работы является следующее:

Теорема. *При условиях 1)–4),a),b) и A)–D) система (1) обладает неотрицательным нетривиальным решением* $x = (x_0, x_1, \dots, x_n, \dots)^T$ *в пространстве ограниченных последовательностей, причем* $x_n \leq \xi, n = 0,1, \dots$ *. Более того,*

$$\sum_{n=0}^{\infty} |\eta - x_n| < +\infty .$$

§ 2. Доказательство основного результата

Доказательство сформулированной выше теоремы разобьем на следующие шаги.

Шаг I. *Априорные оценки.* Сначала заметим, что из условий 2)–3) сразу следует, что

$$a_{n-j} \geq a_{n+j}, \quad n, j = 0,1,2, \dots, \tag{2}$$

С другой стороны, из свойств A)–D) функции Q вытекает существование числа $\varepsilon \in (0,1)$ такого, что функциональное уравнение $Q(u) = \varepsilon u$ имеет положительное решение η_0, причем

$$\eta_0 < \eta < \xi. \tag{3}$$

Для фиксированного $q > 1$ рассмотрим следующее характеристическое уравнение:

$$\sum_{j=-\infty}^{\infty} a_j q^{-p|j|} = \frac{1+\max(a_0, \ \varepsilon)}{2} \tag{4}$$

относительно переменной $p > 0$. Так как в силу условия 1):

$$0 < a_0 < 1, \tag{5}$$

то нетрудно проверить, что функция

$$\chi(p) = \sum_{j=-\infty}^{\infty} a_j q^{-p|j|} - \frac{1+\max(a_0,\ \varepsilon)}{2}. \tag{6}$$

удовлетворяет следующим условиям:

- $\chi \in C(\mathbb{R}^+)$,
- $\chi(0) = \frac{1-\max(a_0,\ \varepsilon)}{2} > 0$,
- $\chi(+\infty) = \lim\limits_{p\to\infty} \chi(p) = a_0 - \frac{1+\max(a_0,\ \varepsilon)}{2} < 0$,
- $\chi \downarrow$ на $\mathbb{R}^+$.

Следовательно, согласно теореме Больцано-Коши, существует единственное положительное решение p_0 уравнения (4). В силу леммы 11 работы [3] имеем следующую оценку снизу:

$$\sum_{j=0}^{\infty}(a_{n-j} - a_{n+j})(1 - q^{-p_0 j}) \geq \frac{1+\max(a_0,\ \varepsilon)}{2}(1 - q^{-p_0 n}),$$
$$n = 0,1,2,\dots . \tag{7}$$

Отметим, что оценка (7) будет играть важную роль в наших дальнейших рассуждениях.

Так как очевидно $\varepsilon < \frac{1+\max(a_0,\ \varepsilon)}{2} < 1$, то в силу условий на функцию Q, уравнение $Q(u) = \frac{1+\max(a_0,\varepsilon)}{2}u$, кроме тривиального решения $u = 0$, имеет также положительное решение ξ_0 – такое, что

$$\eta_0 < \xi_0 < \eta < \xi, \tag{8}$$

при этом

$$Q(u) \leq \frac{1+\max(a_0,\varepsilon)}{2}u, \quad u \in [0, \xi_0]. \tag{9}$$

Шаг II. *Об одной вспомогательной системе*. Наряду с системой (1), рассмотрим следующую систему нелинейных бесконечных алгебраических уравнений:

$$Q(\tau_n) = \sum_{j=0}^{\infty}\big(a_{n-j} - a_{n+j}\big)\tau_j, \quad n \in \mathbb{Z}^+. \tag{10}$$

относительно искомого бесконечного вектора

$$\tau = (\tau_0, \tau_1, \dots, \tau_n, \dots)^T.$$

Введем следующие итерации:

$$Q\left(\tau_n^{(p+1)}\right) = \sum_{j=0}^{\infty} (a_{n-j} - a_{n+j}) \tau_j^{(p)}, \ \ n \in \mathbb{Z}^+, \qquad \tau_n^{(0)} = \eta, \ \ p = 0,1,2,\dots \tag{11}$$

Индукцией по p с применением оценок (9), (7) и (2) можно доказать, что

$$\tau_n^{(p)} \downarrow \text{по} \, p, \tag{12}$$

$$\tau_n^{(p)} \geq \xi_0 (1 - q^{-p_0 n}), \ \ n \in \mathbb{Z}^+, p \in \mathbb{Z}^+. \tag{13}$$

Следовательно, последовательность бесконечных векторов

$$\tau^{(p)} := (\tau_0^{(p)}, \tau_1^{(p)}, \dots, \tau_n^{(p)}, \dots)^T, \qquad p \in \mathbb{Z}^+$$

имеет предел при $p \to \infty$: $\lim\limits_{p\to\infty} \tau_n^{(p)} = \tau_n$, причем

$$\xi_0 (1 - q^{-p_0 n}) \leq \tau_n \leq \eta. \tag{14}$$

Ввиду непрерывности функции Q двойного неравенства (14) и условия 1), заключаем, что предельный вектор удовлетворяет системе (10).

Индукцией также можно проверить, что

$$\tau_n^{(p)} \uparrow \text{по} \, n, \ \ p \in \mathbb{Z}^+. \tag{15}$$

Следовательно, имеет место

$$\tau_{n+1} \geq \tau_n. \tag{16}$$

Обозначим через $\alpha := \lim\limits_{n\to\infty} \tau_n$. Переходя к пределу в обеих частях (10), когда $n \to \infty$ и при этом, учитывая (14) и условия A)–D), приходим к равенству $Q(\alpha) = \alpha$, где $\alpha > 0$, из которого следует, что $\alpha = \eta$.

Проводя рассуждения, аналогичные содержащимся в работе [3], можно доказать, что

$$\sum_{n=0}^{\infty} (\eta - \tau_n) < +\infty. \tag{17}$$

Шаг III. *Последовательные приближения для системы* (1). Рассмотрим для системы (1) следующие итерации:

$$Q\left(x_n^{(p+1)}\right)=\sum_{j=0}^{\infty}(a_{n-j}-a_{n+j})\lambda_j x_j^{(p)},\ \ n\in\mathbb{Z}^+,$$
$$x_n^{(0)}=\tau_n,\ \ p=0,1,2,\dots . \tag{18}$$

Учитывая условие a), неравенство (2) и монотонность функции Q, индукцией по p несложно убедиться, что

$$x_n^{(p)} \uparrow \text{ по } p. \tag{19}$$

Ниже убедимся, что

$$x_n^{(p)} \le \xi, \quad p, n \in \mathbb{Z}^+. \tag{20}$$

При $p = 0$ неравенство (20) сразу следует из (14) и (8). Предположим, что $x_n^{(p)} \le \xi,\ n \in \mathbb{Z}^+$ при некотором натуральном p. Тогда в силу A) и B) из (18) будем иметь

$$Q\left(x_n^{(p+1)}\right) \le \xi \sum_{j=0}^{\infty}(a_{n-j} - a_{n+j})\,\lambda_j \le \xi \sum_{j=0}^{\infty} a_{n-j} +$$
$$+\xi \sum_{j=0}^{\infty}(a_{n-j} - a_{n+j})\,(\lambda_j - 1) \le \xi + \xi\, a_0 \sum_{j=0}^{\infty}(\lambda_j - 1) =$$
$$= (1 + M)\xi = Q(\xi),$$

из которого следует, что $x_n^{(p+1)} \le \xi$.

Итак, в силу (19), (20) последовательность бесконечных векторов $x^{(p)} := (x_0^{(p)}, x_1^{(p)}, \dots, x_n^{(p)}, \dots)^T, p \in \mathbb{Z}^+$ имеет предел, когда $p \to \infty$: $\lim\limits_{p\to\infty} x_n^{(p)} = x_n$, причем

$$\tau_n \le x_n \le \xi,\ n \in \mathbb{Z}^+. \tag{21}$$

Так как $\sum_{j=0}^{\infty}(a_{n-j} - a_{n+j})\lambda_j \le 1 + M,\ n \in \mathbb{Z}^+$, то из (21) и условия A) следует, что $x = (x_0, x_1, \dots, x_n, \dots)^T$ является решением системы (1).

Шаг IV. *Сходимость ряда* $\sum_{n=0}^{\infty}|\eta - x_n|$. Для завершения доказательства сформулированной теоремы остается проверить сходимость ряда $\sum_{n=0}^{\infty}|\eta - x_n| < +\infty$. Сначала заметим, что из (14), (17) и (21) следует существование натурального числа $n_0 \in \mathbb{N}$ – такого, что при $n \ge n_0$

$$x_n \ge x_n^{(p)} \ge \tau_n \ge \frac{\eta}{2}. \tag{22}$$

Введем следующие числовые множества:

$$A_p \coloneqq \left\{n\colon\ n \geq n_0\,,\ x_n^{(p)} \leq \eta\right\},\ B_p \coloneqq \{n\colon\ n \geq n_0,\ x_n^{(p)} > \eta\}. \quad (23)$$

По аналогии, с доказательством теоремы (1) работы [5] можно убедиться, что существует число $c > 0$ – такое, что

$$\sum_{n\in A_p} (x_n^{(p+1)} - \tau_n) + \frac{\tau_{n_0} - Q(\tau_{n_0})}{\eta - \tau_{n_0}} \sum_{n\in B_p} (x_n^{(p+1)} - \tau_n) \leq c + 2\sum_{n=0}^{\infty}(\eta - \tau_n). \quad (24)$$

Из (24), в частности, следует, что

$$\min\left\{1,\ \frac{\tau_{n_0} - Q(\tau_{n_0})}{\eta - \tau_{n_0}}\right\} \sum_{n=n_0}^{\infty} \left(x_n^{(p+1)} - \tau_n\right) \leq c + 2\sum_{n=0}^{\infty}(\eta - \tau_n) \quad (25)$$

или

$$\sum_{n=n_0}^{\infty} \left(x_n^{(p+1)} - \tau_n\right) \leq \frac{c + 2\sum_{n=0}^{\infty}(\eta - \tau_n)}{\min\left\{1, \frac{\tau_{n_0} - Q(\tau_{n_0})}{\eta - \tau_{n_0}}\right\}} \quad (26)$$

Из (26) вытекает, что

$$\sum_{n=0}^{\infty} |x_n - \tau_n| < +\infty. \quad (27)$$

В силу (27), (17) и неравенства треугольника

$$|\eta - x_n| \leq |\eta - \tau_n| + |x_n - \tau_n|$$

приходим к сходимости ряда $\sum_{n=0}^{\infty} |\eta - x_n|$.Теорема доказана.

§ 3. Примеры

В конце работы приведем несколько примеров прикладного характера для функции Q и последовательностей $\{\lambda_j\}_{j=0}^{\infty}$, $\{a_n\}_{n=-\infty}^{\infty}$, удовлетворяющих всем условиям доказанной теоремы.

Примеры функции Q:

I) $Q(u) = u^p, p > 2$ – нечетное число, $u \geq 0$.

II) $Q(u) = au^p + (1 - a)u, u \geq 0$, где $a \in (0,1]$ – числовой параметр.

III) $Q(u) = \ln\frac{\gamma}{\gamma - u}, u \in [0, \gamma)$, где $\gamma \gg 1$ – числовой параметр.

Примеры последовательностей $\{\lambda_j\}_{j=0}^{\infty}$ и $\{a_n\}_{n=-\infty}^{\infty}$:

- $\lambda_j = 1 + \frac{1}{(j+1)^q}$, где $q > 1$ − произвольное число.

- $\lambda_j = 1 + \frac{2^j}{j!}$.
- $a_n = c_0 a^{-|n|}, a > 1, c_0 = \frac{a-1}{a+1}, n \in \mathbb{Z}$.
- $a_n = \frac{1}{2e-1} \cdot \frac{1}{|n|!},\ n \in \mathbb{Z}$.

В конце отметим, что системы с нелинейностью II) возникают в теории p-адической струны, а нелинейности вида III) – в дискретных задачах математической теории пространственно-временного распространения эпидемии (см. [3], [4]).

Автор выражает благодарность своему научному руководителю д.ф.-м.н., профессору Х.А. Хачатряну за постановку задачи и полезные советы при выполнении работы.

ЛИТЕРАТУРА

1. *Владимиров В.С., Волович И.В.* О нелинейном уравнении динамики в теории p-адической струны, ТМФ, Т. 138, № 3 (2004), 355–368.
2. *Владимиров В.С.* О нелинейных уравнениях p-адических открытых, замкнутых и открыто-замкнутых струн, ТМФ. Т. 149, № 3 (2006), 354–367.
3. *Khachatryan Kh.A., Andriyan S.M.* On the Solvability of a Class of Discrete Matrix Equations with Cubic Nonlinearity, Ukrainian Mathematical Journal, vol. 71, № 12 (2020), 1910–1928.
4. *Хачатрян А.Х., Хачатрян Х.А.* О разрешимости некоторых нелинейных интегральных уравнении в задачах распространения эпидемии // Труды МИАН. Т. 306 (2019), 287–303.
5. *Хачатрян Х.А.* О разрешимости некоторых нелинейных граничных задач для сингулярных интегральных уравнении типа свертки // Труды ММО. Т. 81, № 1(2020), 3–40.

ON THE SOLVABILITY OF ONE SYSTEM OF INFINITE ALGEBRAIC EQUATIONS WITH CONVEX NONLINEARITY AND WITH TOEPLITZ-HANKEL MATRICES

A. Sisakyan

ABSTRACT

In this note, a system of nonlinear infinite algebraic equations with matrices of the Toeplitz-Hankel type is studied. This system arises in discrete problems of the dynamic theory of p-adic open-closed strings. The existence of non-trivial non-negative solutions in the space of bounded sequences is proved. At the end of the work, specific examples of these systems are given which have applications in the theory of p-adic strings.

Bibliography: 5 items.

Keywords: nonlinearity, convexity, Toeplitz-Hankel matrix, monotonicity, iteration.

ФИЗИКО-ТЕХНИЧЕСКИЕ НАУКИ

УДК 621.396.67

Поступила: 15.09.2020г.
Сдана на рецензию: 23.09.2020г.
Подписана к печати: 14.10.2020г.

ПРОГРАММА ДЛЯ КОМПЬЮТЕРНОГО МОДЕЛИРОВАНИЯ СВЧ АНТЕННЫХ СИСТЕМ

В.А. Варданян, А.А. Шмавонян, А.И. Тимотин

Российско-Армянский университет
Инженерно-физический институт

v.vardanyan00@gmail.com, arthurshmavonyan@gmail.com, timotin95@gmail.com

АННОТАЦИЯ

В данной научной статье речь идет о времени разработки СВЧ узлов, где важную роль играет математическое моделирование. Значительную часть времени разработки занимает создание 3D-модели СВЧ-узла. Для уменьшения этого времени была проделана работа по написанию программы, производящей расчеты геометрических параметров антенной решетки из заданных частотных характеристик. Так же проделан расчет амплитудного распределения напряжений с последующей симуляцией с помощью взаимодействия программных пакетов.

Ключевые слова: программирование, СВЧ, антенна, моделирование.

Введение

При проектировании СВЧ узлов и антенных решеток, в частности, до получения конечного результата устройство должно пройти следующие этапы разработки: синтез геометрических параметров, определение электрических характеристик антенны на основе теоретических данных, создание 3D-моделей, симуляция и создание опытного образца. Синтез геометрических параметров и создание модели могут занять существенную часть времени. Для уменьшения этого времени используются программы, автоматизирующие процесс синтеза и моделирования. Существующие программы не предоставляют значительной гибкости в проектировании, так как имеют ограниченное количество предустановленных моделей антенн и функций распределения.

Нашей задачей является разработка алгоритма автоматизации синтеза и построения антенной решетки на примере щелевой антенной решетки.

Основное содержание работы

Процесс расчета и моделирования представляет собой стандартную, отработанную схему, которая не требует больших изменений. Соответственно, для ее выполнения можно разработать алгоритм автоматизации. Программа состоит из следующих частей: графического интерфейса, блока расчета параметров волновода, построения геометрии волновода, расчета весовой функции, расположения щелей.

В программном пакете FEKO присутствует возможность написания подпрограмм на языке Lu a.[1]. FEKO дает возможность использования предустановленных функций для создания, редактирования и изменения моделей, переменных, создания графических интерфейсов, а также использование уже готовых моделей.

В качестве примера моделирования была выбрана щелевая антенная решетка [2–3]. Для нее была написана подпрограмма, рассчитывающая и создающая 3D-модель на основе введенных параметров частоты, коэффициента усиления, ширины волновода, глубины волновода и толщины стенок. Для удобства ввода данных был разработан графический интерфейс (Рис. 1).

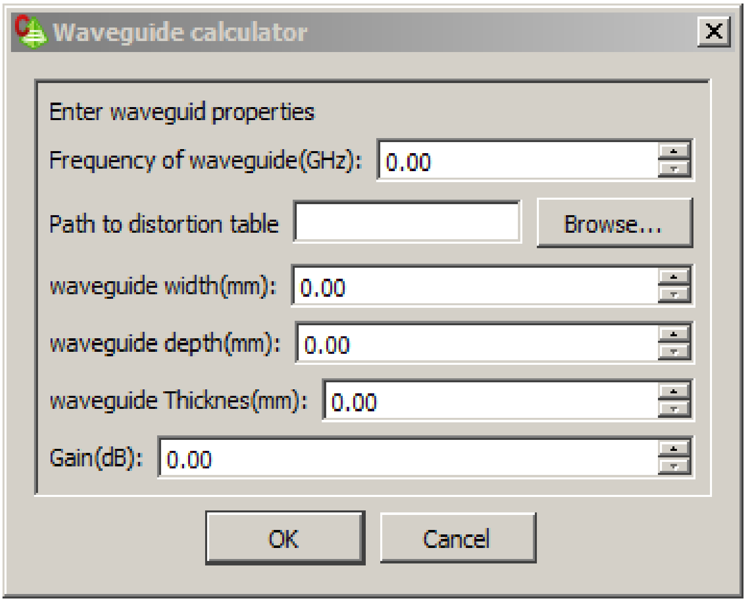


Рис.1. Графический интерфейс.

Антенные решетки обладают высокими параметрами направленности, однако их можно улучшить при использовании функции взвешивания. В нашем случае функция взвешивания применялась к расстоянию от центральной оси волновода до щели (Рис. 2).

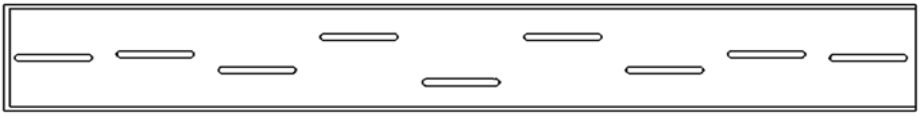


Рис. 2. Схема щелевой антенной решетки.

Подпрограмма работает по следующему алгоритму: после ввода исходных данных они записываются в переменные, затем, на основание КУ и частоты, вычисляется количество щелей и длина волновода. Щели располагаются на широкой стенке волновода с удалением от его центральной оси, согласно выбранному распределению.

Существует множество функций распределения. Они влияют на электрические параметры антенны, приводят к сужению основного лепестка диаграммы направленности, а также к уменьшению боковых лепестков. Нами была выбрана функция Ханна (1).

$$\boldsymbol{\omega(n) = 0.5\left(1 - cos\left(\frac{2\pi n}{N-1}\right)\right)} \qquad (1)$$

где n – номер элемента, а N – количество элементов. Ее распределение и частотный отклик показаны на Рис. 3.

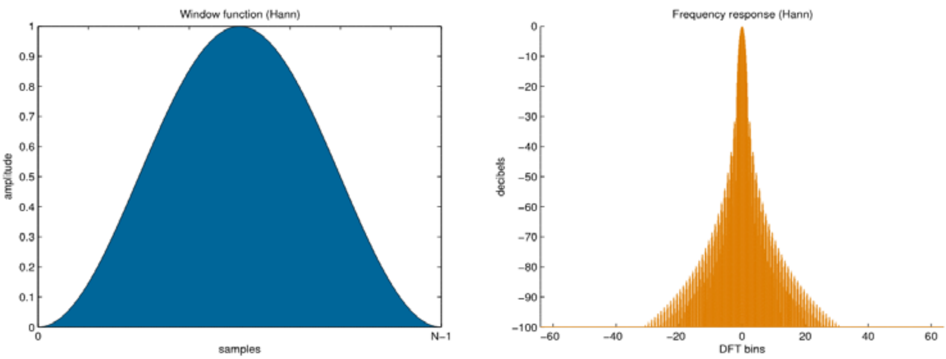


Рис. 3. Функция Ханна.

С помощью написанного нами скрипта была рассчитана щелевая антенная решетка, на частоте 10 ГГц и КУ (коэффициент усиления) 5дБи у выбранного нами волновода широкая стенка была равна 23 мм, а узкая стенка – 10 мм, толщина –2 мм.

Исходя из заданного КУ и частоты, была рассчитана высота, количество щелей, их ширина и длина. Далее расстояние между центральной осью и щелями было перемножено на весовые коэффициенты функции Ханна (Рис. 4).

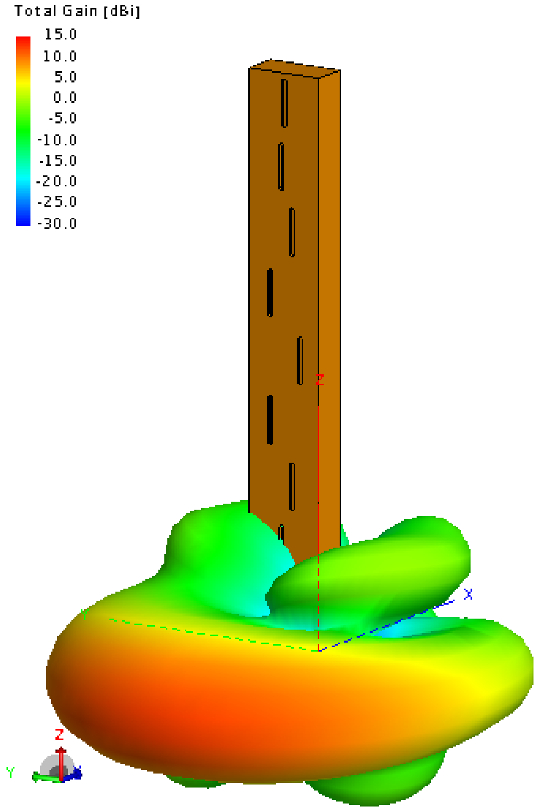


Рис. 4. Полученная щелевая антенная решетка.

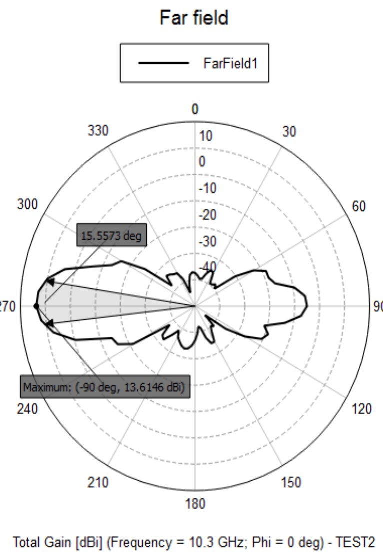


Рис.5. Полученная диаграмма направленности.

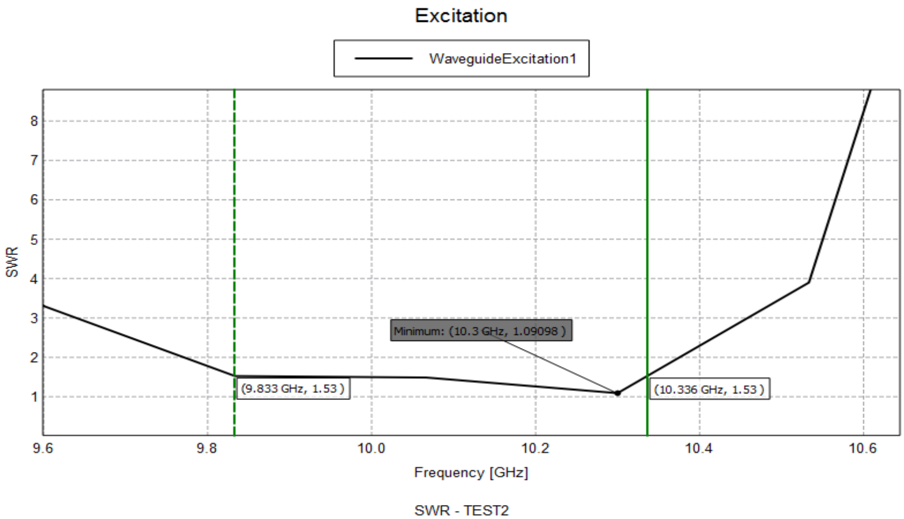


Рис. 6. КСВ в диапазоне 9,6ГГц до 10,4ГГц.

Высота полученной щелевой антенной решетки равняется 176 мм, при количестве щелей равном 9. Симуляция проводилась в диапазоне от 8,9 ГГц до 11ГГц. Наилучшие параметры были зафиксированы на частоте 10,3 ГГц. Согласно полученной диаграмме направленности, ширина основного лепестка равна 15,5 градусам (Рис. 5). КУ, при этом, равно 13,6 дБи. КСВ в диапазоне 9,833ГГц – 10,336 ГГц не превышает 1,53, а на частоте 10,3 ГГц достигает 1,09 (Рис. 6).

Заключение

В данной работе был разработан алгоритм для реализации вопросов, связанных с моделированием и расчетом антенных решеток. Предложенный нами метод решил вопрос автоматизации процесса построения модели щелевых антенных структур. Для улучшения характеристик направленности антенной решетки была использована весовая функция. Благодаря нашему методу удалось сократить время разработки, а также упростить процесс моделирования.

ЛИТЕРАТУРА

1. *Воскресенский Д.И.*Антенны и устройства СВЧ. Проектирование фазированных антенных решеток.1981.107с.
2. *Хармуш А., Радван Д.Б., Зиадех М.* Волноводно-щелевая антенна на согнутом прямоугольном волноводе – T-Comm – Телекоммуникации и Транспорт. 50с.
3. https://www.altairuniversity.com/wp-content/uploads/ 2015/03/ UserManual.pdf.User'sManualSuite 7.0 2014. EMSoftware&Systems-S.A. (Pty) Ltd, 281.

SOFTWARE FOR COMPUTER SIMULATION OF MICROWAVE ANTENNA SYSTEMS

V.Vardanyan, A. Shmavonyan, A.Timotin

Russian-Armenian University
Institute of Engineering and Physics

v.vardanyan00@gmail.com, arthurshmavonyan@gmail.com, timotin95@gmail.com

ABSTRACT

Mathematical modelling plays a vital role in RF device development. Specifically, a large portion of the development time is allocated to creating a 3D model of the device in question. A software solution was found that allows reducing the time overhead associated to modelling, by computing the geometrical parameters of the antenna array based on provided frequency characteristics numerically.Additionally, using appropriate software packages the voltage amplitude distributions were evaluated and subsequently simulated.

Keywords: programming, UFH, antenna, modeling.

УДК 536.7

Поступила: 08.06.2020г.
Сдана на рецензию: 08.06.2020г.
Подписана к печати: 14.06.2020г.

DIFFUSION OF DECENTRAL STATIONARY ENERGY STORAGES

L. Tadevosyan

Russian-Armenian University

mrvosyan@gmail.com

ABSTRACT

Followed by the growth of fluctuating renewable energies, the utility grid demands bigger energy storage possibilities to ensure a stable energy supply. Therefore, the need of decentral stationary energy storages in the form of electrochemical batteries is increasing. The following paper addresses decentralized stationary energy storages (DSES) as an innovation. It establishes the situation of decentral stationary energy storage in Sweden based on an observation using the Charles Edquist system. Characteristics of potential adopters are pointed out, and the Rogers model of decision making is applied to the case of DSES, from persuasion until implementation and confirmation. Finally, the paper suggests five measures in order to spread the use of DSES in Sweden.

Keywords: diffusion, renewable energy, decentralized, stationary energy storage, DSES, Rogers model.

Introduction

The energy market is changing. To mitigate global warming, it is necessary to reduce the emission of greenhouse gases. A solution is the

increasing use of renewable energy. However, the fluctuating nature of renewable resources like sun and wind leads to time differences between availability and demand of electrical energy. Therefore, the energy has to be stored [1]. This is currently happening in big hydroelectric facilities (dams) and combusted air storages. In the future, electrochemical storage can gain more importance as *decentral* energy storage. This is because of decentral stationary energy storages (DSES) impact on the efficiency of the electrical power grid. As the energy demand on the customer-site is evened out by the DSES, the utility sector can concentrate on providing a steady flow of energy. Production capacities can be lower, and the reduction of ramping power plants up and down increases their lifespan [2].

As it has been pointed out, storing the energy is a crucial part of the energy cycle. This is also shown by the recent growth in the electricity storage market [3]. By 2030, the investments in the energy storage market are estimated to be approximately 35 billion US Dollar [4]. Almost half of those investments are expected to be directed to electrochemical batteries like sodium-sulphur, redox-flow and lithium-ion technology.

Currently the main technology for home batteries on the market is lithium-ion. This is because of high energy density, long cycle life and good safety as well as reliability. Those attributes are paid by a relatively high price per kWh. The available products range between 2 to 18 kWh in size with an average price of 800 US Dollars per kWh [5]. A downside of the use of this technology is the scarcity of the resource lithium, which will become harder to produce in the future [6]. Possible increases in lithium production will not satisfy the demand of a revolution in automotive propulsion and of the battery industry in the next decade. Future lithium-based batteries with organic electrodes, solid electrolytes or sodium instead of lithium could decrease the high cost [7].

Other technologies are on the rise but are not yet ready for the market. Sodium sulphur, which is already used in utility scale applications in Japan, could be applied in home batteries. This requires the working temperature of 300° C to be lowered and the safety issues to be resolved. Another promising technology is redox flow, which works with two separate liquids

as electrodes. The main advantage of this technology is the good scalability. Unfortunately, the redox-flow technology is only available in prototypes. An unsolved problem for all types of batteries is pollution, because of the lack of recycling possibilities for the often-hazardous parts of the battery [8].

After understanding the advantages and disadvantages of the technologies that are currently presented in the market, we need to find out how this diffusion can be accelerated.

2. Diffusion Analysis

2.1. Definition

The decentral stationary energy storage is a technological aspect of a process innovation. It is a new type of battery as an improvement to the processes of the utility grid [9]. It should be taken into account that our innovation is an iteration of already existing batteries, the nature of the innovation is sustaining and evolutionary. Indeed, since the beginning of the solar panel market, there has been a demand for home batteries to use off the grid [10]. The innovation is not frugal, as it is relatively expensive [11] [12]. The changes of the innovation are mainly technological in the micro perspective while there are no changes on the marketing level [13]. We conclude that DSES is located somewhere between the development and the diffusion and commercialisation stage in Rogers's model of innovation, because even though there are some products already available, further development is needed to spread the innovation [14].

Next, we have observed the system of the stationary battery innovation according to Charles Edquist [15]. For boundaries, we focus on the geographical and political borders of Sweden, first and foremost because the innovation of home batteries is not yet established in the Swedish market [16]. The Swedish society has a strong interest in nature and a solid knowledge about climate change. Although the Swedish electricity production is already mostly CO_2 neutral, production capacity of the nuclear power plants will be changed to renewables in the long term for reasons of

clear energy [17]. Because of our chosen geological location, the laws of Sweden as well as the European Union pose as our judicial boundaries. Moreover, we focus on the sectors of energy and building. In the system of innovation there are several actors, for example users (e.g. utility companies, property developer, private consumers, and architects), politics (legislators, government), researchers (universities, companies), the battery industry and financial investors.

The function of our system is to improve the diffusion of home batteries in Sweden in order to secure the stability and improve the efficiency of the electrical power grid.

2.2. Application of the Theory of Decision-Making

As stated by Roger, adopters are to be divided into five different groups: innovators, early adopters, early majority, late majority and laggards. The focus of the change agent should lie on the second group of people, as they are the most important one. We have singled out different attributes for the special groups [18].

According to the Roger's model, innovators require a shorter adoption period, are venturesome, mobile, risk takers, apply complex technical knowledge to cope with a high degree of uncertainty and have a higher status.

We look for our innovators in the young technical elite. They are aware of the problem of climate change and are excited to try new technical solutions for this problem. They have enough money to put in risky investments. They supposedly live in urban areas and are highly educated, usually in the area of engineering. They are between 25 and 40 years old, likely have no kids and are working on their careers. The main usage would be in summerhouses or similar off-grid situations.

Early adopters are a bigger user group than innovators. They have an upward social mobility, a greater degree of opinion leadership and are successful and respected by peers. For early adopters we look for upper middle-class families in suburban or rural areas with own property. They are between 50 and 70 years old, with an optional background in science or

engineering. At their point in life, they are earning the most in their career, and their children are starting to sustain themselves. This leads to a situation when they are financially independent [20]. They should have already invested in solar panels as they would understand the benefit from storing the energy of their solar panels.

2.3. Application of the Model on different adopters

Decision-making, according to the Rogers consumer innovation-decision process, is a long process and takes time. We chose to apply Rogers model because it has a broader coverage than similar models.

2.3.1. Knowledge Stage

The first stage in the innovation-decision process is the knowledge stage. In this stage the potential adopter needs to be informed about the availability, handling and principles of the innovation. To find the first potential users of the DSES technology, one has to create awareness about the product for as many people as possible. This can be done with mass media channels like newspapers, TV, internet and social media. After a first impression, people will ideally share the DSES technology by word of mouth.

The second is the how-to knowledge. The change agent should provide a platform of knowledge about the battery which is easy to access and to use. A good webpage on the internet will work for both innovators and early adopters.

Furthermore, principle knowledge about the innovation has to be established. This means showing the basic principles of the innovation. The principles of the electrochemical processes in batteries can be complicated and not easy to understand. Nevertheless, principle knowledge about the basic operation of the home battery can be communicated to a broad audience.

We have to be aware of selective perception and selective retention because every group/individual has their own way of interpreting mass

media. You should present the DSES technology to every group/individual in a different way.

2.3.2 Persuasion Stage

In the persuasion stage, the consumers are forming an opinion about the product. Although the advantages of the product for the society are easy to understand, the possibilities for the private customer are not obvious. As DSES is preventing *future* blackouts and ensuring *future* energy security, it is a preventive innovation. Its biggest benefits are therefore uncertain, while the customer needs to direct time and energy to the adoption. Furthermore, side effects of the increasing use of batteries are not well known. Therefore, we expect the diffusion to be slower than average innovations. Nonetheless, there are several relative advantages of DSES compared to not investing in the technologies.

It is important that the early adopters see an economic motivation in adopting the DSES, especially given that the DSES is an expensive product. However, saving money is not possible with the current prices for electric energy and batteries [21]. Although the Swedish government is supporting the economic factor by giving subsidies, the economic advantage is still not high enough for broader parts of the society [22].

Another relative advantage of the DSES technology is to avoid blackouts and consequently avoid an increase in discomfort. This effect can be seen in developing countries like India, where power outages are more common than in the western world. There, home battery systems diffuse more rapidly and are already used by big parts of the society to provide energy in the hours without electricity from the grid [23].

Furthermore, the possibility to keep the solar- or wind-power self-produced energy and to be therefore self-sustaining can influence the decision in favour of DSES.

It is crucial for home batteries to be compatible with the utility grid, solar panels as well as with smaller regional grids or for self-consumption [24]. A home battery is as easy to install as other electronic devices in the household and thus consumer-friendly (low installation cost).

Although a small-scale trial option is not technically possible, the potential adopters could be inspired by the village of Simris in southern Sweden. In this 160-household village, the community is using a combination of wind-power and solar cells together with DSES [25].

As the chemical process in the battery is not visible, the observability has to be ensured in another way. We propose a good design, which introduces the possibility to install it in a prominent place (e.g. living room, front yard) instead of a utility room in the basement. This adds to the social prestige of the owner as well as creates awareness knowledge with the peers. Moreover, a direct usage as a power bank and the display of battery load through an app or a display are improving the relationship to DSES by an immediate reward.

Besides the characteristics of the innovation, it can be helpful to create positive emotions for DSES with the customer. This can be done by using a strong brand. For example, entrepreneur Elon Musk is using the name of his company Tesla to draw attention for his home battery product.

2.3.3. Decision Stage

The persuasion leads to the decision stage which is the moment where an individual will adopt or reject an SES.

The innovation-decision process can lead to rejection in every part of the process. There are two types of rejection, "active" and "passive". The first one is an active decision of not adopting the DSES innovation after a trial period or after gaining knowledge about the functions as well as advantages and disadvantages. Secondly, "non-adoption" (passive rejection) is about an individual who never knew the innovation [26].

2.3.4. Implementation Stage

After a positive decision, in the implementation stage the user puts one's theoretical decision into practice. During this stage many questions may arise e.g. how to obtain the innovation or how to solve maintenance problems. The change agent has to make sure that the DSES is available for the customer as well as to provide technical assistance and information.

In our case, the implementation will be fast, if we can ensure a good availability. That is because of the easy installation in the existing home grid. As private individuals will use the decentralised SES, the problems of implementation have to be solved by the selling/diffusing company [27].

2.3.5. Confirmation Stage

In the last stage of the innovation-decision process, the consumers check for confirmation. They check if the product is still relevant for them. For example, it might be too expensive to maintain DSES in the future (price for one kWh stored increasing). Furthermore, the adopters of the DSES innovation need some supportive messages to avoid dissonance and to reinforce the decision they have made about the innovation. Such messages are coming with the feedback from other users or from research, but mainly from the declining electricity bill of the adopter.

Once the DSES is adopted, we do not expect a high risk of discontinuance. Provided the product is working fine, it will do its job in the background and not force a second decision about rejecting it.

3. Discussion

In conclusion, DSES technology is still in its infancy, but its importance is growing fast. Although current technology shows many flaws, the research for solutions is promising. Sweden has a high potential to introduce DSES and could therefore avoid the disadvantages of the restructuring of the electrical energy production. After applying the Rogers Model of innovation-decision to our innovators and early adopters, we propose five measures that can accelerate the diffusion of DSES in Sweden.

First, it is necessary to support research about batteries, concerning a decrease in price and the independency from lithium. Another important question is the recycling of used batteries.

Second, the DSES product can be improved in product development by adding new functionalities (e.g. smartphone application, display, direct use).

Thirdly, it is important to acquire knowledge about the belief system of the innovators and early adopters in order to adjust the marketing to their needs and values. With more advertising and mass media coverage it is possible to create awareness knowledge with innovators and early adopters. Furthermore, prototype usage in micro grid villages can demonstrate and distribute how-to knowledge.

In addition to that, more subsidies are needed at the moment, to convince a broader audience to adopt the innovation.

As a last resort, law can regulate home batteries. For example, the government could apply a new legislation by which newly built houses are required to have DSES.

REFERENCES

1. *Kosowatz J.* (2018) Energy storage smooths: The duck curve. Mechanical Engineering, 140(6). PP. 30–35.
2. *Dunn, Bruce, Kamath, Haresh & Tarascon, Jean-Marie* (2011) Electrical energy storage for the grid: a battery of choices. (Author abstract). Science, 334 (6058). PP. 928–935.
3. *Deluzarche C.* (2018) Un an après... les batteries résidentielles de Tesla commencent à décoller (#rediff). [online] Clubic.com. Available at: https://www.clubic.com/pro/entreprises/tesla/actualite-804604-an-batteries-residentielles-tesla-commencent-decoller.html [Accessed 19 Oct. 2018].
4. *Global Market Insights I.* (2018) Stationary Batter Storage Market to cross $35bn by 2030: Global Market Insights, Inc. [online] GlobeNewswire News Room. Available at: https://globenewswire.com/news-release/2018/06/07/1518190/0/en/Stationary-Battery-Storage-Market-to-cross-35bn-by-2030-Global-Market-Insights-Inc.html [Accessed 19 Oct. 2018].
5. *Matasci S.* (2018) 2018 Solar Battery Review: Sonnen, Tesla, Aquion, LG Chem | EnergySage. [online] Solar News. Available at: https://news.energysage.com/tesla-powerwall-vs-sonnen-eco-vs-lg-chem/ [Accessed 20 Oct. 2018].
6. Planetoscope.com. (2018) Planetoscope – Statistiques: Production mondiale de lithium. [online] Available at: https://www.planetoscope.com/matieres-

premieres/671-production-mondiale-de-lithium.html [Accessed 21 Oct. 2018].
7. *Dunn, Bruse, Kamath, Haresh & Tarascon, Jean-Marie* (2011) Electrical energy storage for the grid: a battery of choices. (Author abstract). Science, 334(6058). PP. 928–935.
8. *Zhang, W. et al.* (2018) 'A review on management of spent lithium ion batteries and strategy for resource recycling of all components from them', Waste Management & Research, 36(2). PP. 99–112. doi: 10.1177/0734242X17744655.
9. *Rogers, E.* (2003). Diffusion of innovations. New York: Free Press.
10. Baker Home Energy. (2018) San Diego Energy Storage. [online] Available at: https://www.bakerhomeenergy.com/home-battery/san-diego-energy-storage#off [Accessed 4 Oct. 2018].
11. En.wikipedia.org (2018) Frugal innovation. [online] Available at: https://en.wikipedia.org/wiki/Frugal_innovation [Accessed 19 Oct. 2018].
12. *Prabhu J., Ahuja S., Radjou N. and Roberts K.* (2013) Jugaad innovation. San Francisco, Calif.: Jossey-Bass.
13. *Garcia R. and Calantone R.* (2002) A critical look at technological innovation typology and innovativeness terminology: a literature review. Journal of Product Innovation Management, 19 (2). PP. 110–132.
14. *Rogers E.* (2003) Diffusion of innovations. New York: Free Press.
15. *Edquist Ch.* Reflections on the systems of innovation approach, Science and Public Policy, Volume 31, Issue 6, 1 December 2004. Pages 485–489.
16. Renewableenergyworld.com (2018) Sweden Set to Launch Residential Energy Storage Scheme. [online] Available at: https://www.renewableenergyworld.com/articles/2016/10/sweden-set-to-launch-residential-energy-storage-scheme.html [Accessed 19 Oct. 2018].
17. Nordic Energy Technology Perspectives 2016.
18. *Rogers E.* (2003) Diffusion of innovations. New York: Free Press Page 36.
19. *Rogers E.* (2003) Diffusion of innovations. New York: Free Press Page 248.
20. *Rogers E.* (2003) Diffusion of innovations. New York: Free Press Page 217.
21. *Dzikowski R.and Olek B.,* Capacity sharing – Economic analysis of home battery systems," 2017 14th International Conference on the European Energy Market (EEM), Dresden, 2017. PP. 1–5.
22. Renewableenergyworld.com (2018). Sweden Set to Launch Residential Energy Storage Scheme. [online] Available at:

https://www.renewableenergyworld.com/articles/2016/10/sweden-set-to-launch-residential-energy-storage-scheme.html [Accessed 19 Oct. 2018].
23. Anon 2012. Blackout nation; India's infrastructure. The Economist (US), 404(8796), P.11.
24. *Vivint Solar*. (2018). Everything You Need to Know About Home Batteries | Vivint Solar. [online] Available at: https://www.vivintsolar.com/blog/everything-you-need-to-know-about-home-batteries [Accessed 21 Oct. 2018].
25. Thelocal.se. (2018). Green Sweden to get its first energy self-sufficient village. [online] Available at: https://www.thelocal.se/20170119/sweden-to-get-its-first-energy-self-sufficient-village [Accessed 19 Oct. 2018].
26. *Rogers E.* (2003) Diffusion of innovations. New York: Free Press Page 177–179.
27. *Rogers E.* (2003) Diffusion of innovations. New York: Free Press Page 177–179.

РАСПРОСТРАНЕНИЕ ДЕЦЕНТРАЛИЗОВАННЫХ СТАЦИОНАРНЫХ НАКОПИТЕЛЕЙ ЭНЕРГИИ

Л. Тадевосян

АННОТАЦИЯ

В данной научной статье рассматриваются децентрализованные стационарные накопители энергии (ДСНЭ), акцентируя внимание на них как на нововведении. Вслед за ростом колебаний возобновляемых источников энергии энергосистема требует больших возможностей хранения энергии для обеспечения стабильного энергоснабжения, поэтому возрастает потребность в децентрализованных стационарных накопителях энергии в виде электрохимических батарей. В статье описывается ситуация с ДСНЭ в Швеции на основе наблюдений с использованием системы Чарльза Эдквиста. Выделяются также характеристики потенциальных потребителей, и модель принятия решений Роджерса применяется в случае ДСНЭ, от убеждения до внедрения и подтверждения. Наконец, в статье предлагается ряд мер по распространению использования ДСНЭ в Швеции.

Ключевые слова: диффузия, возобновляемые источники энергии, децентрализованый, стационарные накопители энергии, ДСНЭ, модель Роджерса.

УДК 621.3.049.77 Поступила: 26.04.2020г.
Сдана на рецензию: 06.05.2020г.
Подписана к печати: 18.05.2020г.

METHOD OF INCREASING CURRENT DAC LINEARITY WITH CONSIDERING ITS RANDOM VARIABLES FOR MODELLING RISK OR UNCERTAINTY

A. Atanesyan[1], M. Grigoryan[2], H. Margaryan[2], H. Aghayan[2], G. Hakobyan[2]

[1]Institute of Radiophysics and Electronics,
[2]Synopsys Armenia Educational Department

atanesya@synopsys.com, manvelg@synopsys.com, hmargar@synopsys.com, haghayan@synopsys.com, garikh@synopsys.com

ABSTRACT

In this article the method of increasing current DAC linearity by taking into account modeling risk and uncertainty impact on circuit is presented. The main idea of the method is to distribute DNL error over all codes and to decrease DNL for critical codes. The method shows significant improvement and DAC performing properly even for 4.5 sigma. The main disadvantage of this method is output voltage range decrease.

Keywords: digital to Analog converter, DNL, INL, Monte Carlo, 4.5 sigma.

Introduction

Nowadays digital to analog converters (DAC) and analog to digital converters (ADC) are commonly used in modern integrated circuits. The

degradation of performance parameters of DACs and ADCs can cause total errors in integrated circuit operating. To avoid this kind of problems, a great number of solutions have been suggested. Yet in most cases because of linearity parameters improvement other parameters have degradation: for example, area increase or high-power consumption.

The approach discussed in this article is aimed to avoid degradation of other parameters while increasing the linearity of DACs and ADCs. And only minor parameters are injured.

The DAC overviewed in this paper is designed to cancel offset between differential legs of circuits. Regardless of matching technique in layout, technological variations cause an offset between differential legs of circuits which can decrease the system's performance. There are used techniques with comparator and current DAC circuits which cancel offset for differential legs by calibrating offset after producing chip and using current of DAC. In this way offset has been decreased to a minimal step of current DAC (LSB). To achieve the necessary performance, the current DAC must provide the needed linearity. In case where linearity is poor, some current values will be unachievable.

For all known types of DACs and ADCs the least significant bit (LSB) is the smallest measurement unit. LSB is the average voltage increment for digital code step sensible for DAC and ADC. For the N-bit converter LSB definition is given in the formula below [1]:

$$\boldsymbol{LSB} = \frac{V_{2n-1} - V_0}{n^2} \tag{1}$$

where n^2 is the number of steps in total and V_0 and V_{2n-1} are the output voltage range produced by the converters.

The ADC and DAC linearity are summarized with two parameters: integral nonlinearity (INL) and differential nonlinearity (DNL) the measure unit of which is LSB.

For k bit DNL and INL are given by the formulas below [2, 3]:

$$\boldsymbol{DNL} = \frac{V_{i+1} - V_i}{LSB} - 1 \tag{2}$$

$$INL = \frac{V_i - V_0}{LSB} - i \qquad (3)$$

The DNL error can lead to a case when some current values from DAC output range can be missed.

The method purposed in this article gives an opportunity to avoid the problem.

Detailed description of the problem and proposed solution

The article discusses the 8-bit current DAC linearity parameters improvement after Monte Carlo variation. The current DAC is designed for offset cancelation purposes. To avoid DC voltage difference between differential lags in circuit, the mentioned DAC is used.

To have the needed currents for each code of DAC, current sources with different currents are designed. The different currents are obtained by current source transistors with different sizes.

The DAC structure is shown in the picture below:

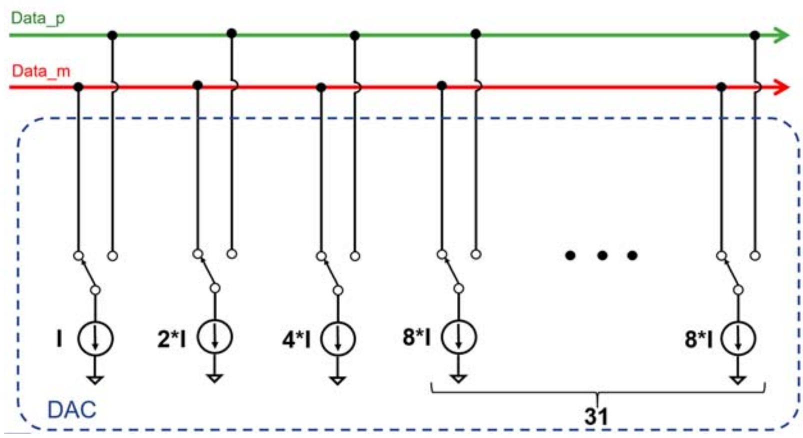


Fig. 1. DAC structure.

To avoid glitches on the output of DAC during code calibration, 5 binary bits are converted to a thermometric code as shown in DAC architecture.

The current difference between differential legs depending on code can be found by the formula shown below:

$$I_p - I_m = (2 * code - 256) * I_{ref} \quad (4)$$

Because of technological variations linearity parameters can be degraded so much that normal circuit operation will be impossible. So, there has been proposed a method of reducing DNL error by impacting the most significant DNL error contributor legs.

The main propose of the method is to avoid having a DNL error of more than 1 LSB. Having an error greater than 1 LSB is the most dramatic case because some of the current values can be lost. The thermal controlled legs have the greatest current value, so most cases of DNL error are related to those legs. Thus, by decreasing the current of those legs, the DNL error will also be reduced and it will have a negative value. Hence, the DAC output range will decrease. Increasing the binary controlled legs current will give the opportunity to avoid this problem.

The method described above is visualized in the chart below:

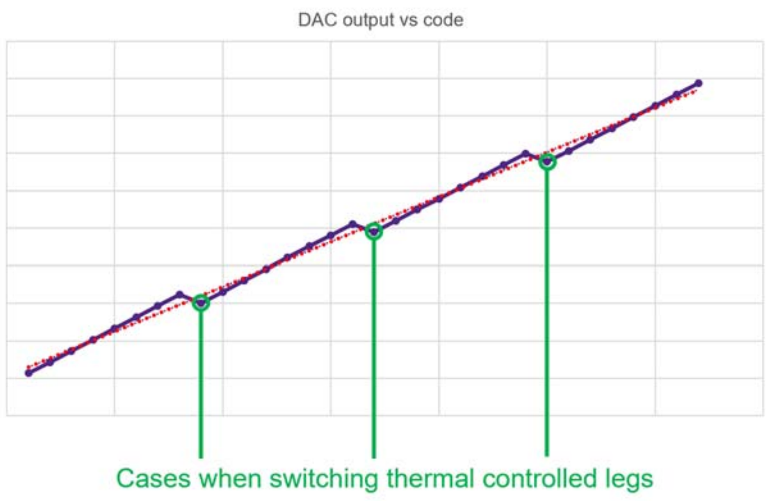


Fig. 2. Visualization of proposed method.

As shown in the chart, for each case when the thermal controlled leg is switched, current values have an overlapping. Hence, in these cases DNL has a negative value. The negative value will warranty a margin for DNL and after Monte Carlo variations it will be less than 1LSB.

Simulation Results

The current DAC with an 8-bit resolution has been modeled. There has been used binary and thermal controlling: 3-bit for binary and 5-bit for thermal. Simulation and modeling have been conducted with Custom Compiler [4] and HSPICE [5] tools. The circuit has been designed by using SAED14nm [6] technology.

There have been done preliminary simulations without considering DAC random variables for modeling risk or uncertainty. The obtained results over PVT are shown in the picture below:

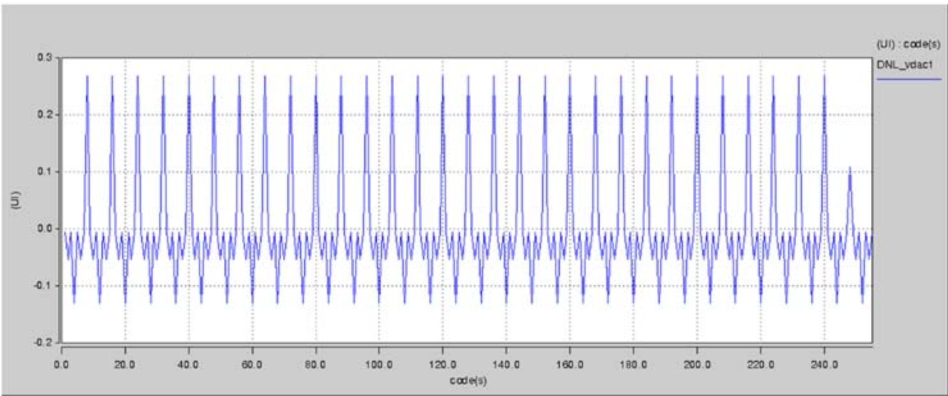


Fig.3. DNL results for worst case over PVT.

The simulation results show that maximum DNL error over PVT variation for the worst case is less than 1LSB. However, after Monte Carlo simulation some corners have a DNL error much greater than

1LSB. The results of Monte Carlo simulations for the worst case are shown below:

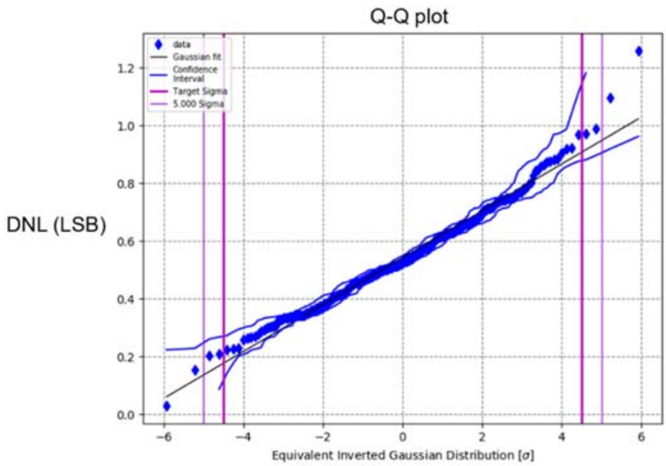


Fig. 4. DNL Q-Q plot for worst case over PVT.

After the reduction of the current of thermal controlled legs and the increase in that of binary controlled legs, DAC DNL error over Monte Carlo has decreased as shown in the picture below:

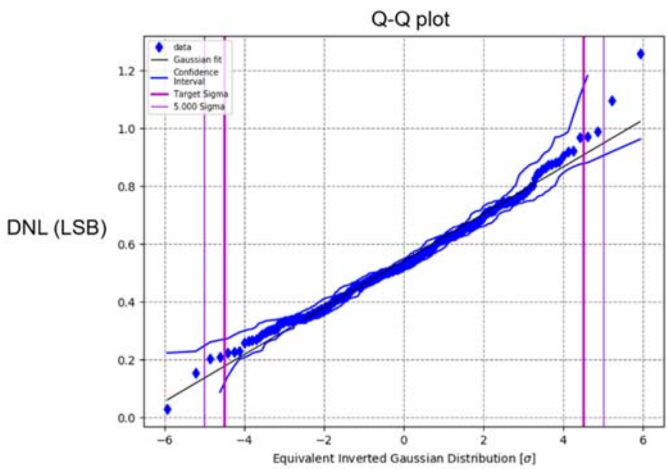


Fig. 5. DNL Q-Q plot for worst case over PVT.

Conclusion

The proposed method of increasing the linearity of DAC after Monte Carlo variation shows significant improvement of linearity parameters. This method has shown improvement of linearity by 70% after the Monte Carlo analysis. The distribution of DNL error thus becomes equal for all codes. The disadvantage of this method is output voltage range decrease.

REFERENCES

1. Bit numbering: https://en.wikipedia.org/wiki/Bit_numbering
2. Differential nonlinearity: https://en.wikipedia.org/wiki/Differential_nonlinearity
3. Integral nonlinearity: https://en.wikipedia.org/wiki/Differential_nonlinearity
4. Galaxy Custom Designer Schematic Editor User Guide, Synopsys Inc. 2014. 236 p.
5. Hspice Application Manual, Synopsys Inc. 2013. 196p.
6. *Melikyan V., Martirosyan M., Melikyan A., Piliposyan G.* 14nm Educational Design Kit: Capabilities, Deployment and Future // Small Systems Simulation Symposium Niš, Serbia, February, 2018. PP. 37–41.

МЕТОД УВЕЛИЧЕНИЯ ЛИНЕЙНОСТИ ТОКОВОГО ЦАП, УЧИТЫВАЯ СЛУЧАЙНЫЕ ОТКЛОНЕНИЯ И НЕТОЧНОСТИ ЕГО ПЕРЕМЕННЫХ КОЭФФИЦИЕНТОВ

А. Атанесян, М. Григорян, А. Маргарян, А. Ахаян, Г. Акобян

АННОТАЦИЯ

В данной статье представлен метод увеличения линейности токового ЦАП-а с учетом риска моделирования и влияния неточностей на схему. Основная идея метода состоит в том, чтобы распределить дифференциальную нелинейную ошибку по всем кодам и уменьшить дифференциальную нелинейность для критических кодов. Метод показывает значительное улучшение, и рабочий диапазон ЦАПа имеет охват 4,5 сигма случаев. Основным недостатком этого способа является сужение диапазона выходного напряжения.

Ключевые слова: токовый ЦАП, дифференциальная нелинейность, интегральная нелинейность, линейность ЦАП, Монте-Карло.

БИОЛОГИЧЕСКИЕ НАУКИ

УДК 616.053.(053.3)

Поступила: 04.06.2020г.
Сдана на рецензию: 06.06.2020г.
Подписана к печати: 02.11.2020г.

RESEARCH ON ARTIFICIAL NEURAL NETWORKS AND ELABORATION OF THEIR OBTAINING METHODOLOGY PRINCIPLES

A. Grigoryan, Kh. Gejagezyan

Russian-Armenian University,
National Polytechnic University of Armenia

anna.grigoryan@rau.am, khcho.gejagezyan@gmail.com

ABSTRACT

In this paper we review the two most popular supervised and unsupervised neural network types, as well as provide some foundation for networks design with a special focus on topology, selection of network sizes and number of layers for multilayer networks. We believe that this could be a useful entry point for non-specialists, especially for the biology/chemistry fields.

Keywords: Artificial neural network, formal neuron, Von Neumann architecture, electrical model, software solution.

The artificial neural network is a mathematical representation of the brain's neuron system (*Fig. 1*). The natural analogue shows that many problems that cannot be solved by standard algorithmic approaches can easily be solved with the help of a neural network.

Based on artificial neural networks, intellectual systems allow a successful solution to problems of image recognition, predictive implementation, optimization, associative memory and management. Traditional approaches to solving these problems do not always have the necessary flexibility [1].

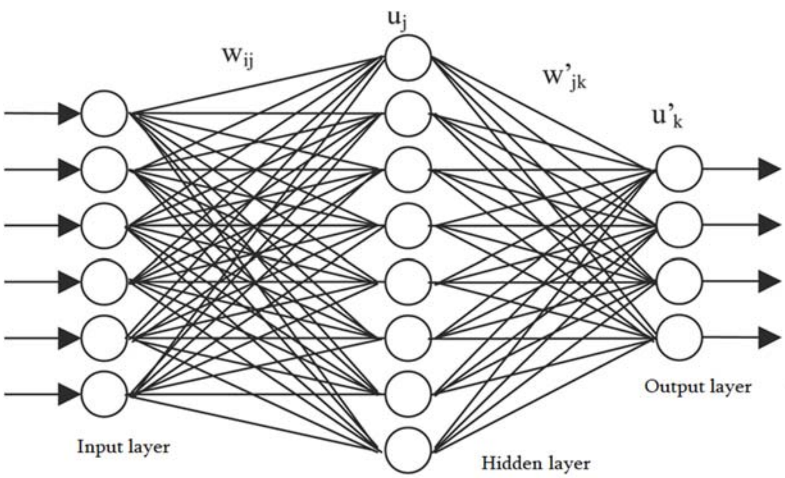


Fig.1. Neuron network in general.

During evolution, the human brain has acquired features that are lacking in Von Neumann's computer architecture. These are:

- Imagination about information and parallel estimation;
- Ability to learn and generalize;
- Adaptability;
- Tolerance for mistakes;
- Low energy consumption.

The equipment based on the principles of biological neurons has the enumerated characteristics: this can be considered a great achievement in the data processing industry. Achievements in neurophysiology allow developing an idea about the mechanism of thinking where information is stored in the form of complex images. The process of storing information as an image, the use of images (classification, detection, segmentation), and the solution to the given problem is a new direction of information processing which provides the creation of parallel networks and their training, without using traditional programming [2].

The human brain has been studied for more than 1,000 years. Modern electronics has made it possible to visualize the process of thinking through devices. The prospects of neural networks application in solving non-traditional problems are great. Currently, research is focused on the production of 3 types of AI accelerators (neurochips): digital, analogue and optical [5].

A neural network is a set of interconnected, interactive neurons designed to receive, process, and extract discrete information. Depending on the nature of the interaction, neural networks are generally divided into two types: random and deterministic. If the connections between network neurons are random, such a network is called random or stochastic. One subtype is possible networks. In such networks, the process of developing information is random.

The function or behavior of stochastic networks can be predicted in advance (by known mathematical relations). If the neural connections in the network and the interactions are predicted and described by known mathematical relations, such a network is called deterministic. The function of this network is completely predictable. Let us consider two of the most popular artificial neural networks.

Multilayer perceptron (*Fig.2*): This is the most popular and the oldest architecture, where there are several layers of neurons: an input layer, one or more hidden layers and an output layer.

It is almost always trained by the method of reverse propagation of the error, i.e. the set of "input vector – exact output" pairs must be presented for training. In this case, the input vector will be transmitted to the input of the network, the state of all intermediate neurons will be calculated successively, and the output vector will be formed at the output, which must be compared with the exact vector. The difference will be the error which can be sent back through the network connections (negative feedback), estimate the role of each neuron in the error and correct its weights to eliminate the error. The repetition of these processes for several thousand times will enable training the network.

These types of networks solve problems effectively where:

1. The answer depends only on the value given to the network input and does not at all depend on the previous values of the inputs, i.e. this is not a dynamic process.
2. The answer does not depend or weakly depends on the high number of parameters.
3. There is a big training set of samples; it is desirable to have at least one hundred examples for each network connection. This is due to the fact that having many coefficients, the network can remember more specific examples and give excellent results in that case, but if such examples are given to the input that is not from the training system, all the assumptions of the network will have no relation with the real answer (called overfitting).

The advantages of the perceptron network are that it was extensively studied, the scope of its applications is well defined and limitations are well known. It works well with its problems, and if it does not work with a specific problem, it can be argued that the problem was more complicated than it seemed to be.

The disadvantages of the network are the inability to work with dynamic processes and the need for multiple instructional samples [3].

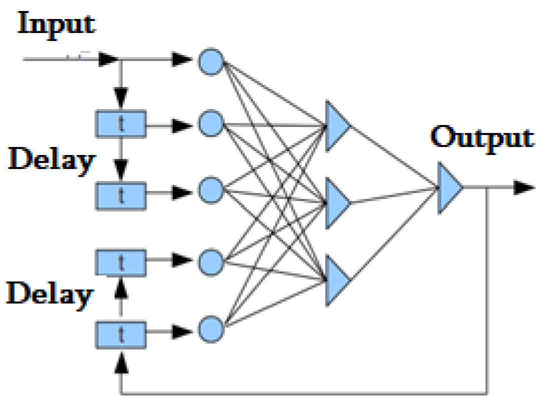


Fig. 2. Multi-layer perceptron structure.

Kohonen neural network: The problem of input images and the location of clusters in space are being solved in the Kohonen network (*Fig. 3*). The Kohonen network is unsupervised. During the training, the neurons weight vectors strive to the cluster centers of the training sample vector clusters. After the training, the network combines the presented image with one of the clusters, i.e. one of the outputs.

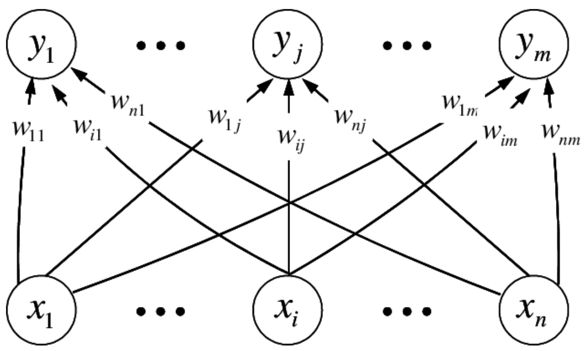


Fig. 3. Kohonen network.

In the general case, the clustering problem is presented as follows:

- There are objects that are characterized by the vector of parameters $x^p \epsilon$ x X, the parameters have the component N, $x^p = (x_1^p, \dots, x_N^p)$.
- There is an invested set of $C^1, \dots, C^M = \{C^m\}$ classes, in the C class space (M≤N, M = N).

It is necessary to determine the nuclei of classes $\{C^m\} = C^1, \dots, C^M$ in the space of C class so that the dimensions of proximity $d(x^p, c^M)$ are minimal, that is,

$$\sum_p d\left(x^p, c^{m(p)}\right) \rightarrow min\,, d(x,y) = \sum_i (x_i - y_i)^2$$

Usually d is an Euclidean size.

The m (p) function, which determines the class of objects for the set of objects x p according to the index p, gives the division of classes and is the solution to the problem of classification.

The initial values are given with the help of a random number generator. Each weight is given a small value. However, it is desirable for the Kohonen network to distribute the weight values evenly from the beginning, for which the method of convex combinations is used.

The schematic representation of Kohonen network is provided in Figure 3.

Kohonen network training takes place as follows:

- One of the x p vectors is given to the input;
- The Kohonen layer output is calculated and the m_i number of the gain neuron is determined, the output of which is maximal;
- We specify only m_0 gaining weights

$$W_{m_0} = W_{m_0} + \propto (x^p - W_{m_0})$$

where α is the training speed, the monotone decreasing α (t) function is usually used. The training takes place until the weights get stabilized [3].

Development of neural network synthesis (obtaining) method

The synthesis of neural networks (NEs) involves the selection of the structure of the neural network and, consequently, the learning algorithm, the neuron model (activation function), the number of layers, and the number of neurons in each layer. The choice of the neural network and the algorithm is made according to the sphere and the set of the problem where it will be applied. The choice of the model of the neuron, the number of layers, the choice of the number of neurons in each layer are very complex problems, and there is no regulated method for their selection. Thus, the designers usually use statistical data and their own experience. That is, by changing the number of neurons, the models evaluate the effectiveness of the ANN for the selected problem. Various error functions are used as criteria for such efficiency:

$$MSE = \sum_{i=1}^{N} \frac{(y_i - d_i)^2}{N}\ ,\ MAPE = \frac{100}{N} \sum_{i=1}^{N} \left| \frac{(y_i - d_i)}{\overline{y_i}} \right|\ ,$$

$$MAE = \frac{1}{N} \sum_{i=1}^{N} |y_i - d_i|$$

where y_i and d_i are the corresponding actual output and predictable (desirable) values of the output, $\overline{y_i}$ is the real mean output value and N is the number of examples. The number of formal neurons in each layer determines the complexity of the ANN and, at the same time, the functionality which has not been fully studied. For researchers, the creation of ANN is a more complex task [4].

Selection of the number of layers. If all formal neurons of a multi-layered perceptron have linear activation functions, it is easily proved by linear algebra that the multi-layered perceptron having any number of layers can be reduced to a standard double layer input - output construction.

In general, one hidden layer is enough for most problems, and the reality is that the addition of the second, third, and other layers leads to a small improvement in the effectiveness of the ANN.

Using the Kolmogorov theorem, Kurkova showed that any function can be approximated by at least 4 layers [6]. Necht-Nielsen has shown that the 3^{rd} is enough, and at the same time he noted that in case of a large number of layers, the total number of FNs in the hidden layer decreases [7]. However, the results of the publications show that in most practical problems, 1 and sometimes 2 hidden layers are enough. Such practical and theoretical discrepancy is probably due to the fact that in practice there are fewer real problems than it is theoretically possible [4].

Selection of formal neurons (FN) quantity. The number of neurons in the input is equal to the measurement of the input output signals, but there is no method for selecting the number of neurons in the hidden layer.

In the case of a large number of neurons in the hidden layer, the ANN has the ability to process so much information that a limited amount of information in the teaching multitude is not enough to train all neurons in the hidden layer. And even with enough instructional examples, the training process becomes unacceptably great.

Nielsen used Kolmogorov's theorem to determine the upper margin of the number of neurons in the hidden layer, according to which the function of any *n* variable can be represented by a superposition of 2n + 1 one-dimensional functions [7]. That L_W margin is equal to twice the number of input elements plus one:

$$L_W \leq 2n+1$$

In order to determine the upper limit of weight coefficients, Upadaya and Yerurek used the fact that the number of parameters required to encode N binary sequences is equal to $\log_2 P$ used to determine the boundary factor.

$$W = n\log_2 N:$$

In order to get a good generalization, it is necessary to choose fewer formal neurons in the hidden layer. There exist certain rules that are the starting point in the design of ANN [5].

1. The number of neurons in the hidden layer must be between the number of neurons in the output and input layers:

$$m \leq L_W \leq n, \text{ or } n \leq L_W \leq m$$

   where L_W, n, m is the number of neurons in hidden, input and output layers, respectively.

2. The number of neurons in the hidden layer should be equal to 2/3 of the number of neurons in the input layer (or 70% to 90%) and if it is sufficient, the number of neurons in the output layer can be increased:

$$L_w = \frac{2}{3}n + m$$

3. The number of neurons in the hidden layer must be twice as small as the number of neurons in the input layer:

$$L_W < n/2$$

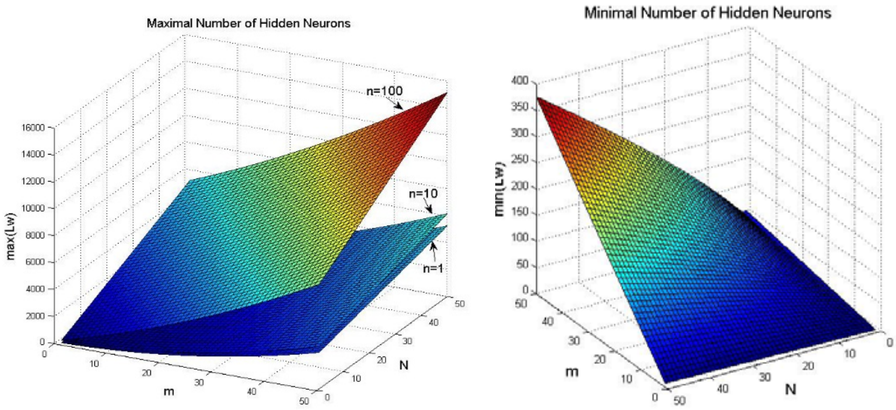
4. The number of neurons in the hidden layer should not exceed the sum total of the number of neurons in the output and input layers:

$$L_W \leq n + m$$

5. In the case of sigmoid activation function, a rough estimate of the number of neurons in the hidden layer is given by the following rule of Kolmogorov:

$$\frac{mN}{1 + log_2 N} \leq L_W \leq m\left(\frac{N}{m} + 1\right)(n + m + 1) + m,$$

where N is the number of instructional examples. The dependencies of the minimum and maximum values of L_W from the parameters m, N and n are shown in Figs. 4 a and b, where the corresponding dependency graphs were obtained due to specially designed software, for the design of which modern programming capabilities have been applied: c # programming language and program constructing WPF technology [5].



a) b)

Fig. 4. The maximum (a) and minimum (b) numbers of neurons in the hidden layer depend on the measurement of the output signal (m), the number of instruction samples (N), depending on the n = 1, n = 10, n = 100 cases of the input signal.

In the case of a single hidden layer, the number of neurons in the hidden layer is determined as follows:

$$L = \frac{L_W}{n + m}$$

By selecting:

$$L_W = \frac{[\min(L_W) + \max(L_W)]}{2}$$

we get the dependence of the number of neurons in the hidden layer on the measurements of the input and output signals. Fig. 5:

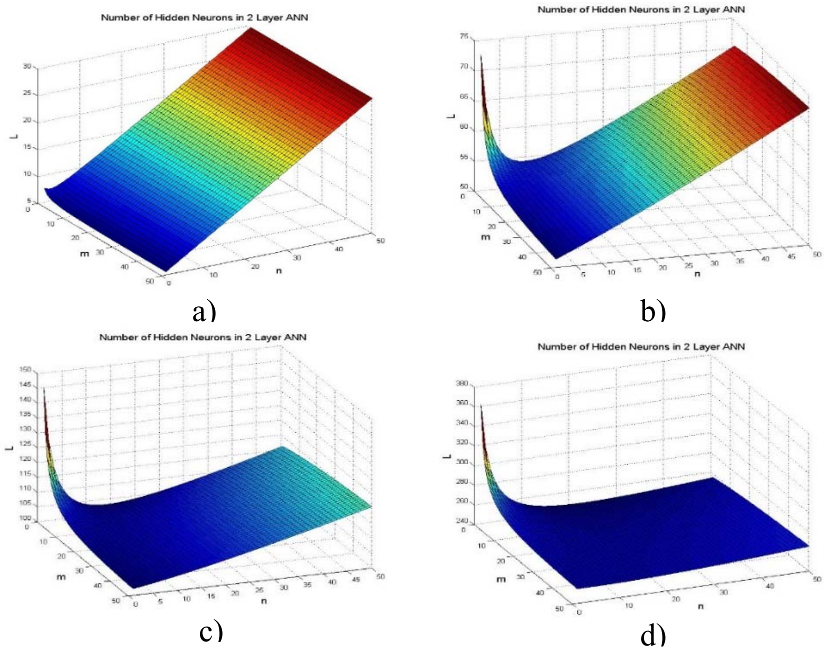


Fig. 5. The number of neurons in the hidden layer depending on the measurements of the output and input signals a) N = 10 b) N = 100 c) N = 200 d) N = 500

REFERENCES

1. *Klyukin V.I., Nikolaenkov Yu. K.* Electrical and mathematical models of neurons. NS direct distribution. Tutorial. Publishing Center of Voronezh State University, 2008. 63p.
2. *Chizhov A.V.* Mathematical models of ion channels, neurons and neural populations // From neuron to consciousness. St. Petersburg, 2009. PP. 91–110.
3. *Chizhov A.V., Turbin A.A.* From models of single neurons to models of neuron populations // Neuroinformatics. No. 1, 2006. PP. 76–88.
4. *Osipov G.V.* Synchronization in the processing and transmission of information in neural networks. Training materials on the continuing education program “Storage and processing of information in biological systems” Nizhny Novgorod, 2007. 99p.
5. *Tarkov M.S.* Neurocomputer systems – Internet University of Information Technologies-INTUIT.ru, BINOM. Laboratory of Knowledge, 2006. 144p.

6. *Kurkova, V.* Kolmogorov's Theorem and Multilayer Neural Networks. Neural Networks 5, 501–506 (1992).
7. *Hecht-Nielsen, R.* Counter Propagation Networks. In: Proc. IEEE Int. Conf. Neural Networks, vol. 2, PP. 19–32 (1987).

ИССЛЕДОВАНИЕ ИСКУССТВЕННЫХ НЕЙРОННЫХ СЕТЕЙ И РАЗРАБОТКА МЕТОДОЛОГИИ ИХ ПОЛУЧЕНИЯ

А.М. Григорян, Х.А. Геджагезян

АННОТАЦИЯ

Данная статья посвящена исследованию искусственных нейронных сетей (ИНС): были рассмотрены несколько сетей ключевого значения, описанных в своих структурных особенностях, алгоритме работы, с преимуществами и недостатками. В результате изучения искусственных нейронных сетей становится ясно, что создание нейросистем, принцип работы которых, по возможности, приближен к работе естественных нейронных сетей человека, сыграл важнейшую роль в области нейрокибернетики и позволяет успешно решать проблемы распознавания изображений, прогнозирования, оптимизации, ассоциативной памяти и управления, традиционные подходы к решению которых (с использованием обычных компьютеров) не всегда имеют необходимую гибкость.

В результате исследования принципов синтеза искусственных нейронных сетей и внедрения процессов разработки стало ясно, что существуют определенные правила, которые имеют ключевое значение в процессе проектирования ИНС. В рамках изучения этих правил были использованы некоторые хорошо известные математические уравнения для определения числа формальных нейронов в скрытом слое, и были представлены соответствующие графики зависимостей. Для построения графиков было разработано специальное программное решение, для разработки которого были применены современные возможности программирования – такие, как «Язык программирования» с # и технология WPF (Windows Presentation Foundation) для проектирования и построения компьютер-ных моделей.

Ключевые слова: искусственная нейронная сеть, формальный нейрон, архитектура фон Неймана, электрическая модель, программное решение.

УДК 577.11

Поступила: 04.09.2020г.
Сдана на рецензию: 14.09.2020г.
Подписана к печати: 28.09.2020г.

IRON OXIDE Fe_2O_3 BIOGENIC NANOPARTICLES SYNTHESIS USING *Ocimumbasilicum* L. EXTRACTS, THEIR QUANTITIVE ANALYSIS AND CHARACTERISTICS

L. Farsiyan, A. Hovhannisyan, S. Tiratsuyan

Russian-Armenian University
Institute of Medical Biochemistry and Pharmacy
the laboratory of analytical biochemistry and biotechnology

lilit.farsiyan@rau.am

ABSTRACT

Biogenic ("green") synthesis method, that uses plant extracts, allows to obtain non-toxic iron oxide NPs, is environmentally friendly and cost-effective. In current study, iron oxide NPs have been synthesized using various standardized plant extracts of *O. basilicum* with high antiradical activity. As a confirmation of the nature of obtained NP's during the green synthesis, spectral and transmission electron microscopy (TEM) analyses were performed. The effect of β-glucosidase on the yield of NPs in aqueous extracts was investigated as well. Results showed, that obtained NPs belonged to Fe_2O_3cluster, and had a round shape and the size raging in 3-16 nm. Besides, the used method provided a high yield of nanoparticles in the range of 95-25078 mg/g of the dry mass for various extracts. Aqueous extracts had the highest yield.

Keywords: green nanoparticles, Fe_2O_3, *Ocimum basilicum.*

Introduction

Rapidly developing nanotechnology creates the possibility of producing on an industrial scale a wide range of NPs of various compositions, shapes and sizes. Nanobiotechnology is a part of modern nanotechnology, which has received attention due to its wide application. This is a multidisciplinary approach based on the use of NPs in biological systems, in the fields such as biology, chemistry, engineering, physics, medicine, etc. In addition, it is one of the most important methods for developing cost-effective and environmentally friendly procedures for the congregation of non-toxic metallic NPs.

Currently, iron oxide NPs are synthesized using physical, chemical, and biological methods. Physical and chemical synthesis is more laborious and hazardous compared to biological synthesis that has a high yield, solubility and stability, as well as have high bioavailability and biocompatibility. Therefore, there is a need to develop environmentally friendly procedures that do not use toxic chemicals in NP synthesis protocols. In addition, some of the conditions necessary for the synthesis of iron oxide NPs cannot be reproduced for production in large volumes. The choice of medium and the selection non-toxic reducing and stabilizing solvent agents are the most important issues that should be considered in green synthesis of NPs.

The use of biogenic or "green" synthesis methods helps to avoid many disadvantages of physical and chemical methods, for example, instead of the toxic stabilizers, are used plant extracts that have a number of positive biological properties [8]. Extracts of various plants are used as reducing and stabilizing agents for the biosynthesis of iron oxide NPs. Besides that, synthesis of NPs using plants is very cost effective and therefore can be used as an economical and valuable alternative for large scale NPs production.

Ocimumbasilicum is widely used in traditional medicine and as a herb in a national cuisine. Basil contains high levels of phenolic compounds that are involved in protecting cells from free radicals [4]. The antioxidant

potential of herbs and spices correlates with the presence of phenolic compounds and, due to their redox properties, they can act as reducing agents, hydrogen donors and singlet oxygen quenchers [2].According to the literature the major phenolic component of basil is rosmarinic acid [3], and other caffeic acid derivatives. The presence of rosmarinic acid in medicinal plants, herbs and spices has beneficial effects on health. Rosmarinic acid has a number of biological activities [6], including antibacterial, anti-inflammatory and antioxidant, antimutagenic, antiviral. Due to *O. basilicum* high antioxidant properties it becomes a good candidate for NP's synthesis.

Materials and methods

For extraction of fresh and dried leaves of *O.basilicum* were used 50% and 96% ethanol and distilled water. The synthesis of iron oxide NPs was carried out by adding a solution of 1M ferric chloride salt to those extracts [11].

The total content of flavonoids (TCF) was determined by the ability of flavonoids to form yellow colored complexes with Al^{3+} ions, detectable at 430 nm [10].

Antiradical activity (ARA) was determined by quenching the free stable radical of 2,2-diphenyl-1-picrylhydrazyl (DPPH) [7].

The amount of NPs obtained from the extracts (both with fresh and dried leaves) was calculated taking into account the dry weight of leaves (mg/g of dry weight).

Extracts, containing NPs, were treated with β-glucosidase (Sigma-Aldrich, USA).

The UV–v is absorption spectra of the samples were recorded by a spectrophotometer (SPECTRO UV – 18 MRC, Israel) from 200 nm to 800 nm [5].

For the characterization of the crystalline structure and shape of Fe_2O_3 NPs TEM (LEO 912 AB omega, Carl Zeiss, Germany) was conducted.

Statistical analysis of the results was carried out on the basis of the complex application of standard statistical methods: calculating mean

values, standard deviations, standard mean errors. Biological repetition of experiments is 4–6 times, with carrying out 2–3 series of experiments in each. The tables, graphs and diagrams show the arithmetic means and their standard errors (n = 8–12), $p \leq 0.05$.

Results and discussion

Rapidly developing nanotechnology makes possible producing wide range of NPs of various compositions, shapes and sizes on an industrial scale. NPs are known to be used in both technology and biomedicine due to their superior physical, chemical and biological characteristics due to discrete physical and optical properties and biochemical functionality [1].

As it can be seen from the obtained results (Fig. 1–2), the extracts we chose had a high ARA. The radical neutralizing activity of all extracts showed a dose-dependent character. The total content of flavonoids (TCF) of *O.basilicum* various extracts are presented in Table 1.

Table 1.

The total content of flavonoids of *O.basilicum* extracts

Extract	TCF µg/ml
O.basilicum (dried) 96%	2.44±0,04
O.basilicum (dried) 50%	36.34±1,8
O.basilicum (dried) aqueous	11.17±0,46
O.basilicum (fresh) 96%	1,3±0.02
O.basilicum (fresh) 50%	2,99±0.15
O.basilicum (fresh) aqueous	2,29±0.1

From the study of basil's dried leaves antiradical activity results it is clear that all extracts have a high ARA (Fig. 1), which is most pronounced in 50% ethanol extract of *O.basilicum*. Aqueous and 96% ethanol extracts were less active. Thus, it can be concluded that ARA of dry *O.basilicum* extracts positively correlates with TCF.

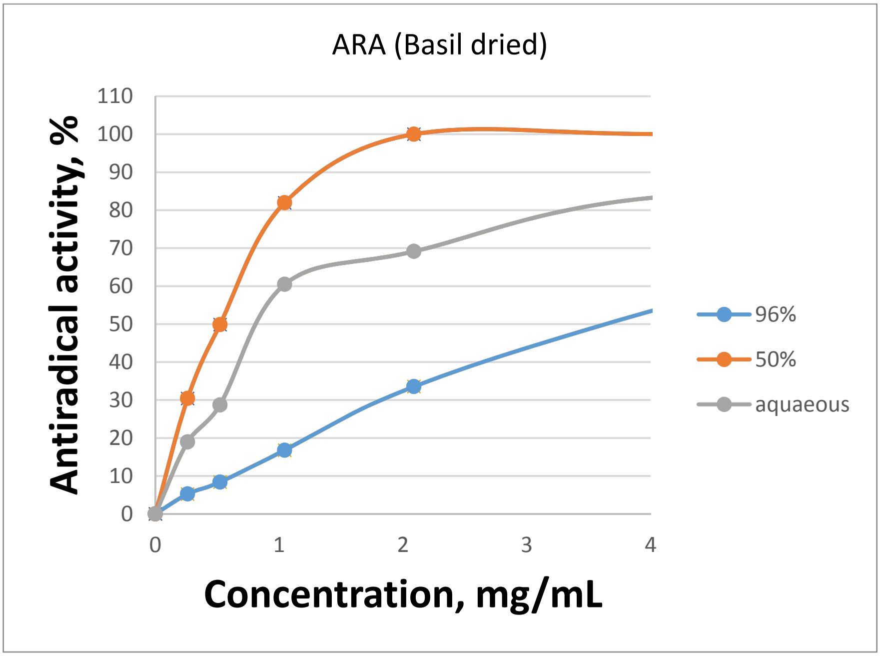


Fig. 1. Antiradical activity of O. basilicum dried leaves extracts.

Among the extracts of fresh basil leaves, 96% ethanol extract of *O.basilicum* was the most active, although the other two samples also had high ARA (Fig. 2). The lowest activity was observed in the aqueous extract. It should be noted that ARA is significantly lower than that of dry *O.basilicum* extracts and does not correlate with the TCF.

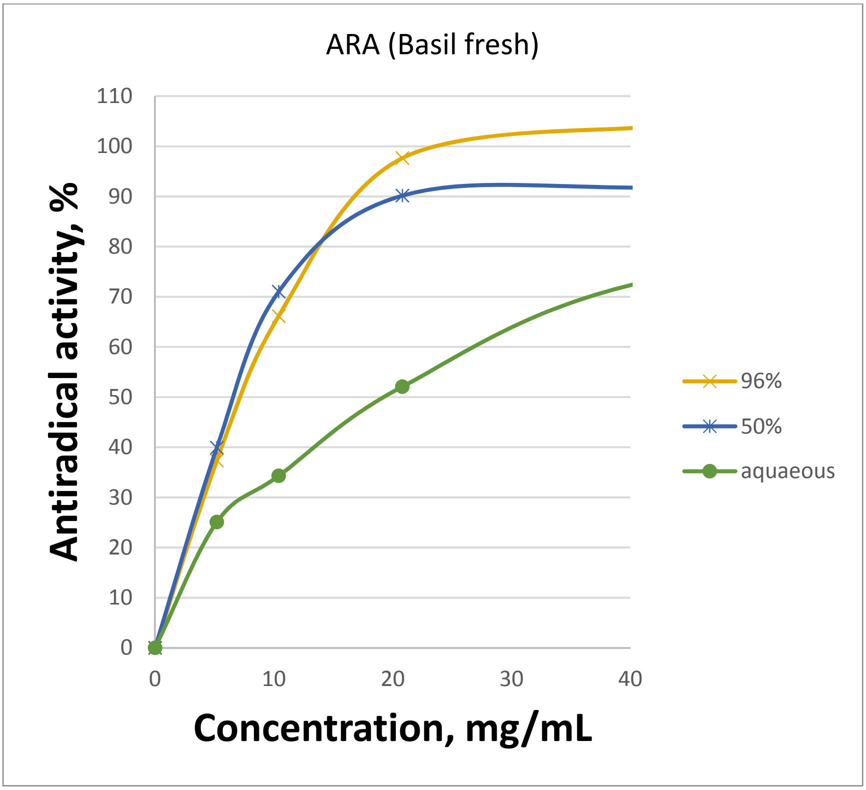


Fig. 2. Antiradical activity of O.basilicum fresh leaves extracts.

From the obtained results it can be seen that by definition of ARA, the most active is 50% ethanol extract of dry basil, and the least – aqueous extract of fresh basil (Fig. 1, 2). Due to the presence of the antioxidant components in the extracts, it is possible to carry out a congregation of NPs.

UV–v is absorption spectroscopy was also carried out in the range of 200–800 nm of the following samples: extract, salt solution, supernatant, and iron oxide NPs (Fig. 3). As it can be seen from the figure, the curves differ in optical characteristics. In the absorption spectrum prevails a peak with a maximum of 300 nm, which is absent in the extract and in the salt solution. This directly indicates a congregation of NPs. Detection by the analog method is also found in the literature [5].

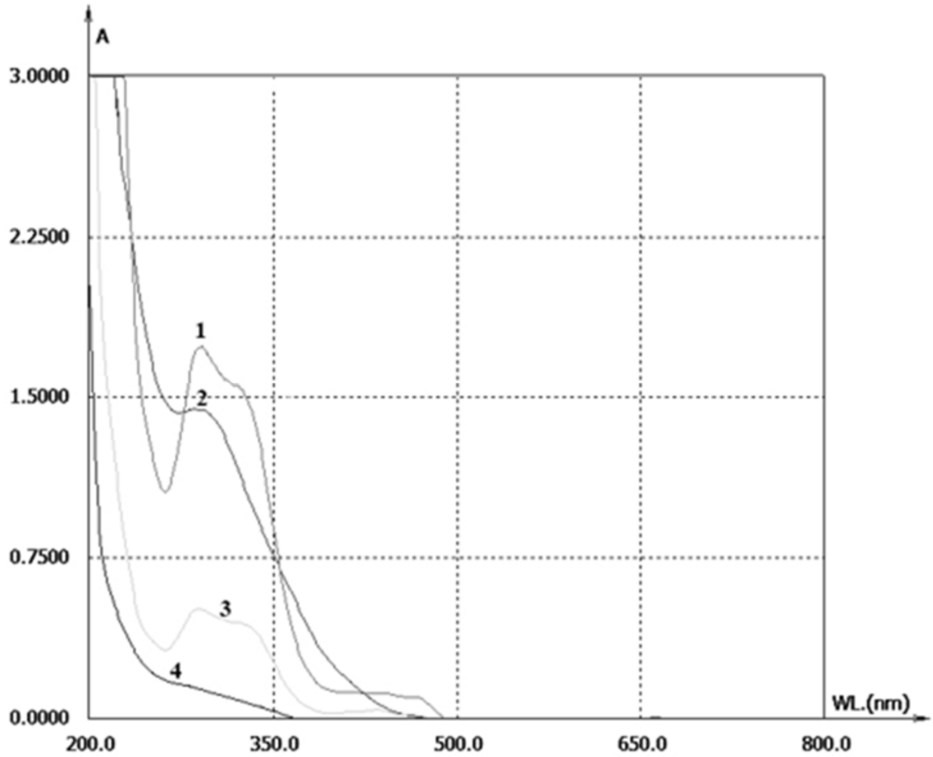


Fig. 3. Absorption spectra of complexes of the extract and salt (1), $FeCl_3$- $6H_2O$ salt (2), basil ethanol extract (3), and supernatant (4).

As a result of the synthesis of Fe_2O_3 NPs, a black precipitate formed, which initially indicates the correctness of the process. To prove the formation of Fe_2O_3NPs, to determine the nature of the material formed and to detect the size and shape of the low frequency, TEM was carried out.Samples were stored in the dark and allowed to dry for 2 h. TEM images were taken immediately after drying. The Fe_2O_3 NPs were spherical and round shaped and had a single-crystalline structure. Size of NPs varies from 3 to 16 nm in diameter (Fig. 4). The average size of synthesized Fe_2O_3 was determined on the base of 10 different images and was found to be 12 ± 2 nm. In addition, the obtained NPs were not in an aggregated state, which is an important problem in other methods of synthesis.

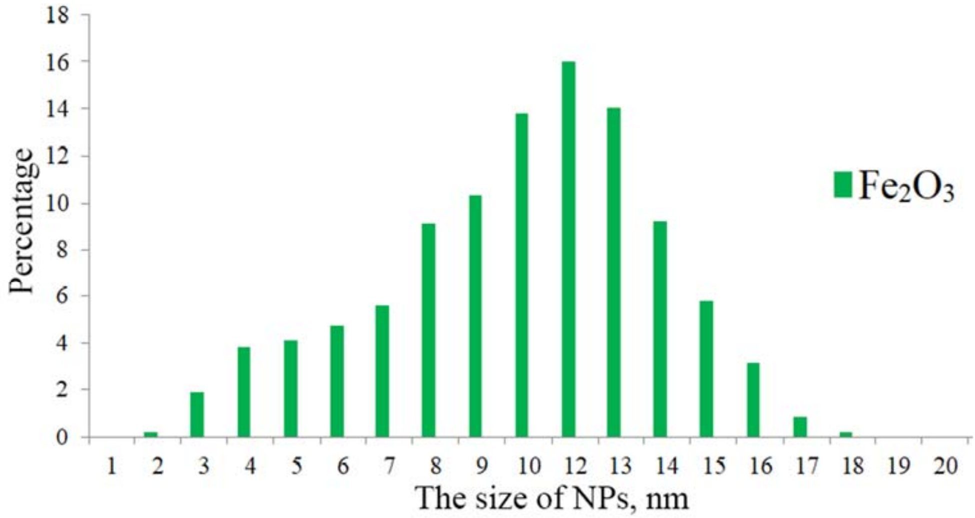


Fig. 4. The content of the synthesized Fe_2O_3 NPs sizes (%).

The crystalline structure of NPs was also investigated by electron-diffraction method [9]. The electron diffraction patterns of the reference specimen Fe_2O_3 and Fe_2O_3NPs coincided, indicating that the NPs have a single-crystalline structure.

For measuring the yield of the obtained NPs, they were dried to the state of a powder. As our results had shown, the largest number of NPs (mg/g of dry weight) were obtained from aqueous extracts; in particular, the greatest amount of NPs was obtained from *O.basilicum* fresh leave saqueous extract: 25078.1 ± 99, and the smallest from *O.basilicum* dried leaves 50% ethanol extract: 75 ± 3.1. But in general, all the aqueous extracts, compared with the other extractants provided a high yield of NPs. The following diagram shows the comparative yield of iron oxide NPs (Fig. 5).

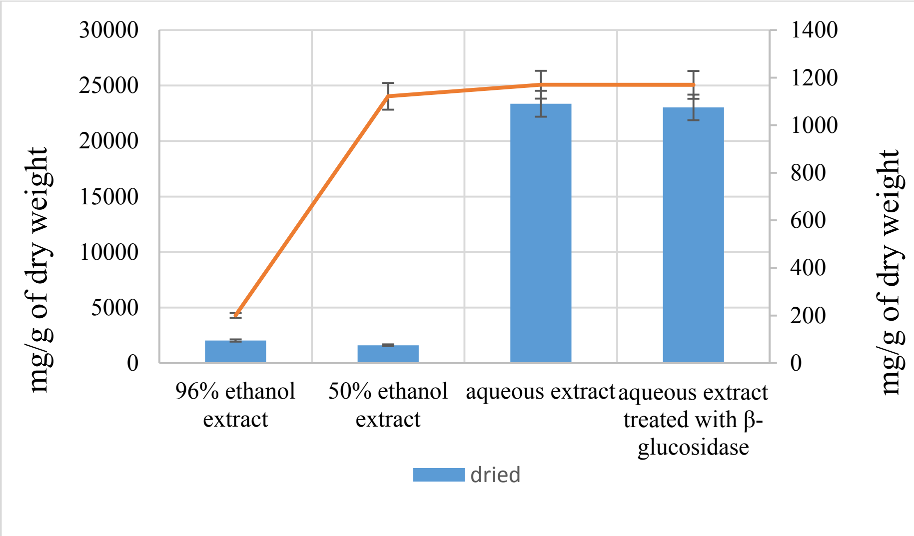


Fig. 5. Yield of the Fe_2O_3NPs based on O.basilicum extracts.

As soon as the highest yield of NPs was obtained by aqueous extracts containing water-soluble polysaccharides, therefore, to determine the effect of polysaccharides on the congregation of iron oxides NPs, the aqueous extract of fresh and dried leaves of *O.basilicum* were treated with β-glucosidase, after which the synthesis of NPs was carried out. Then, the obtained iron oxide NPs were dried and their yield was compared with the yield of NPs obtained from the untreated β-glucosidase extracts. The results showed (Fig. 5) that the yield of NPs in both cases practically did not differ. In particular, for *O.basilicum*dried leaves aqueous extract the yield of NPs was 1090 ± 98 and 1075 ± 84 mg/g of dry weight for β-glucosidase-untreated and β-glucosidase-treated extracts, respectively. For *O.basilicum* fresh leaves aqueous extract the yield of NPs was 25078.1 ± 99 and 25066 ± 65 mg/g of dry weight for β-glucosidase-untreated and β-glucosidase-treated extracts, respectively. Thus, can be concluded that the polysaccharides do not have a significant effect on the Fe_2O_3 NPs yield.

Conclusion

Thus, this study demonstrated that biogenicly synthesized NPs belong to Fe_2O_3 cluster, are round-shaped and aren't aggregated. Size of obtained NPs was in 3–16 nm range. The highest yield of NPs was obtained from aqueous extracts of *O.basilicum*. The biogenic synthesis of iron (III)oxide nanoparticles provide high yield, which doesn't depend on polysaccharides content in aqueous extracts.Fe_2O_3NPs can be used for various applications due to their unique properties: for targeted drug delivery, as agents for magnetic resonance imaging studies, in biosensors, for purifying water from pesticides and dyes, etc.

"This work was made possible by a research grant from the Yervant Terzian Armenian National Science and Education Fund (ANSEF) based in New York, USA"

REFERENCES

1. *Ahmmad B., Leonard K., Islam M.S., Kurawaki J., Muruganandham M., Ohkubo, T. and Kuroda Y.* (2013) Green synthesis of mesoporous hematite (α-Fe2O3) nanoparticles and their photocatalytic activity. Advanced Powder Technology, 24(1). PP.160–167.
2. *Caragay A.B.* (1992) Cancer-preventive foods and ingredients. Food technology (Chicago), 46(4). PP. 65–68.
3. *Lee J. and Scagel C.F.* (2009) Chicoric acid found in basil (Ocimum basilicum L.) leaves. Food Chemistry, 115(2), PP. 650–656.
4. *Lee J. and Scagel C.F.* (2010) Chicoric acid levels in commercial basil (Ocimum basilicum) and Echinacea purpurea products. Journal of functional foods, 2(1). PP. 77–84.
5. *Mahdavi M., Namvar F., Ahmad M.B. and Mohamad R.* (2013) Green biosynthesis and characterization of magnetic iron oxide (Fe_3O_4) nanoparticles using seaweed (Sargassum muticum) aqueous extract. Molecules, 18 (5), PP. 5954–5964.
6. *Petersen M. and Simmonds M.S.* (2003) Rosmarinic acid. Phytochemistry, 62 (2), PP. 121–125.

7. *Vardapetyan, H.R., Tiratsuyan, S.G., Hovhannisyan, A.A. and Martirosyan, A.S.,* (2012) Elucidation of DPPH antiradical and photodynamic activities of Hypericum perforatum extracts. Հայաստանիկենսաբանականհանդես Biological Journal of Armenia Биологический журнал Армении, 64(2). PP.111–116.
8. *Wei Y., Fang Z., Zheng L., Tan L. and Tsang E.P.* (2016) Green synthesis of Fe nanoparticles using Citrus maxima peels aqueous extracts. Materials Letters, 185, PP. 384–386.
9. *Zhuang L., Zhang W., Zhao Y., Shen H., Lin H. and Liang J.* (2015) Preparation and characterization of Fe_3O_4 particles with novel nanosheets morphology andmagnetochromatic property by a modified solvothermal method. Scientific reports, 5. P. 9320.
10. *Тихонов Б.Б., Сидоров А.И., Сульман Э.М., Ожимкова Е.В.* (2011) Комплексная экстракция гликанов и флавоноидов из растительного сырья. Вестник ТвГТУ, 128(19). PP.57–63.
11. *Фарсиян Л.М., Оганесян А.А.* (2019) Синтез зеленых наночастиц оксидов железа и изучение их цитотоксичности // «Вестник Российско-Армянского университета: сер.: физико-математические и естественные науки» (1). PP.73–80.

СИНТЕЗ БИОГЕННЫХ НАНОЧАСТИЦ ОКСИДА ЖЕЛЕЗА Fe_2O_3 ПОСРЕДСТВОМ ЭКСТРАКТОВ *Ocimumbasilicum L.*, ИХ КОЛИЧЕСТВЕННЫЙ АНАЛИЗ И ХАРАКТЕРИСТИКИ

Л.М. Фарсиян, А.А. Оганесян, С.Г. Тирацуян

АННОТАЦИЯ

Метод биогенного («зеленого») синтеза с использованием экстрактов растений позволяет получить нетоксичные наночастицы (НЧ) оксида железа и является экологически чистым и экономически выгодным. Целью данного исследования является синтез НЧ оксида железа с использованием стандартизированных разных экстрактов *O. basilicum*, обладающих высокими антирадикальными активностями. Для подтверждения природы полученных НЧ в процессе зеленого

синтеза были выполнены спектральный и трансэмисионно-электроно микроскопический анализы. Также было исследовано влияние β-глюкозидазы на выход НЧ, полученных посредством водных экстрактов. В результате анализа подтвердилось, что полученные НЧ относятся к кластеру Fe_2O_3 и имеют округлую форму и размеры в пределах 3–16 нм. Используемый метод получения зеленых НЧ обеспечивает высокий выход в пределах 95–25078 мг/г сухого веса для разных экстрактов. Наиболее высоким выходом обладают водные экстракты.

Ключевые слова: зеленые наночастицы, Fe_2O_3, *Ocimumbasilicum*.

УДК 577.29(577.322.9)

Поступила: 05.11.2020г.
Сдана на рецензию: 05.11.2020г.
Подписана к печати: 16.11.2020г.

COMPARATIVE ANALYSIS OF THE INTERACTION OF ARTEMISININ AND SCH772984 INHIBITOR WITH ERK2

S.V. Ginosyan[1], H.V. Grabski[1], S.G. Tiratsuyan[2]

[1]Department of Medical Biochemistry and Biotechnology
[2]Department of Bioengineering, Bioinformatics and Molecular Biology
Institute of Biomedicine and Pharmacy
Russian-Armenian University (RAU)

siranush.ginosian@student.rau.am, susanna.tiratsuyan@rau.am

ABSTRACT

Sesquiterpene trioxane lactons are secondary metabolites of plants of the genus *Artemisia anua* have multiple biological and pharmacological effects, including antimalarial, anti-imflammatory, vasodilative, antitumor, antiviral, antibacterial, antifungal, neuroprotective and other properties. However, specific molecular targets and mechanisms of action of artemisinin family compounds have not been sufficiently studied. It is assumed that the neuroprotective action of artemisinin is mediated through signalling pathway of ERK2. The purpose of the work was to study the peculiarities of direct interaction of artemisinin with ERK2. We carried out docking analysis- of artemisinin with ERK2 and compared it with inhibitor SCH772984. The results showed that both artemisinin and SCH772984 interact directly with ERK2 with high binding affinity. The artemisinin binding site coincides with one of the inhibitor binding sites, which corresponds to that of ATP. At the same time, the endoperoxide bridge in C ring of artemisinin, is not involved in the interaction with the protein,

which suggests that artemisinin binding to ERK2 can modulate it without ROS formation.

Keywords: *Artemisia anua*, artemisinin, neuroprotective agent, ERK2, SCH772984, docking analysis.

Introduction

Among most diverse classes of plant compounds that have healing properties, a special place is occupied by sesquiterpene lactones - secondary metabolites of *Artemisia*, as antimalarial, anti-imflammatory, vasodilating, antitumoral, antiviral, antibacterial, antifungal agents. [1] Nowadays, more and more attention is being paid to the neuroprotective properties of artemisinin (ART) and its derivatives such as dihydroartemisinin, artesunate, and many other semi-synthetic analogs [8].Recent studies have shown that artemisinins can have a neuroprotective effect by inhibiting oxidative stress via modulating various signaling pathways, such as ERK [13].

However, to this day, specific molecular targets and mechanisms of action of artemisinin family compounds have not been sufficiently studied.

The aim was to study the peculiarities of direct interaction of artemisinin with ERK2.

Materials and methods

AutoDock Tools and AutoDock Vina [10] software packages were used for "blind" and local docking. Three-dimensional ERK2 structures with inhibitor (3R)-1-(2-oxo-2-{4-[4-(pyrimidin-2-yl)phenyl]piperazin-1-yl}ethyl)-N-[3-(pyridin-4-yl)-2H-indazol-5-yl]pyrrolidine-3-carboxamide (SCH772984) (PDB ID: 4QTA) was obtained from RCSB Protein Data Bank [3]. 3D structure of ART [CID: 68827] was taken from PubChem Data Bank. The ligand topology for additional analysis was generated using Acpype software [5], which is compatible with General Amber Force Field [12].

The entire ERK2 protein was studied using box dimensions of 66 × 50 × 88 Å. The "exhaustiveness" value was set to 128. The molecular docking simulations were performed 10 times and the number of binding modes was set to 20. As a result, 200 ligand conformations were obtained. Large number of conformations was necessary to obtain good sampling for further analysis. After that, the binding site for ART and 2SH was determined based on the largest distribution of ligand conformations. Then local docking was carried out with this site with a box size of 16 × 26 × 12 Å. Hydrophobic interactions and hydrogen bonds were analyzed using Ligplot+ [11]. Visualization of docking conformations was done using Pymol [6].

Results and Discussion

The accuracy of the docking analysis was estimated by re-docking the crystallized SCH772984 ligand with ERK2 protein obtained by X-ray crystallography [3]. The RMSD value between two superimposed conformations between crystallized SCH772984 associated with ERK2 and its conformation obtained after re-docking was 1.339 Å (Fig. 1a), which indicates a good prediction quality [10].

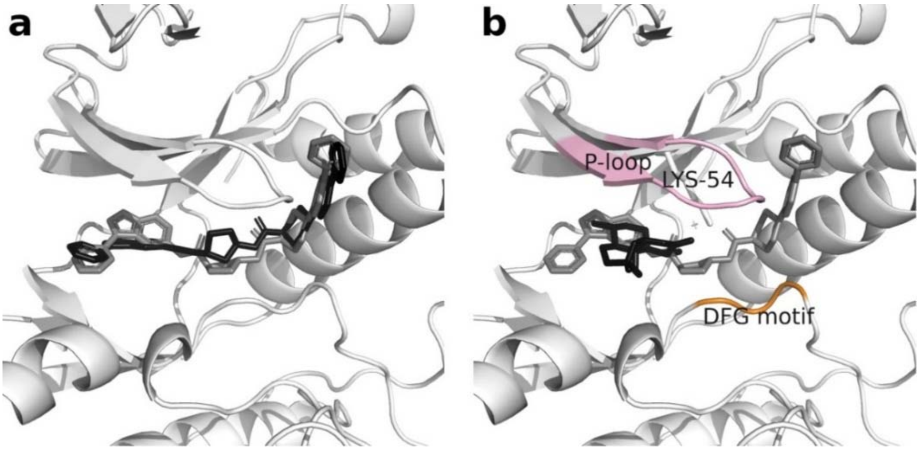


Fig. 1. a). Superimposition of docked conformation SCH772984 (gray) with its crystal structure (black). RMSD value 1.339 Å. b). Docking analysis of SCH772984 (gray) and ART (black) with ERK2.

The binding affinity of the bound conformation of SCH772984 after docking analysis is -9.4 kcal/mol, which indicates a rather strong interaction. The NZ group of side chain Lys54 formed a hydrogen bond with carboxylic C3 of SCH772984 at a distance of 3.31 Å. The aminoacid residues Ile31, Ala35, Tyr36, Val39, Ala52, Ile56, Ser57, Pre58, Tyr64, Arg67, Thr68, Thr110, Asp111, Asp167 were involved in numerous hydrophobic interactions with SCH772984 (Fig. 1b, 2a).

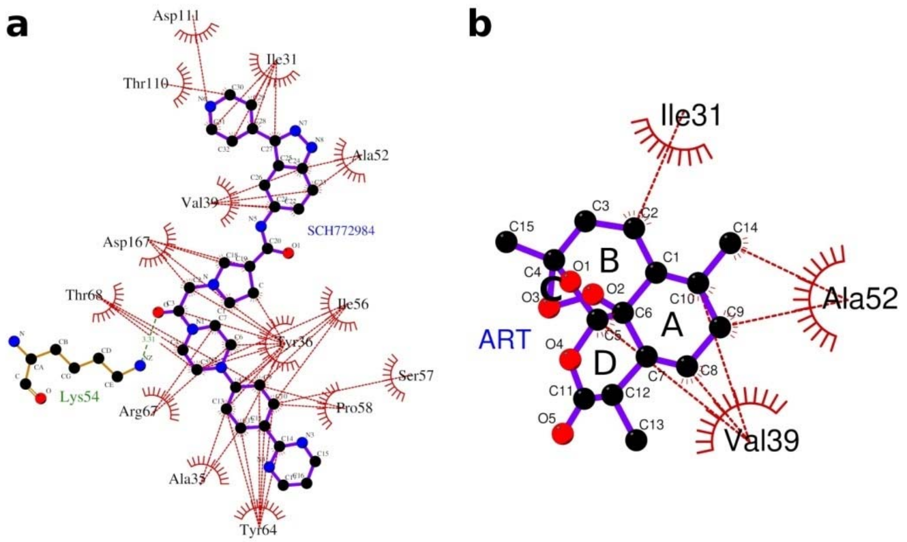


Fig. 2. Analysis of hydrogen bonds and hydrophobic interactions of SCH772984 (a) and ART (b) with ERK2.

The ERK2 protein has specific areas, whose conformational change determines its activity. Such sites are, for example, P-loop and DFG motif. The results of our docking analysis showed that SCH772984 affects these sites and forms a hydrogen bond with Lys54, which is one of the key amino acids that bind ATP and inhibitors. Thus, our results coincide with the literature data [3].

According to the results of the docking analysis, the binding site of artemisinin to ERK2 coincides with one of SCH772984 inhibitor binding

sites (Fig. 1b) H., and artemisinin is located directly in the ATP binding site. Artemisinin interacts with ERK2 with a binding affinity of -8.7 kcal/mol, which is slightly lower than the binding affinity of SCH772984. The interaction of artemisinin with ERK2 is due to hydrophobic interactions: Ile31 with C2 (ring B) of artemisinin, Val39 with C5 (D), C8 and C10 (A), Ala52 with C9 and C14 (A) of artemisinin (Fig. 2b). Artemisinin as well as SCH772984 interact with the amino acids of P-loop.

The ERK/CREB pathway is a central signaling component that induces cellular antioxidant mechanism and plays a role in initiating and regulating cellular processes such as proliferation, survival and differentiation [9]. Artemisinin increased the phosphorylation of ERK1/2 [4]. Phosphorylated and activated ERK1/2 can regulate the activity of a transcription process, thus causing a protective effect [7]. Artemisinins can protect cells from death by inhibiting oxidative stress,apoptosis, and restoring mitochondrial function [4].

We have shown *in silico,* theinteraction of artemisinin with the hydrophobic pocket of the allosteric site ERK1/2 as a modulator. As we can see, ART binds to ERK2 with a binding affinity that is close to SCH772984. While the inhibitor interacts with more amino acids than artemisinin. The C ring of artemisinin, which contains the endoperoxide bridge is not involved in the interaction. It is known that the biological activity of artemisinins leading to cell death is mainly related to the endoperoxide bridge, which leads to the formation of ROS [2]. Therefore, it can be assumed that artemisinin during interaction with ERK2 will not contribute to ROS formation. Our results suggest that artemisinin can be developed to prevent neuronal cell from death. It should be noted molecular dynamics simulations are being performed for getting more detailed insight of the interaction of artemisinin with ERK2.

Acknowledgement

This work was made possible by a research grant from the Yervant Terzian Armenian National Science and Education Fund (ANSEF) based in

New York, USA. We are grateful for the financial support to the Ministry of Education and Science of the Republic of Armenia (grant № 10-2/I-4).

REFERENCES

1. *Ali M. et al.* Strategies to enhance biologically active-secondary metabolites in cell cultures of Artemisia–current trends //Critical reviews in biotechnology. 2017. Vol. 37. №. 7. PP. 833–851.
2. *Cai H. H. et al.* Visual characterization and quantitative measurement of artemisinin-induced DNA breakage // Electrochimica acta. 2009. Vol. 54. №. 13. PP. 3651–3656.
3. *Chaikuad A. et al.* A unique inhibitor binding site in ERK1/2 is associated with slow binding kinetics // Nature chemical biology. 2014. Vol. 10. №. 10. P. 853.
4. *Chong C.M., Zheng W.* Artemisinin protects human retinal pigment epithelial cells from hydrogen peroxide-induced oxidative damage through activation of ERK/CREB signaling //Redox biology. 2016. Vol. 9. PP. 50–56.
5. *Da Silva A.W.S., Vranken W.F.* ACPYPE-Antechamber python parser interface //BMC research notes. 2012. Vol. 5. №. 1. P. 367.
6. *DeLano W.L. et al*. Pymol: An open-source molecular graphics tool //CCP4 Newsletter on protein crystallography. 2002. T. 40. №. 1. CC. 82–92.
7. *Oh Y. T. et al.* Correction: Oncogenic Ras and B-Raf proteins positively regulate death receptor 5 expression through co-activation of ERK and JNK signaling //The Journal of Biological Chemistry. 2020. Vol. 295. №. 26. P. 8870.
8. *Shi Z. et al.* Resolving neuroinflammation, the therapeutic potential of the anti-malaria drug family of artemisinin //Pharmacological Research. 2018. Vol. 136. PP. 172–180.
9. *Sugiura S. et al.* CRE-mediated gene transcription in the peri-infarct area after focal cerebral ischemia in mice //Journal of neuroscience research. 2004. Vol. 75. №. 3. PP. 401–407.
10. *Trott O., Olson A. J.* AutoDock Vina: improving the speed and accuracy of docking with a new scoring function, efficient optimization, and multithreading //Journal of computational chemistry. 2010. Vol. 31. №. 2. PP. 455–461.

11. *Wallace A.C., Laskowski R.A., Thornton J.M.* LIGPLOT: a program to generate schematic diagrams of protein-ligand interactions //Protein engineering, design and selection. 1995. Vol. 8. №. 2. PP. 127–134.
12. *Wang J. et al.* Development and testing of a general amber force field //Journal of computational chemistry. 2004. Vol. 25. №. 9. PP. 1157–1174.
13. *Zhelyazkova M., Hadjimitova V., Hristova-Avakumova N.* Antioxidant and prooxidant properties of artemisinin and epirubicin on in vitro biophysical models // Bulgarian Chemical Communications. 2019. Vol. 51. Special Issue A. PP. 119–124.

СРАВНИТЕЛЬНЫЙ АНАЛИЗ ВЗАИМОДЕЙСТВИЯ АРТЕМИЗИНИНА И ИНГИБИТОРА SCH772984 С ERK2

С.В. Гиносян, О.В. Грабский, С.Г. Тирацуян

АННОТАЦИЯ

Сесквитерпеновые триоксановые лактоны – вторичные метаболиты растений рода *Artemisia anua* обладают мультиплетным биологическим и фармакологическим действием, включающим антималярийные, противоимфламматорные, сосудоукрепляющие, противоопухолевые, противовирусные, антибактериальные, противогрибковые, нейропротекторные и т.д. свойства. Тем не менее, специфические молекулярные мишени и механизмы действия соединений семейства артемизининовых недостаточно изучены. Предполагается, что нейропротекторное действие артемизинина опосредуется через ERK2. Целью представленной работы было изучение особенностей непосредственного взаимодействия артемизинина с ERK2. Нами был проведен докинг анализ артемизинина с ERK2 и сравнение с ингибитором SCH772984. Результаты показали, что как артемизинин, так и SCH772984 непосредственно с высокой энергией взаимодействуют с ERK2. Сайт связывания артемизинина совпадает с одним из сайтов связывания ингибитора, который соответствует таковому АТФ. При этом С кольцо артемизинина, которое содержит эндопероксидный мостик, не вовлечено во взаимодействие с белком, из чего можно заключить, что артемизинин, связываясь с ERK2, может его активировать без образования АФК.

Ключевые слова: *Artemisia anua*, артемизинин, нейропротектор, ERK2, SCH772984, докинг-анализ.

UDK612/902, 622, 3147

Поступила: 28.10.2020г.
Сдана на рецензию: 05.11.2020г.
Подписана к печати: 12.11.2020г.

BINDING OF PHOTOSENSITIZERS TO CERULOPLASMIN WITH A CHANGE IN THE SALT COMPOSITION OF THE MEDIUM

A. Zakoyan

Institute of Biochemistry NAS RA

ann.zakoyan@yandex.ru

ABSTRACT

It is shown that cationic porphyrins and metalloporphyrins, as well as anionic porphyrin (Chlorin e_6) non-covalently bind to ceruloplasmin (CP) in sufficient quantities, while the neutral photosensitizer (PS) Al-phthalocyanine binds very weakly. It is determined that an increase in the concentration of NaCl in the environment can cause a partial release of PSs from protein. Modeling of physiological conditions has shown that CP can be used as a protein-carrier of PSs, but not an active agent for photodynamic therapy of tumors (PDT).

Keywords: Photodynamic therapy of tumor (PDT), photosensitizers, cationic porphyrins, ceruloplasmin, salt composition of the medium.

Introduction

Cancer is one of the fastest growing causes of fatal diseases that people face around the world, and is thought to be the second leading cause of death, accounting for 15% of all deaths [1,11]. Photodynamic therapy of tumor (PDT) compared with other types of cancer treatment is considered

to be a promising non-traditional method with many advantages: it is non-toxic and invasive; it can be used in places where surgery is not possible, and it can be used for many types of cancer [4, 3, 9, 10]. In PDT three components act simultaneously: a photosensitizer (PS), a light source, and oxygen. The PS and the light source must be harmless to the target cell [13, 17]. In PDT, the activation of PS preparations with a certain wavelength of light leads to the transfer of energy to oxygen molecules or other substrates in the surrounding areas, while cytotoxic active forms of oxygen (ROS) are generated which can cause the death of necrotic tumor cells by apoptosis or necrosis [3, 9]. In the absence of a photoactivating light source, PS drugs are minimally toxic and are gradually eliminated from the body. The ultimate goal of PDT is the selective destruction of tumor cells with minimal damage to surrounding healthy tissues [8]. Among porphyrins used in PDT, a special role is played by cationic porphyrins, due to their own high selectivity of the accumulation in malignant cells [10]. A large class of cationic (metal) porphyrinsvarious peripheral functional groups and different central metal atoms (Zn, Ag, Co, Fe, Mn, Cu, etc.) were synthesized earlier in Armenia [14, 19].

It is known that the main carriers of PSs in the blood are proteins and lipoproteins [2, 12, 15]. Earlier we studied the binding of some PSs to various blood proteins and it was shown that in addition to serum albumin, hemoglobin, and transferrin, ceruloplasmin (CP) can also participate in porphyrin transport in the body [5, 6]. The effect of two types of irradiation (natural solar radiation and irradiation with a tungsten lamp) on the optical absorption of the complexes of human CP with some PSs has also been studied and changes in the absorption spectra have been shown [21]. Changes in physiological conditions (pH and salt composition of the medium) during the transfer of porphyrins by proteins can have a significant effect on the complexation and on the efficiency of transfer of PSs by proteins. CP is an important copper-containing glycoprotein; among its many functions it is necessary to note its participation in copper transport [16] and iron metabolism [20]. The aim of this research was to study the complexation and desorption of CP by cationic porphyrins and some known

PSs when changing the salt composition of the medium (NaCl) and to determine the possibility of using complexes for PDT tumors.

Materials and Methods

Binding of CP to PSs. The study of non-covalent complexation and desorption of PSs with human CP was carried out in vitro. Preliminary incubation of PSs ((metal) porphyrins, Chlorin e_6, Al-phthalocyanine) and purified protein was carried out in a ratio of 4:1 for 72 hours in cold conditions (6–8 °C). Non-covalent complexation of PSs with CP and further separation of unbound PSs were performed on a Sephadex G-25 column balanced with 0.01 M phosphate buffer pH 7.2. Control of the concentration of bounded PSs with CP was carried out by two independent methods of absorption and fluorescence spectroscopy.

Absorption and fluorescence spectra. The analysis of the spectra was carried out by two independent methods: absorption and fluorescence spectroscopy. Absorption spectra of PSs and their complexes were recorded on a Shimadzu UV-VISIBLE Recording Spectrophotometer UV-2100 spectrophotometer (Japan) in a quartz cuvette (0.1 or 1 cm). Changes in the absorption spectra of cationic porphyrins and metalloporphyrins were recorded for the Soret band (420–440 nm), and for Chlorin e_6 (λ_{max} = 671 nm) and for Al-phthalocyanine (λ_{max} = 678nm) at their absorption maxima in the near infrared region. Fluorescence spectra were recorded on a MPF 44 spectrofluorimeter (Perkin-Elmer, USA) in a quartz cuvette (0.1 or 1 cm). All measurements were carried out at room temperature.

PSs. The cationic porphyrins and metalloporphyrins produced in Armenia and the UK were used in the work, as well as the anionic porphyrin Chlorin e_6 and the neutral PS Al-phthalocyanine, known and currently used in PDT of tumors. All over reagents were on analytical grade.

CP. The isolation and purification of human CP was carried out by gel filtration chromatography on Sephadex G-150 and G-25 columns, as well as by ion-exchange chromatography on a DE-52 ion exchanger

(Whatman). CP was obtained from the donor blood plasma in monomeric form in a homogeneous state with a high purity index: $I = A_{280} / A_{610} < 20$ [18].

The influence of the salt composition of the medium on the binding of PSs to CP. The salt composition of the CP binding medium with PSs (0.01 M phosphate buffer /PBS/ pH 7.2) was changed by adding sodium chloride solution with the highest possible molarity to obtain the desired salt concentration. The analysis of the absorption and fluorescence spectra was carried out for 5 points (0% (H_2O), 0.1%, 0.2%, 0.4%, 0.9% NaCl) of each of the studied solutions.

Statistical analysis. The statistical parameters (mean values, standard deviation) used in the experiments were calculated using Microsoft Excel and Origin 7.0 (Origin Lab Corporation).

Results and discussion

Due to significant differences in the structure and charges of the studied PSs (cationic (metal) porphyrins, anionic porphyrin Chlorin e_6 and neutral Al-phthalocyanine), significant changes in their complexation with human CP are observed with a change in the salt composition of the medium. The binding of PSs was observed by the change in absorption at the peak of the Soret band (420-440 nm) for cationic (metal) porphyrins, for anionic Chlorin e_6 (λ_{max} = 671nm) and for neutral Al-phthalocyanine (λ_{max} = 678nm) with a change in the salt composition of the medium. Absorption and fluorescence spectra were measured for all compounds. Figures 1–4 show the typical absorption spectra of the studied compounds.

It is seen from the absorption spectra that the binding of PSs to CP occurs very quickly (less than 3 minutes) when CP is added to the PS solution. For all the studied PSs, a hypochromic effect (a decrease in the absorption of the Soret band (448 nm) and a bathochromic effect (shift of the absorption peak) are observed: for cationic (metal) porphyrins and anionic Chlorin e_6 in the long-wavelength region, and in the case of neutral Al-phthalocyanine into the shortwave region. These changes indicate the

interaction of PSs with CP and the formation of complexes. The calculated data from the analysis of the absorption and fluorescence spectra are shown in Table 1 for 5 points (0% (H_2O), 0.1%, 0.2%, 0.4%, 0.9% NaCl) of each of the studied solutions.

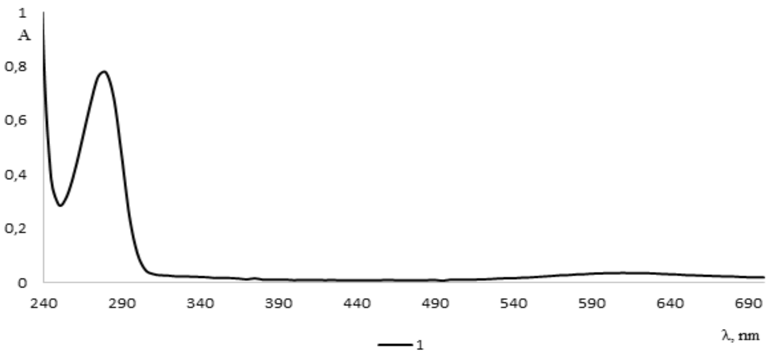


Fig. 1. Absorption spectrum of the isolated and purified human CP in 0.01 M PBS, pH 7.2, with a ratio of A_{610} / A_{280}> 0.049, having a characteristic blue color.

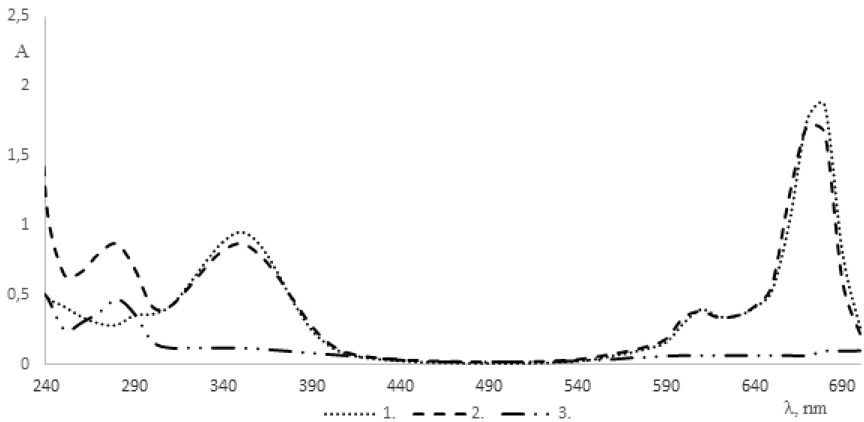


Fig. 2. Absorption spectra of neutral Al-phthalocyanine and its change upon binding to CP. 1 – 1.6 × 10^{-4} M Al-phthalocyanine in 0.01 M PBS, pH 7.2; 2 – spectrum of the complex [CP + Al-phthalocyanine] 3 minutes after protein binding to Al-phthalocyanine (in 0.01 M PBS); 3 – spectrum of the complex [CP + Al-phthalocyanine] after purification from unbound Al-phthalocyanine on Sephadex G-25 (in 0.01 M PBS).

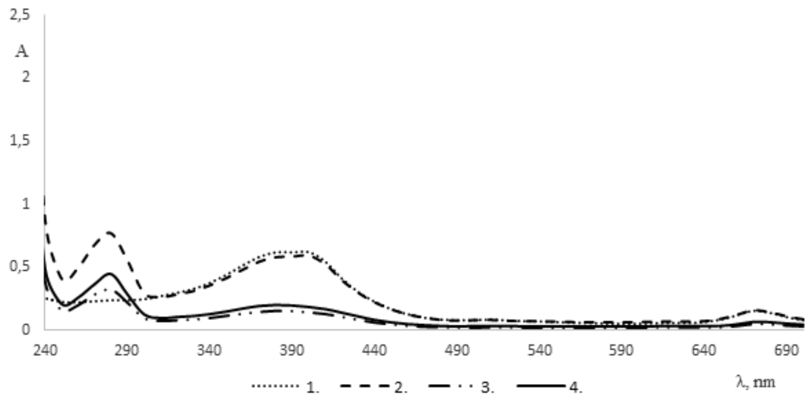


Fig. 3. Absorption spectra of Chlorine$_6$ and their change upon binding to CP. 1 – 1.6 × 10^{-4} M Chlorine$_6$ in 0.01 M PBS, pH 7.2; 2 – spectrum of the complex [CP + Chlorine$_6$] 3 min after protein binding to Chlorine$_6$ (in 0.01 M PBS); 3 – spectrum of the complex [CP + Chlorine$_6$] after purification from unbound Chlorine$_6$ on Sephadex G-25 (in 0.01 M PBS); 4 – spectrum of the complex [CP + Zn-TOEt4PyP] in 0.01 M PBS with 0.9% NaCl.

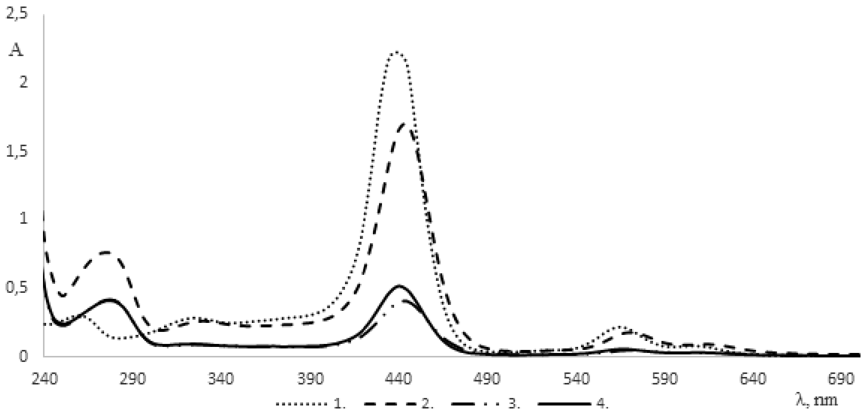


Fig. 4. Absorption spectra of cationic metalloporphyrin Zn-TOEt4PyP(Armenia) and their change upon binding to CP. 1 - 1.6 × 10^{-4} M Zn-TOEt4PyP (Armenia) in 0.01 M PBS, pH 7.2; 2 – spectrum of the complex [CP + Zn-TOEt4PyP(Armenia)] 3 min after protein binding to porphyrin (in 0.01 M PBS); 3 – spectrum of the complex [CP + Zn-TOEt4PyP(Armenia)] after purification from unbound porphyrin on Sephadex G-25 (in 0.01 M PBS); 4 - spectrum of the complex [CP + Zn-TOEt4PyP(Armenia)] in 0.01 M PBS with 0.9% NaCl.

From the obtained results according to absorption spectroscopy, it follows that the neutral PS Al-phthalocyanine binds very weakly (3.28%) to the CP molecule, while the anionic porphyrin Chlorin e_6 binds to CP better than all PSs. For complexes with all PSs, the number of PSs per one CP molecule decreases with increasing NaCl concentration in the medium. At 0.9% NaCl in the medium, which corresponds to the salt composition of human blood, a significant decrease in the number of PSs per one molecule of CP is observed. This means that there are conformational changes in the protein CP and a partial separation of PSs from the complex. Upon injection of [CP + PS] complexes into the blood, partial separation of PSs from the complex may occur; however, a significant part of PSs can remain in a bound state. Therefore, such complexes can exist in human blood and CP can be a carrier of PSs in human blood.

Table 1.*

Spectral studies of the binding of PSs to human CP molecules with a change in salt composition

N	Complex [CP + PS]	Shift of the Soret peak	% NaCl Intheme-dium	Number of PSs to 1 protein molecule (by absorption spectra)	% PSs on the protein surface (by fluorescence spectra)
I	CP + Zn-TOEt4PyP (Armenia)	4	H_2O	1.02	5.54%
			0.1%	0.94	5.99%
			0.2%	0.85	6.73%
			0.4%	0.84	8.01%
			0.9%	0.65	10.47%
II	CP + Zn-TOEt4PyP (UK)	5	H_2O	0.95	6.11%
			0.1%	0.92	6.12%
			0.2%	0.86	6.12%
			0.4%	0.85	6.13%
			0.9%	0.63	9.77%

III	CP + TOEt4PyP (Armenia)	3	H_2O	0.57	2.46%
			0.1%	0.51	2.75%
			0.2%	0.51	2.75%
			0.4%	0.26	5.56%
			0.9%	0.26	7.79%
IV	CP + TOEt4PyP (UK)	5	H_2O	0.51	3.27%
			0.1%	0.49	3.44%
			0.2%	0.49	3.56%
			0.4%	0.43	3.94%
			0.9%	0.3	8.45%
V	CP + Zn-TBut4PyP (UK)	3.5	H_2O	0.93	3.54%
			0.1%	0.84	6.87%
			0.2%	0.82	6.43%
			0.4%	0.81	8%
			0.9%	0.32	15.6%
VI	CP + Chlorin e_6 (λ_{max} = 671 nm)	0.5	H_2O	1.81	3.25%
			0.1%	1.78	2.55%
			0.2%	1.75	2.55%
			0.4%	1.70	2.4%
			0.9%	1.38	2.28%
VII	CP + Al-phthalocyanine (λ_{max} = 678 nm)	-2.5	3.28 % - a very low binding percent		

* The average values of five independent experiments are given (n = 5). The standard deviation of the values does not exceed 5%. $P \leq 0.05$.

According to fluorescence data (Table 1), for complexes with cationic (metal) porphyrins, the percentage of bound PSs on the surface of CP increases with increasing NaCl concentration in the medium. This means a change in the microenvironment of cationic (metal) porphyrins and the

possible release of negatively charged amino acid residues of the CP molecule on the surface of the protein and binding to cationic (metal) porphyrins. The opposite picture is observed for the [CP + Chlorin e_6] complex: with an increase in the concentration of NaCl in the medium and a change in the microenvironment of this complex, the percentage of bound Chlorin e_6 molecules on the surface of the protein decreases. This indicates a partial transition of these PSs to the internal structures of the protein and a partial separation of Chlorin e_6 from the protein molecule.

Thus, CP can form complexes with PSs [CP + PS] and is a carrier of PSs in the blood, but not an active agent for PDT tumors, due to the protein part of the complex (CP) quenching the fluorescence of most associated PSs [7].

REFERENCES

1. *Akhtar M.J., Ahamed M., Alhadlaq H.A., Alrokayan S.A., Kumar S.* Targeted anticancer therapy: Overexpressed receptors and nanotechnology. Clin. Chim. Acta, 436, 78–92, 2014.
2. *Cohen S., Margalit R.* Binding of porphyrin to human serum albumin. Structure-activity relationships. Biochemical J., 270, 325–330, 1990.
3. *Dolmans D.E., Fukumura D., Jain R.K.* Photodynamic therapy for cancer. Nat. Rev. Cancer, 3, 380–387, 2003.
4. *Ethirajan M., Chen Y., Joshi P., Pandey R.K.* The role of porphyrin chemistry in tumor imaging and photodynamic therapy. Chem. Soc. Rev. 40, 340–362, 2011.
5. *Gyulkhandanyan A.G., Parkhats M.V., Knyukshto V.N., Lepeshkevich S.V., Dzhagarov B.M., Zakoyan A.A., Gyulkhandanyan Aram G., Sheyranyan M.A., Kevorkian G.A., Gyulkhandanyan G.V.* Binding of cationic porphyrins andmetalloporphyrins to thehuman transferrin for photodynamic therapy of tumors. Proc. of SPIE, 10685, 1068504-1-1068504-9, 2018.
6. *Gyulkhandanyan A.G., Zakoyan A.A, Gyulkhandanyan A.G., Parkhats M.V., Dzhagarov B.M, Lazareva E.N., Tuchin V.T., Gyulkhandanyan G.V.* Ceruloplasmin – a potential carrier of photosensitizers for photodynamic therapy of tumors. Proc. of SPIE, Vol. 11079. PP. 110791T-110791T-3, 2019.

7. *Gyulkhandanyan A.G., Zakoyan A.A., Mkrtchyan L.V., Gyulkhandanyan A.G., Parkhats M.V., Dzhagarov B.M., Sheyranyan M.A., Simonyan G.M., Lazareva E.N., Tuchin V.V., Gyulkhandanyan G.V.* Binding of ceruloplasmin with cationic porphyrins: pH and salt composition of a medium. Proc. SPIE, 11363, Tissue Optics and Photonics, 1136329, 2020.
8. *Hong E.J., Choi D.G., Shim M.S.* Targeted and effective photodynamic therapy for cancer using functionalized nanomaterials. Acta Pharm. Sin. B, 6, 297–307, 2016.
9. *Hopper C.* Photodynamic therapy: a clinical reality in the treatment of cancer. Lancet Oncol, 1, 212–219, 2000.
10. *Hudson R., Boyle, R.W.* Strategies for selective delivery of photodynamic sensitizers to biological targets. J. Porphyrins Phthalocyanines, 8, 954–975, 2004.
11. *Jemal A., Center M.M., DeSantis, C., Ward E.M.* Global patterns of cancer incidence and mortality rates and trends. Cancer Epidemiol. Prev. Biomark. 19(8), 1893–1907, 2010.
12. *Kongshaug M., Moan J., Brown, S.B.* The distribution of porphyrins with different tumor localizing ability among human plasma proteins, British Journal of Cancer 59, 184–188, 1989.
13. *Lim M.E., Lee Y.-L., Zhang Y., Chu J.J.H.* Photodynamic inactivation of viruses using upconversion nanoparticles. Biomaterials, 33, 1912–1920, 2012.
14. *Madakyan V.N., Kazaryan R.K., Khachatryan M.A., Stepanyan A.S., Kurtikyan T.S., Ordyan M.B.* Synthesis of new water-soluble cationic porphyrins, Khimiyaheterociklicheskikhsoedinenii, 2, 212–216, 1986.
15. *Moan J., Rimington C., Western A.* The binding of dihematoporphyrin ether (photofrin II) to human serum albumin. Clinica Chimica Acta, 145, 227–236, 1985.
16. *Musci G., Fraterrigo T.Z., Calabreze L., McMillin D.R.* On the lability and functional significance of the type 1 cooper pool in ceruloplasmin. J. Biol. Chem., 4, 441–446, 1999.
17. *Mroz P., Hashmi J.T., Huang Y.-Y., Lange N., Hamblin M.R.* Stimulation of anti-tumor immunity by photodynamic therapy. Expert Rev. Clin. Immunol. 7(1), 75–91, 2011.
18. *Sokolov A.V., Dadinova L. A., Petoukhov M.V., Bourenkov G., Dubova K.M., Amarantov S.V., Volkov V.V., Kostevich V.A., Gorbunov P.A., Grudinina N.A.,*

Vasilyev V.B., Samygina V.R. Structural Study of the Complex Formed by Ceruloplasmin and Macrophage Migration Inhibitory Factor. Biochemistry, 83 (6), 701–707, 2018.
19. *Tovmasyan A.G., Ghazaryan R.K., Sahakyan L., Gasparyan G., Babayan N., Gyulkhandanyan G.* Synthesis and anticancer activity of new water-soluble cationic metalloporphyrins. European Conferences on Biomedical Optics 2007, Munich, Germany, Technical Abstract Summaries, 71–72, 2007.
20. *Yoshida K., Furihata K., Takeda S., Nakamura A., Yamamoto K., Morita , NM Hiyamuta S., Ikeda S., Shimizu N. Yanagisawa N.* A mutation in the ceruloplazmin gene is associated with systemic hemosiderosis in humans. Nat. Genet., 9 (3), 267–72, 1995.
21. *Zakoyan A.A.* The Effect of Light on the Optical Absorption of Photosensitizers and Their Complexes with Human Ceruloplasmin. Medical Science of Armenia, 60 (3), 62–70, 2020.

СВЯЗЫВАНИЕ ФОТОСЕНСИБИЛИЗАТОРОВ С ЦЕРУЛОПЛАЗМИНОМ ПРИ ИЗМЕНЕНИИ СОЛЕВОГО СОСТАВА СРЕДЫ

А.А. Закоян

АННОТАЦИЯ

В данной научной статье показано, что катионные порфирины и металлопорфирины, а также анионный порфирин (хлорин e_6) нековалентно связываются с церулоплазмином (ЦП) в достаточных количествах, тогда как нейтральный фотосенсибилизатор Al-фталоцианин связывается очень слабо. Определено, что увеличение концентрации NaCl в окружающей среде может вызвать частичное высвобождение фотосенсибилизаторов из белка. Моделирование физиологических условий показало, что ЦП может быть использован в качестве белка-переносчика фотосенсибилизаторов, но не активным агентом для фотодинамической терапии опухолей.

Ключевые слова: Фотодинамическая терапия опухолей (ФДТ), фотосенсибилизаторы, катионные порфирины, церулоплазмин, солевой состав среды.

УДК 577.29(577.322.9)

Поступила: 06.11.2020г.
Сдана на рецензию: 10.11.2020г.
Подписана к печати: 18.11.2020г.

СРАВНИТЕЛЬНЫЙ АНАЛИЗ ПОТЕНЦИАЛА ВЗАИМОДЕЙСТВИЯ ДИГИДРОАРТЕМИЗИНИНА, ДИМЕРА ДИГИДРОАРТЕМИЗИНИНА И ИБУПРОФЕНА С β-АМИЛОИДНОЙ ФИБРИЛЛОЙ И BACE-1 МЕТОДАМИ МОЛЕКУЛЯРНОГО МОДЕЛИРОВАНИЯ

***Е.Р. Амбарцумян*[1]*, С.В. Гиносян*[1]*, С.Г. Тирацуян*[2]**

[1]*Кафедра Медицинской биохимии и биотехнологии*
[2]*Кафедра Биоинженерии, биоинформатики и молекулярной биологии*
Институт Биомедицины и Фармации
Российско-Армянский университет

yelena.hambarcumyan@rau.am, *siranush.ginosian.student@rau.am*, *susanna.tiratsuyan@rau.am*

АННОТАЦИЯ

Болезнь Альцгеймера – глобальная проблема здравоохранения, которая оказывает огромное влияние на людей и общество. Согласно гипотезе амилоидного каскада, важнейшее молекулярное событие в патогенезе «Болезнь Альцгеймера» – протеолитическое расщепление белка-предшественника амилоида β-секретазой BACE-1, приводящее к образованию нерастворимых форм β-амилоидных пептидов. Известно, что артемизинины, являющиеся вторичными метаболитами растения полыни однолетней (*Artemisia Annua*), обладают аниамилоидогенными, противовоспалительными, антиоксидантными, когнитивно-стимулирующими, антибактериальными и другими свойства-

ми. Данная работа посвящена изучению взаимодействия дигидроартемизинина и его димера с амилоидной фибриллой18$A\beta_{9-40}$ и BACE-1 и последующему сравнению с таковым нестероидного противовоспалительного препарата ибупрофена методами молекулярного моделирования. Нами было выявлено, что ибупрофен способен предотвращать образование амилоидной фибриллы, в то время как дигидроартемизинин препятствует образованию и стабилизации, а его димер предотвращает рост амилоидной фибриллы. Подобно остальным лигандам, димер дигидроартемизинина способен модулировать активность BACE-1, что дает возможность рассматривать его в качестве потенциального соединения для лечения болезни Альцгеймера.

Ключевые слова: Болезнь Альцгеймера, артемизинины, димер дигидроартемизинина, ибупрофен,18$A\beta_{9-40}$, BACE-1.

Введение

Болезнь Альцгеймера (БА) – это глобальная проблема здравоохранения, которая оказывает огромное влияние на людей и общество [1]. Как основная причина прогрессирующих когнитивных нарушений, приобретенных в результате деменции, БА в значительной степени препятствует повседневной деятельности. Согласно данным ВОЗ, 35,6 млн. человек во всем мире страдают деменцией, и это число увеличится почти вдвое к 2030 году, достигнув 65,7 млн. и 115,4 млн. к 2050 году [2]. БА стала третьей по частоте причиной инвалидности и смерти среди пожилого населения, уступая сердечно-сосудистым заболеваниям и злокачественным опухолям. Драматическая роль, которую БА и другие виды деменции будут играть в системах здравоохранения в будущем, неоспорима и подчеркивает огромную важность успешной разработки лекарств и методов лечения против БА [3].

БА – комплексное заболевание, в котором участвует множество факторов. Поскольку основными патологическими признаками БА являются внеклеточные отложения β-амилоидных пептидов (Aβ) в виде

сенильных бляшек, внутриклеточные отложения гиперфосфориллированных белков тау в нейрофибриллярных клубках и потеря нейронной функции, Aβ долгое время рассматривались в качестве потенциальной мишени для разработки препаратов для лечения БА [4]. Самая прямая стратегия анти-Aβ-терапии – снижение образования Aβ таргетированием β- и γ-секретаз [5, 6]. С тех пор, как был диагностирован первый пациент с БА, управление по санитарному надзору за качеством пищевых продуктов и медикаментов (FDA) одобрило только 5 препаратов, которые, однако, не смогли замедлить прогрессирование БА и имели некоторые побочные эффекты [7].

Артемизинин и его полусинтетические производные обладают противовирусными, противовоспалительными, когнитивно-стимулирующими, антиамилоидогенными, антиоксидантными, нейропротекторными и другими свойствами. Данные последних лет показали, что их можно рассматривать в качестве потенциальных терапевтических средств при лечении заболеваний ЦНС, включая БА, так как они способны ингибировать воспалительные процессы [8].

Цель данной работы – изучение исравнение непосредственного взаимодействия дигидроартемизинина (DHA), димера дигидроартемизинина(DDHA), ибупрофена (IBU) с амилоидной фибриллой 18Aβ_{9-40} и BACE-1.

Материалы и методы

3D структуры десяти моделей 18Aβ_{9-40} [PDB ID: 2LMP], BACE-1 [PDB ID: 2WJO] в формате PDB взяты из базы данных RCSB Protein Data Bank (RCSB PDB) [9]. 3D структуры DHA [CID: 456410], DDHA [CID: 44564070], IBU [CID: 3672] были получены из базы данных PubChem [10]. Докинг анализ фибрилы и BACE-1 с DHA, DDHA и IBU проводили программными пакетами AutoDock Tools и AutoDock Vina [11]. Анализ водородных связей и гидрофобных взаимодействий проводили с помощью Ligplot^{+} [12]. Визуализация полученных данных

проводилась при помощи Pymol [13]. Расчет молекулярных характеристик лигандов проводился с помощью PreADME [14].

Результаты и обсуждение

Нами был проведен докинг анализ десяти моделей с DHA, DDHA и IBU. Результаты показали, что наибольшая аффинность 18Aβ$_{9-40}$ ко всем лигандам наблюдается для модели 2.

Докинг анализ взаимодействия DDHA (ΔG_{bind}=-10,7 ккал/моль) со 2-й моделью фибриллы 18Aβ$_{9-40}$выявил гидрофобные взаимодействия с Gly37 P и Q цепей.DHA (ΔG_{bind}= -9,4 ккал/моль) гидрофобно взаимодействует с Ala21 (A), и образует водородную связь с Lys28 (C). IBU (ΔG_{bind} = -7,4 ккал/моль) гидрофобно взаимодействует с Ala21 (G), Ala21 (H) (Рис. 1).

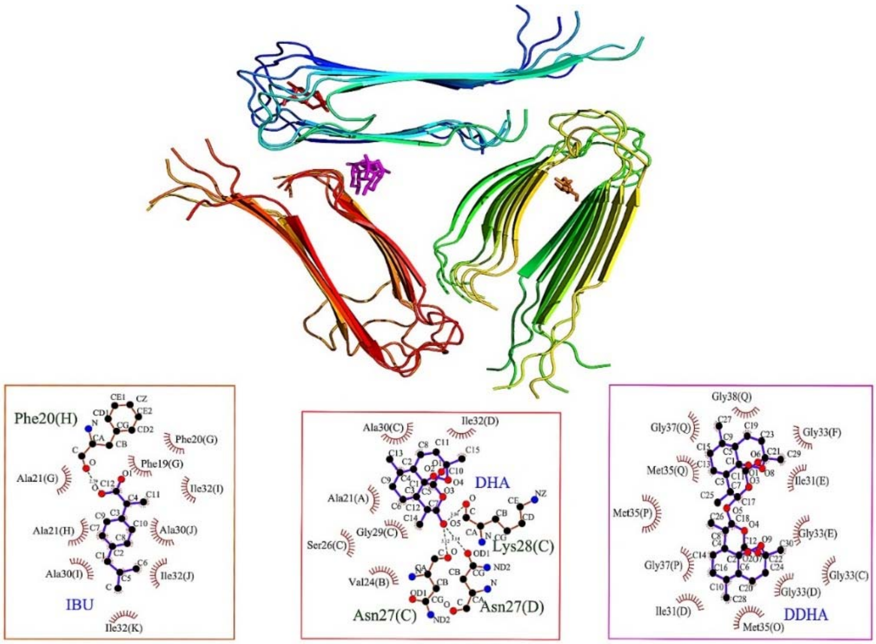


Рисунок 1. Докинг (сверху)и анализ водородных связей и гидрофобных взаимодействий (снизу) DDHA(сиреневый),DHA (красный) и IBU (оранжевый) со 2-й моделью 18Aβ$_{9-40}$.

Известно, что за образование, рост и стабилизацию фибриллы ответственны Leu17-Ala21, Gly37-Ala42, Lys28-Asp23 [15]. Из трех лигандов IBU предотвращает образование, DDHA – рост, а DHA препятствует образованию и стабилизации амилоидной фибриллы (Табл. 1).

Таблица 1.

Взаимодействие DDHA (фиолетовый), IBU (оранжевый) и DHA (красный) с аминокислотами, ответственными за образование, рост и стабилизацию фибриллы.

Структура	Образование		Рост		Стабилизация	
	Leu17	Ala21	Gly37	Ala42	Lys28	Asp23
18Aβ_{9-40}		**DHA (A), IBU (G, H)**	**DDHA (P, Q)**		**DHA(C)**	

Анализ докинга DDHA (ΔG_{bind}=-10,1 ккал/моль) с BACE-1 выявил гидрофобные взаимодействия с Tyr71 (P). DHA (ΔG_{bind}=-7,9 ккал/-моль) гидрофобно взаимодействует с Tyr71, и образует водородную связь с Asp32. IBU гидрофобно взаимодействует с Tyr71 BACE-1 (ΔG_{bind}= -6,7 ккал/моль) и образует водородную связь с Ser35 и Asn37 (Рис. 2).

Аффинность для предпочтительных конформаций связывания лигандов с фибриллой, а также для BACE-1 можно расположить в следующем убывающем порядке: DDHA > DHA > IBU.

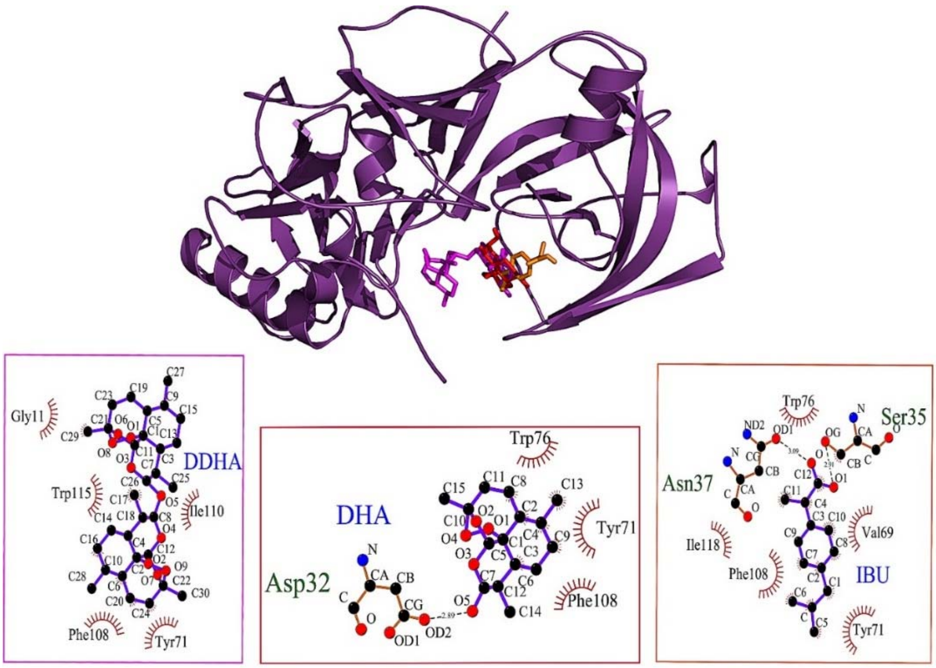


Рисунок 2. Докинг DDHA(сиреневый),DHA (красный) и IBU (оранжевый) с BACE-1 (сверху), анализ водородных связей и гидрофобных взаимодействий (снизу).

Активный центр BACE-1состоит из Asp32 и Asp228, которые консервативны для аспарагиновых протеиназ эукариот [16]. Известно, что консервативная молекула воды (W2) образует три водородные связи с остатками Tyr71, Asn37 и Ser35. Это приводит к образованию непрерывной цепи связанных с водородом остатков Trp76-Tyr71-W2-Ser35-Asp32. Существует механизм, который на начальных стадиях катализа способствует высвобождению протона из карбоксильной группы Asp32 и усвоению протона после расщепления субстрата, а Ser35 помогает усвоению протонов и высвобождению Asp32 во время каталитического цикла [17].

Все лиганды взаимодействуют с Tyr71 и только DHA взаимодействует с аминокислотой (Asp32) активного центра фермента.

Были проанализированы фармакологические характеристики, такие как абсорбция (HIA) и гематоэнцефалический барьер (BBB) (Табл. 2). Как видно из таблицы, лиганды проявляют высокую степень всасываемости и способны преодолевать BBB в той или иной степени.

Таблица 2.

Анализ физико-химических свойств лигандов.

CID	Соединение	Log (BBB)	HIA (%)
3672	**IBU**	0.103	98.38
456410	**DHA**	-0.003	93.58
44564070	**DDHA**	-0.648	99.06

В соответствии с полученными результатами можно заключить, что ибупрофен способен предотвращать образование амилоидной фибриллы, в то время как дигидроартемизинин препятствует образованию и стабилизации, а его димер предотвращает рост амилоидной фибриллы. Подобно остальным лигандам, димер дигидроартемизинина способен модулировать активность BACE-1, что дает возможность рассматривать его в качестве потенциального соединения для лечения БА.

Благодарность

Работа выполнена при поддержке Гранта № 10-2/I-4 ГКН МОН РА.

ЛИТЕРАТУРА

1. *Duthey B.* Background Paper 6.11 Alzheimer Disease and Other Dementias, Update on 2004; World Health Organization: Geneva, Switzerland, February 2013. PP. 1–77.
2. *Eurostat.* Population Structure and Ageing. Available online: http://ec.europa.eu/eurostat/statisticsexplained/index.php/Population_structure_and_ageing

3. *Alzheimer's Association.* 2017 Alzheimer's disease facts and figures. Alzheimer's Dement. 2017, 13, 325–373.
4. *Sharma P., Sharma A., Fayaz F., Wakode S., Pottoo F.H.* Biological Signatures of Alzheimer's Disease. Curr. Top. Med. Chem. 2020, 20, 770–781.
5. *Uddin, M.S., Al Mamun A., Rahman M.A., Behl T., Perveen, A., Hafeez A., Bin-Jumah M.N., Abdel-Daim M.M., Ashraf G.M.* Emerging proof of protein misfolding and interactions in multifactorial Alzheimer's disease. Curr. Top. Med. Chem. 2020, 20.
6. *Uddin M.S., Kabir M.T., Jeandet P., Mathew B., Ashraf G.M., Perveen A., Bin-Jumah M.N., Mousa S.A., Abdel-Daim M.M.* Novel Anti-Alzheimer's Therapeutic Molecules Targeting Amyloid Precursor Protein Processing. Oxid. Med. Cell. Longev. 2020, 2020, 1–19.
7. *Ali G-C, Guerchet M., Wu Y-T, Prince M., Prina M.* Chapter 2: The global prevalence of dementia. In: Prince M, Guerchet M, Ali G-C, Wu Y-T, Prina M, editors. The Global Impact of Dementia. An analysis of prevalence, incidence, cost and trends. London: Alzheimer's Disease International (ADI); 2015. PP. 10–29.
8. *Shi Z., Chen Y., Lu C., Dong L.M., Lv J.W., Tuo Q.H., Zhu X.X.* Resolving neuroinflammation, the therapeutic potential of the anti-malaria drug family of artemisinin. Pharmacol Res, 136, 172–180, 2018.
9. *Berman H.M. et al.* The protein data bank //Acta Crystal lographica Section D: Biological Crystallography. 2002. Vol. 58. №. 6. PP. 899–907.
10. *Bolton E.E. et al.* PubChem: integrated platform of small molecules and biological activities //Annual reports in computational chemistry. Elsevier, 2008. Vol. 4. PP. 217–241.
11. *Trott O., Olson A.J.* Auto Dock Vina: improving the speed and accuracy of docking with a new scoring function, efficient optimization, and multithreading //Journal of computational chemistry. 2010. Vol. 31. №. 2. PP. 455–461.
12. *Wallace A.C., Laskowski R.A., Thornton J.M.* LIGPLOT: a program to generate schematic diagrams of protein-ligand interactions //Protein engineering, design and selection. 1995. Vol. 8. №. 2. PP. 127–134.
13. *De Lano W.L.* The PyMOL molecular graphics system //http://www. pymol. org. 2002.
14. *Lee S.K. et al.* The PreADME: Pc-based program for batch prediction of Adme properties //EuroQSAR. 2004. Vol. 9. PP. 510.

15. *Han W., Schulten K.* Fibril elongation by Ab17–42: kinetic network analysis of hybrid-resolution molecular dynamics simulations. J. Am. Chem. Soc. 2014. 136, 12450–12460.
16. *Venugopal, C., et al.:* Beta-secretase: structure, function, and evolution. CNS Neurol Disord Drug Targets (Formerly Curr Drug Targets CNS NeurolDisord). 2008. Vol. 7. PP. 278–294.
17. *Mishra S., Caflisch A.* Dynamics in the active site of b-secretase: a network analysis of atomistic simulations. //Biochem. 2011. Vol. 50. PP. 9328–9339.

COMPARATIVE ANALYSIS OF THE POTENTIAL OF INTERACTION OF DIHYDROARTEMISININ, DIHYDROARTEMISININ DIMER AND IBUPROFEN WITH β-AMYLOID FIBRIL AND BACE-1 BY MOLECULAR MODELING METHODS

Y. Hambardzumyan, S. Ginosyan, S. Tiratsuyan

ABSTRACT

Alzheimer's disease is a global health problem that has a huge impact on people and society. According to the hypothesis of the amyloid cascade, the most important molecular event in the pathogenesis of Alzheimer's disease is the proteolytic cleavage of the amyloid precursor protein by β-secretase BACE-1, leading to the formation of insoluble forms of β-amyloid peptides. It is known that artemisinins, which are secondary metabolites of the plant *Artemisia Annua*, have anti-amyloidogenic, anti-inflammatory, antioxidant, cognitive-stimulating, antibacterial and other properties. This work is devoted to the study of the interaction of dihydroartemisinin and its dimer with the amyloid fibril $18A\beta_{9\text{-}40}$ and BACE-1, and the subsequent comparison with nonsteroidal anti-inflammatory drug ibuprofen using molecular modeling methods. We have found that ibuprofen is able to prevent the formation of amyloid fibrils, while dihydroartemisinin prevents the formation and stabilization, and its dimer prevents the growth of amyloid fibrils. Like other ligands, the dihydroartemisinin dimer is capable of modulating the activity of BACE-1, which makes it possible to consider it as a potential compound for the treatment of Alzheimer's disease.

Keywords: Alzheimer's disease, artemisinins, dihydroartemisinin dimer, ibuprofen, $18A\beta_{9\text{-}40}$, BACE-1.

СВЕДЕНИЯ ОБ АВТОРАХ

Агаян А.А.	студент четвертого курса по специальности «Радиофизика и электроника» ЕГУ, инженер в ЗАО «Синопсис Армения»
Акопян Г.А.	инженер в ЗАО «Синопсис Армения»
Амбарцумян Е.Р.	аспирант второго года обучения по направлению «Биологические науки» (направленность «Биохимия») РАУ
Атанесян А.А.	аспирант Института радиофизики и электроники НАН РА
Варданян В.А.	студент второго курса магистратуры по направлению подготовки «Инфокоммуникационные технологии и системы связи» РАУ
Гарибян А.	аспирант третьего года обучения кафедры Дискретной математики и теоретической информатики Ереванского государственного университета
Геджагезян Х.А.	аспирант Национального Политехнического университета Армении
Гиносян С.В.	аспирант третьего года обучения по направлению «Биологические науки» РАУ
Грабский О.В.	преподаватель кафедры Медицинской биохимии и биотехнологии РАУ
Григорян А.М.	к.х.н., зав.кафедрой Общей и фармацевтической химии РАУ
Григорян М.Т.	инженер в ЗАО «Синопсис Армения»

Гукасян Ц.Г.	аспирант кафедры Системного программирования РАУ, заведующий лабораторией им. В.П. Иванникова
Закоян А.А.	младший научный сотрудник Института биохимии НАН РА
Маргарян А.В.	студент второго курса магистратуры по специальности «Радиофизика и электроника» ЕГУ, инженер в ЗАО «Синопсис Армения»
Оганесян А.А.	к.б.н., доцент, заведующая кафедрой медицинской биохимии и биотехно-логии РАУ
Сисакян А.А.	ассистент кафедры высшей математики и физики Национального Аграрного университета Армении
Тадевосян Л.А.	студент первого курса магистратуры по направлению подготовки «Электроника и наноэлектроника» РАУ
Тигранян Ш.Т.	студент четвертого курса по направлению подготовки «Прикладная математика и информатика» РАУ
Тимотин А.И.	инженер Ереванского научно-исследовательского института связи
Тирацуян С.Г.	к.б.н., доцент, заведующая кафедрой Медицинской биохимии и биотехнологии РАУ
Фарсиян Л.М.	аспирант третьего года обучения по направлению «Биологические науки» (направленность «-Биохимия») РАУ
Шмавонян А.А.	студент четвертого курса по направлению подготовки «Инфокоммуникационные технологии и системы связи» РАУ.

СОДЕРЖАНИЕ

Главный редактор РНИ – *М.Э. Авакян*
Корректор – *Ш.Г. Мелик-Адамян*
Компьютерная верстка – *А.Г. Антонян*

Адрес Редакции научных изданий
Российско-Армянского
университета:

0051, г. Ереван, ул. Овсепа Эмина, 123
тел./факс: (+374 10) 27-70-52 (внутр. 42-02)
e-mail: redaction.rau@gmail.com

Заказ № 18
Подписано к печати 20.12.2020г.
Формат 70x100 1/16. Бумага офсетная № 1.
Объем 8 усл. п.л. Тираж 100 экз.